Dissertation zur Erlangung des Doktorgrades

der Fakultät für Chemie und Pharmazie

der Ludwig-Maximilians-Universität München

The Value of Fluorescence and B$_{22}$ Techniques as Complementary Approaches in Protein Stability Analyses

Miriam Printz

aus Köln

2011

Erklärung

Diese Dissertation wurde im Sinne von § 13 Abs. 3 bzw. 4 der Promotionsordnung vom 29. Januar 1998 (in der Fassung der vierten Änderungssatzung vom 26. November 2004) von Herrn Prof. Dr. Wolfgang Frieß betreut.

Ehrenwörtliche Versicherung

Diese Dissertation wurde selbständig, ohne unerlaubte Hilfe erarbeitet.

München, den 15.04.2011

_____
Miriam Printz

Dissertation eingereicht am 15.04.2011

1. Gutachter: Prof. Dr. Wolfgang Frieß

2. Gutachter: Prof. Dr. Gerhard Winter

Mündliche Prüfung am 01.06.2011

Ludwig Maximilians University of Munich

Department of Pharmacy

Pharmaceutical Technology
and Biopharmaceutics

ACKNOWLEDGEMENTS

_____

Thank you!

Miriam

Simon

Table of Contents

CHAPTER 1

Formulation Development and Its Relation to Protein Aggregation and Particles

CHAPTER 2

Individual Second Virial Coefficient (B$_{22}$) Determination of Monomer and Oligomers in Heat Stressed Protein Samples using Size Exclusion Chromatography and Light Scattering

_____

CHAPTER 3

Simultaneous Detection and Analysis of Protein Aggregation and Protein Unfolding by Size Exclusion Chromatography with Post Column Addition of the Fluorescent Dye BisANS

III

CHAPTER 4

Kinetics of Protein Aggregates during Storage

CHAPTER 5

Fluorescence Microscopy of Protein Particles on Filter Surfaces

_____

CHAPTER 6

Front Face Fluorescence Spectroscopy of Lyophilised Protein

_____

CHAPTER 7

General Summary and Outlook

CHAPTER 1

Formulation Development and Its Relation to Protein Aggregation and Particles

ABSTRACT

Parenteral protein formulations not only have to be physiologically acceptable but also must maintain the stability of the protein molecules. A limited spectrum of formulation variables, including pH, ionic strength, the addition of surfactants or a restricted number of other stabilizers are used to meet the demands of protein pharmaceuticals. One major concern in protein formulation is the formation of protein aggregates which may be inactive or potentially cause adverse effects and therefore have to be minimized. Aggregates may be formed during manufacturing, storage or transportation. Typically an integrated approach to the analysis of protein aggregates and particles has to be accomplished during formulation development, considering various types of protein aggregates. Triggers and causes for aggregation and particle formation may be a variation in temperature, agitation stress such as stirring, pumping and shaking as well as the exposure to different surfaces.

_____

1 INTRODUCTION

During protein formulation development, a bunch of analytical methods is required to analyze the entire size range and types of protein aggregates. Hence, the current European Medicines Agency (EMA) draft guideline suggests the use of orthogonal methods, which means the use of a combination or a variety of different analytical methods, each having its own characteristic measuring principle, for example, by size, quantification or structure, etc. [1]. For quantification and / or size estimation typically methods such as high performance liquid chromatography (HPLC), asymmetrical flow field flow fractionation (AF4) applying various detectors, e.g., UV-, fluorescence- and multi angle laser light scattering (MALLS) detector, analytical ultracentrifugation (AUC), and sodium dodecyl sulfate polyacrylamide gel electrophoresis (SDS-PAGE) are used. In addition, static and dynamic light scattering, light obscuration, UV spectroscopy and turbidity are commonly used analytical tools in formulation development. For characterization of protein aggregates and structural analysis of proteins, spectroscopic methods such as circular dichroism (CD), and Fourier transform infrared spectroscopy (FTIR), second derivative UV absorption spectroscopy, and fluorescence spectroscopy are applied.

An additional challenge during formulation development can arise from the availability of only small amounts of protein and limited time, so that not all analytical tools can be fully applied. Thus, accelerated stability studies of protein pharmaceuticals are implemented and extrapolation, as far as practicable, of the gained data is performed to identify the most suitable formulation. But as aggregation kinetics do not typically follow Arrhenius' behaviour, the extrapolation to predict aggregation and stability behaviour at lower storage temperature over longer storage time remains challenging [2]. In the context of limited availability of material as well as for high throughput formulation screening approaches, it appears necessary to select analytical methods enabling miniaturisation. Consequently methods for aggregate analysis which can be adapted to well plate systems are of interest which includes UV-Vis and fluorescence spectroscopy, nephelometry, turbidity, dynamic light scattering, SE-HPLC and lab on a chip gel electrophoresis [3]. These setups allow the use of robotic systems and the application of different stress methods can

be combined with factorial design of experiment or also enable the evaluation of lyophilized formulations in micro-plates [4; 5].

Other questions have to be raised in the context of freeze-thaw stability testing. Freeze-thaw stability testing is advised to be performed at genuine scale, but might have to be conducted with much smaller volumes as the availability of protein material is limited in early stages. Therefore, the obtained data might contingently not correlate to the freeze-thaw behaviour and stability data at manufacturing scale [1]. Furthermore, agitation stress has to be simulated. By using mechanical stress testing devices such as horizontal or vertical shakers [6], stirred reactors [7] and pumps [8], accelerated mechanical stress situations are imitated. However, it remains difficult to predict the extent of mechanical stress that a protein is confronted with during manufacturing and transport [1]. All of this also has to be considered against the background of the differences in type and quality of surfaces of containers, stoppers or tubings used in the various stages of product development and manufacturing. Another aspect in this context are environmental factors, which could change during development and manufacturing and thereby influence the quality of the product, such as temperature fluctuations, influence of light exposure and a possible dilution effect in infusion liquids.

2   STABILITY OF LIQUID PROTEIN PHARMACEUTICALS DURING STATIC STORAGE

During formulation development of liquid protein pharmaceuticals, a main focus is the stability of the protein in solution (for dried products see 6), especially under static conditions. The intended storage temperature is typically set between 2 and 8°C for liquid protein pharmaceuticals and dried proteins, whereas drug substance (bulk) is frequently stored frozen. In case of accelerated temperature studies during formulation development, typically temperatures like 25°C, 30°C and 40°C are utilized for protein pharmaceuticals, in accordance to the conditions of the International Conference on Harmonization of Technical Requirements for Registration of Pharmaceuticals for Human Use (ICH) guidelines. One can

_____

indisputably state that there is no single protein aggregation pathway but a variety of pathways resulting in different aggregation end states. As a consequence, the type of aggregates formed a protein molecule upon quiescent storage can be different depending on the solution conditions. The stabilizing effects of cosolutes as described by Timasheff and colleagues are attributed to the protein solvent interaction and not directly to the protein-excipient interplay [9]. The molecules are preferentially excluded from the surface of the native protein [10] and lead to a thermodynamically unfavourable situation and an entropically unfavourable state. As denaturation would lead to an enhanced contact surface between protein and additive, which is thermodynamically even more disadvantageous, the native monomer structure is preferred which is one major aspect of protein stability. Due to this complexity a broad aggregate analysis approach is essential covering a wide range of aggregate sizes and structures [1; 6; 11-13] and a limited application of e.g. only size-exclusion chromatography (SEC) or visible inspection leaves many open questions. Although SE-HPLC is considered the working horse in protein formulation development, various challenges have been described using SE-HLPC. The single use of a SE-HPLC method could lead to artefacts due to dilution [14], adsorption of protein to the column [10], and the influence of high salt concentration in the mobile phase [15].

Every technique offers a range of benefits, but also goes along with its restrictions. For instance, using SDS-PAGE the detection of non-covalently linked aggregates is not possible, as they are split during sample preparation [16]. AF4 is currently orthogonally used to SE-HPLC, but also here artefacts due to the measuring principle have been described [15]. AUC might be disturbed by stabilizers such as sugars [18]. DLS is not capable to quantify aggregates and exogenous particles interfere [1]. At least a combination of small soluble aggregate analysis, e.g., by SE-HPLC supplemented by orthogonal methods covering the several nm to µm range e.g., by turbidity testing or sub-visible and visible particle analysis is necessary [19; 20]. Recently, it was shown that freeze thaw-, thermal-, shaking- and stirring stresses in liquid formulations lead to different aggregates in quality, quantity and morphology [6; 12; 21]. Whereas shaking and freeze thaw stress led to pronounced formation of subvisible particles observed by light obscuration, the increase in soluble aggregates

detectable by SE-HPLC was only slight [21]. However, aggregation upon static storage at elevated temperature could not be substantiated by visual inspection, turbidity measurements or light obscuration. Only SE-HPLC detected changes. Significant differences in physico-chemical characteristics of aggregates induced after thermal and freeze thaw stress were also reported by Hawe et al. Thermal stress led to an increased formation of dimers and soluble oligomers traceable by SE-HPLC and AF4. Evolved aggregates smaller than 30 nm after thermal stress were measured by DLS, as well as slightly elevated particle levels in the µm range by light obscuration. Aggregates created by heating were in part covalently linked as seen in SDS-PAGE and made up of conformationally perturbed monomers as observed in CD, ATR-FTIR and extrinsic dye fluorescence. Thus, a clear picture of the aggregation characteristics could be derived. In contrast, freeze–thawing stress primarily induced particles in the µm range. These aggregates were non-covalently linked (SDS-PAGE) and composed of native-like monomers (CD, ATR-FTIR, extrinsic dye fluorescence spectroscopy) [12].

Regarding formulation properties, pH and ionic strength are considered to be the most important parameters for aggregation. But, e.g., for the stability of FK506-binding protein it could be shown that in the pH range of 5-9, the pH dependence of the unfolding free energy from residual charge-charge interactions in the unfolded state was negligible. The negligible contribution was attributed to the lack of sequentially neighboring charged residues around groups that are titrated in this pH range. Salt lowered both conformational and colloidal protein stability at low salt concentrations, but raised stability at high concentrations which could be explained by two opposing types of protein-salt interactions: the Debye-Hückel type, modeling the response of the ions to protein charges, favors the unfolded state while the Kirkwood type, accounting for the disadvantage of the ions moving towards the low-dielectric protein cavity from the bulk solvent, disfavors the unfolded state [22]. The initial decrease in folding stability with increasing salt concentration could be attributed to a stronger effect of the Debye-Hückel type interaction over the Kirkwood type. As the concentration increase further, the relative strengths of the two types of interactions reversed and a net stabilization was obtained. In contrast, for hydrophobic cytokines charge shielding with increasing salt concentrations leads to

_____

substantial aggregate formation [19]. Electrostatic repulsion has been shown to be responsible for the absence of aggregation of RNAse using low pH [23]. The influence of pH is consequently complex. At low pH and high pH charges increase leading to repulsion and reduced conformational stability. Consequently most proteins have maximal thermodynamic stability around the isoelectric point. But, if a protein is already unfolded, the aggregation of the denatured molecules could be enhanced if the electrostatic repulsion is reduced at a pH close to the isoelectric point.

3 MECHANICAL STRESS STABILITY DURING FORMULATION AND SHIPMENT

During processing and handling of proteins as well as during transport of protein solutions, the protein may be exposed to various kinds of mechanical or interfacial stresses. Such mechanical stress conditions are known to potentially induce protein aggregation. Aggregates formed by mechanical and interfacial stresses can appear in a variety of morphologies, requiring the analysis of the full spectrum of potential aggregates [6; 7]. So far there are only few general guidelines regarding extent and accomplishment of mechanical stress to mimic the protein exposure to interfacial and agitational stress during processing, fill and finish and shipment. The American Society for Testing and Materials (ASTM) addresses issues related to process control, design, and performance, as well as quality acceptance / assurance tests for the pharmaceutical manufacturing industry and published guidance regarding standard test methods for, e.g., vibration testing for shipping containers (D 999-01) or standard practice for performance testing of shipping containers and systems (D 4169-08). Beyond, the International Safe Transit Association (ISTA) provides test procedures (ISTA 1A 2001 packaged-products 150 lb (68kg) or less) [24-26].

Typically, horizontal and vertical shakers, stirred reactors, rotation, vortexing and pumps are used as mechanical stress methods during formulation or process development [6]. Mechanical stress studies on various proteins revealed that agitation methods like shaking and stirring induced diverse species, sizes and

quantities of non-covalent aggregates. Shaking involves an enhanced interplay of protein with air- and glass-liquid interfaces, which leads to aggregation and an enhanced transportation of aggregated proteins into the solution [27]. In contrast, stirring may provoke shearing, interfacial effects between the protein and stirrer bar/glass bottom, cavitation, local thermal effects and rapid transportation of either aggregated or adsorbed protein into solution [6]. Shear stress alone is not supposed to cause unfolding [27].

Surfactants such as polysorbates are commonly employed to stabilize the protein against aggregation through agitation, but their mechanism of protection is still under discussion. By adding surfactants an adsorption competition between surfactant and protein to these interfaces is described. Protein is displaced from the interfaces and thereby protected from the surface induced denaturation and aggregation [11]. Another theory describes the interaction between surfactant and exposed hydrophobic areas of the protein. The hydrophobic surfaces of the proteins are supposed to be covered by surfactants and aggregation of protein is therewith inhibited [11]. However, typically these interactions are very weak and the effect may actually favor unfolding due to preferential interaction of structures exposing more hydrophobic sites [28]. Another theory is in the potential ability of surfactants to act as chaperones and facilitate the refolding of partially unfolded proteins [29; 30]. Surfactants are typically applied at concentrations slightly close to or above the critical micelle concentration to ensure surface coverage [31].

Most frequently used non-ionic surfactants in protein pharmaceuticals are polysorbate 20 and 80 [6; 30; 32; 33; 34]. They appear to be less effective in stabilization of protein exposed to stirring stress [6]. Also negative effects of polysorbates on protein stability are mentioned in the literature. After long term storage at elevated temperatures increased protein aggregation was observed [34]. Peroxide contamination of polysorbates might be a reason for oxidation of proteins [35-37].

The surfactant-protein-ratio seemed to be essential for stabilizing effects, as at low polysorbate 80 concentration destabilization can occur [6; 38-40]. Different stabilizing effects were mentioned by Matheus et al. working on the selection of the optimal buffer system at pH 6.0 for a 100 mg/ml IgG formulation (Fig. 1 and 2) [38].

Whereas protein in acetate buffer was characterized by a low level of larger aggregates and precipitates during horizontal shaking, the increase in degradation products in SE-HPLC and SDS-PAGE after exposure to accelerated temperature conditions was rather high. In citrate buffer, the monomer fraction could be kept at the highest level during exposure to accelerated temperatures, particularly at 40 mM citrate. However, the increased susceptibility of this formulation to the formation of large-sized aggregates upon mechanical agitation as well as to deamidation was a major obstacle for citrate buffer. The histidine-buffered protein solutions behaved similarly to the citrate-buffered ones, since protein aggregation during storage at 40°C / 75 % r.h. could be reduced, but in contrast, the unfavourable formation of medium to large size aggregates was extremely pronounced during shaking and even more at accelerated thermal storage conditions.

Thus, the 10 mM phosphate buffer system was chosen as a "golden mean" to maintain protein stability in a liquid 100 mg/ml formulation, keeping both, aggregate formation and protein degradation under stress conditions at a moderate rate. The effect appeared to be less related to ionic strength, but a stabilizing increased positive charge density in the presence of histidine was discussed. Furthermore, the reduced buffer strength was found sufficient to maintain the pH. Slight differences in protein structure affect the aggregate formation behaviour upon mechanical stress as shown for IgG1 antibodies [40]. The amount of insoluble, visible particles of an IgG1 was increased after mechanical stress, but there was no increase in soluble aggregates observed by SE-HPLC or turbidity [40], whereas an increase in soluble aggregates was reported for a different IgG1 [6; 33].

Another impact factor on protein aggregation characteristics in its final container is the fill volume and with that the headspace. It was shown that surfactant free

formulations without headspace in vial - similar to a prefilled syringe - remained essentially free of aggregates upon shaking similar to a formulation with 0.005 % polysorbate 20 with head space [13]. The same formulation in vial with headspace with less polysorbate showed substantial formation of native-like aggregates detectable by SE-HPLC, turbidity, light obscuration and visual inspection. During stirring, less polysorbate 20 was necessary to inhibit the formation of large particles whereas higher amounts of surfactant were required to suppress the creation of smaller particles [13].

_____
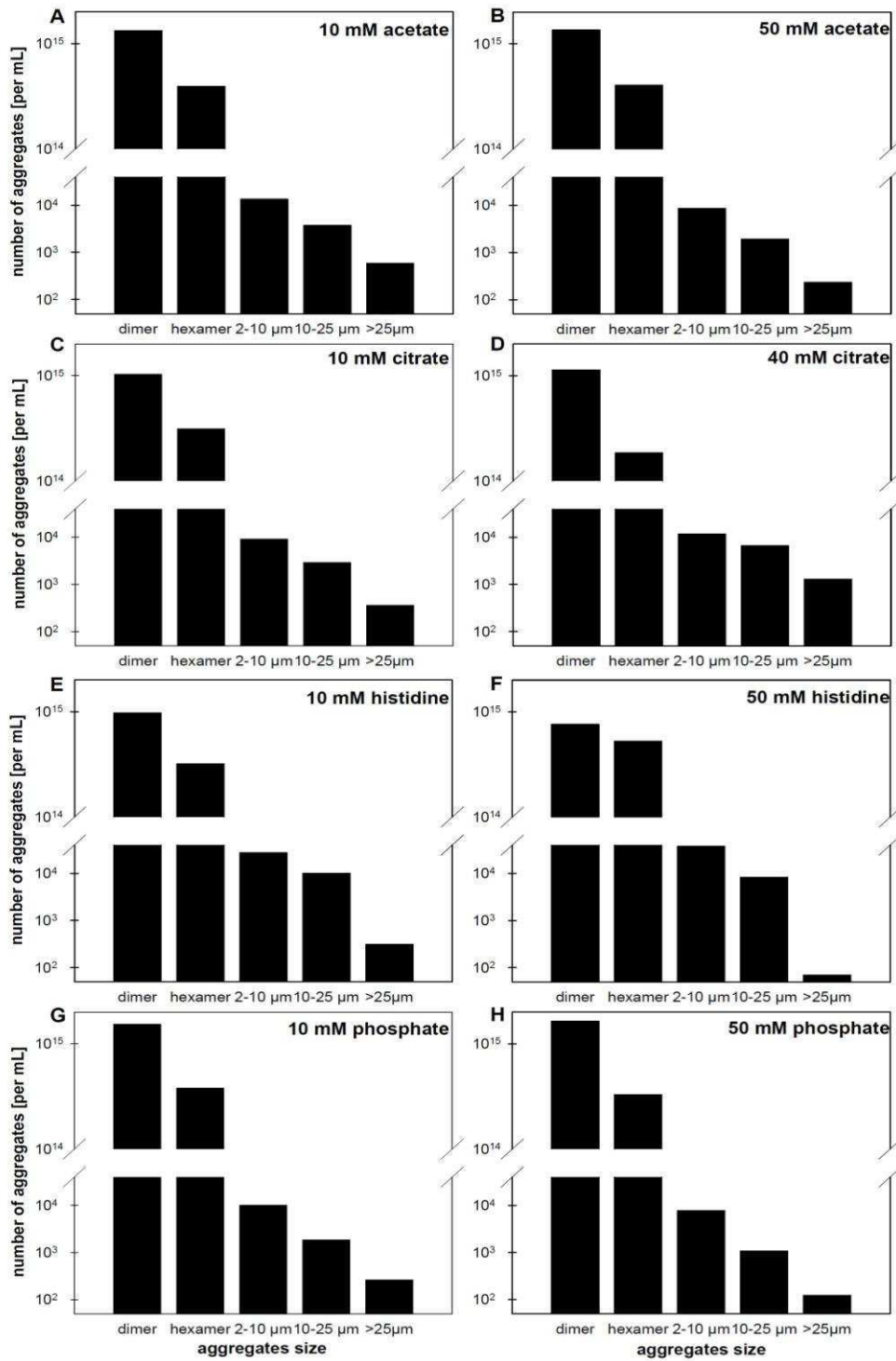
Figure 1: Number of soluble aggregates, as measured by SE-HPLC, and of sub-visible particles (2 – 10, 10 – 25 and ≥ 25 μm), as measured by light obscuration of different 100 mg/ml IgG1 formulations in (A, B) 10/50 mM acetate, (C, D) 10/40 mM citrate, (E, F) 10/50 mM histidine or (G, H) 10/50 mM phosphate buffer, at pH 6.0 after 168 h shaking, courtesy of Susanne Matheus [38].
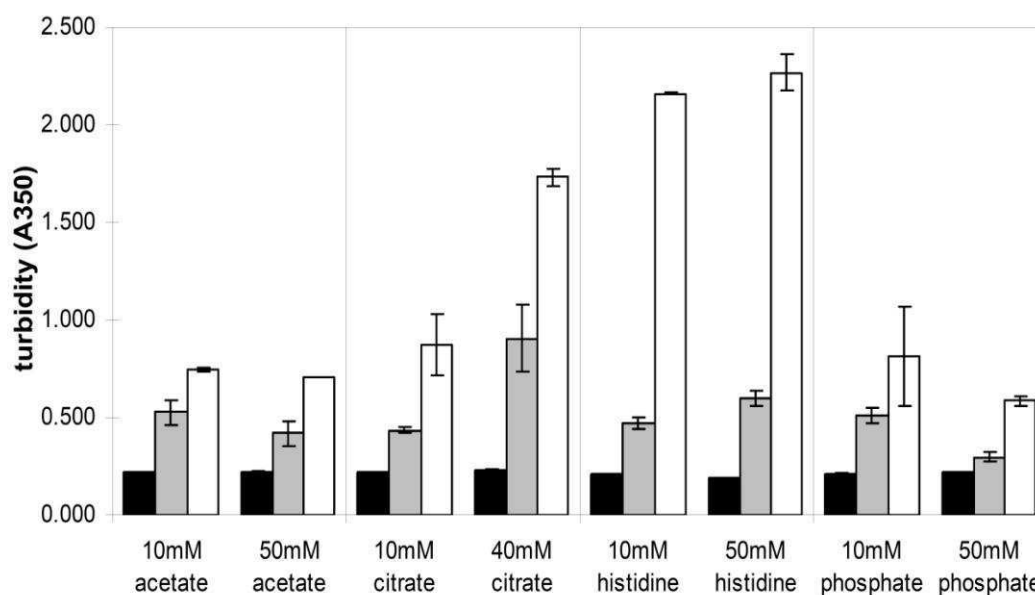
Figure 2: Turbidity of 100 mg/ml IgG1 pH 6.0 in different buffer formulations before (black columns) and after applying shaking stress for 24 h (grey columns) or 168 h (blank columns), courtesy of Susanne Matheus [38].

4   STABILITY DURING FREEZE-THAW

Protein solutions, both as bulk substance or as final product, may undergo freezing or freeze-thawing processes either during manufacturing or later shipment and/or storage either intended (as part of the process) or accidentally. During freezing several changes occur to the protein microenvironment. As ice crystals evolve, the concentration of both protein and excipients increases, which can come along with a drastic decrease in pH at the eutectic point, depending on chosen buffer, bulk volume, and freezing rates etc [41; 42; 43]. If the excipients, which are concentrated to high concentrations while freezing, show a preferential binding to the protein surface, the protein may be destabilized and denatured during freezing.

Moreover, the cooling and warming rates show an impact on the loss of protein activity during freezing and thawing as well. An inverse correlation between cooling rate and loss of protein activity is mentioned in several articles [42; 44; 45]. Various

studies have shown that freeze-thaw stress induces the formation of small quantities of native-like insoluble aggregates [12; 46-49]. Hawe et al. showed that visible aggregates formed upon freeze-thaw in an antibody solution but only about 0.15% of the total protein content became aggregated. CD and extrinsic fluorescent dye analysis of the whole samples and FTIR of the precipitates confirmed that the native structure of the IgG was retained to a high degree [12]. It has been found that excipients have similar positive or negative effects on protein stability both in solution and during freeze-thawing due to the postulated same mechanism of preferential exclusion [50]. Bhatnagar studied the individual contribution of ice formation and freeze concentration on the stability of a sucrose- and citrate-containing LDH solution during freezing and could identify ice formation itself as the critical destabilizing factor [51]. In addition to optimized pH, ionic strength and co-solute supplementation, cryoprotectants can be employed to protect proteins against denaturation upon freeze-thaw such as sugars, polyols, amino acids, polymers and diverse other substances (see also 6 Special Challenges in dried Protein Pharmaceuticals).

5 SPECIAL CHALLENGES IN HIGH CONCENTRATION PROTEIN FORMULATIONS

The use of protein formulations for subcutaneous delivery has attracted substantial attention as it is more convenient and facilitates home administration. As a consequence e.g. for some antibodies, high protein concentration in subcutaneous formulations containing 100 mg/mL and more might be desired, because of limitation of the volume for subcutaneous administration. Challenging aspects of highly concentrated protein formulations are on the one hand higher viscosity, which can make the formulation difficult to manufacture or to administer. On the other hand concentration dependent reversible self-association, also considered as "native-like aggregation" resulting in opalescent solution or precipitation occurs [16; 52; 53]. Reversible self-association can be described as intermolecular interaction of native protein molecules and precipitated protein associates can be re-dissolved and yield native protein molecules again. Solubility of a protein as the thermodynamic activity at the equilibrium of a saturated solution is difficult to measure and indirect analysis methods may be required [54].

Tangential flow filtration (TFF) is the industry standard for buffer exchange and concentrating proteins. The viscosity of high concentration products should be controlled, since viscous protein solutions can significantly increase the process time and might lead to higher back-pressure during TFF. Some of these viscosity-related problems may be manageable by improving equipment, design, operation and formulation parameters [16; 53]. Depending on the protein's propensity to aggregate or precipitate, this could lead to decreased flux and eventually membrane clogging [54; 55-57]. Rosenberg et al. presented an optimized method for ultrafiltration, with adapted transmembrane pressure and cross-flow conditions, resulting in minimized aggregate formation for three monoclonal antibodies [55]. The formation of aggregates was monitored by turbidity, SE-HPLC, light obscuration, DLS and a microscopic method and the aggregate structure analyzed by FT-IR. The analytics revealed that mostly large insoluble and structurally perturbed aggregates form during the ultrafiltration/concentration process. The optimized method did not significantly reduce the high-molecular-weight species, as detected by SE-HPLC, but substantially reduced large aggregate formation as studied by turbidity and DLS.

Measuring the second virial coefficient (B_{22}) could be relevant for the prediction of protein aggregation as well as viscosity. Up to now there is only rare information on the correlation between B_{22} and protein aggregation [58-60]. A study on lysozyme could show a correlation of B_{22} and physical protein stability as analyzed by turbidity [60]. Comparing B_{22} of an IgG1 with stability over 12 weeks at 40 °C demonstrated that histidine 5mM was the most promising buffer candidate according to B_{22} and showed a slightly better physical stability as assessed by turbidity and SE-HPLC compared to the other tested formulations. The effect of buffer species on the stability of interferon-tau (IFN-tau) was compared to B_{22} determined by self-interaction chromatography [58]. At pH 7 and 20 mM buffer systems, IFN-tau formulated at 1 mg/ml and thermally stressed formed aggregates in the 20 to 40 nm range in phosphate and Tris buffer, but not in histidine buffer. In SE-HPLC the aggregate formation rate was the highest in phosphate buffer, whereas both Tris and histidine resulted in less aggregate formation. Only slight differences in B_{22} were measured suggesting that modulation of protein-protein interactions is probably a

_____

minor component of the stabilization mechanism for IFN-tau, at least with respect to thermally-induced aggregation [58].

Protein self-association is an important factor to consider in high concentration protein formulations [54]. Most aggregation reactions are reported to be of second or higher order and would be enormously accelerated in high concentration protein formulations [1; 2; 6; 8; 61]. On the basis of the mechanism of excluded volume an increased volume fraction is occupied by the protein molecules themselves at higher protein concentrations. The related decrease in the effective volume available and in turn the higher apparent protein concentration pushes the reaction equilibrium of protein self-association towards the associated state [54]. In contrast, the reaction rate of macromolecular association can be either limited by the conversion of the activated complex to a fully formed dimer or by the diffusion controlled formation of the activated complex. Due to the larger and/or more asymmetric form of the denatured state, the equilibrium of the protein unfolding reaction is driven towards the compact native conformation by the volume exclusion as a consequence of increasing protein concentrations [62]. Consequently, crowding would increase the reaction rate of self-association, whereas, if the system is diffusion limited, a diminished reaction rate results, owing to the fact that crowding considerably lowers the diffusional mobility of macromolecules (Fig.2 and 3) [62; 63]. Therefore, an increase in protein concentration could actually stabilize the protein against the formation of insoluble aggregates [64; 65] or with respect to agitation induced aggregation [34; 66].

Thus, the relationship between protein concentration and aggregation tendency has to be evaluated on a case to case basis and formulation development at the concentration of interest is essential.
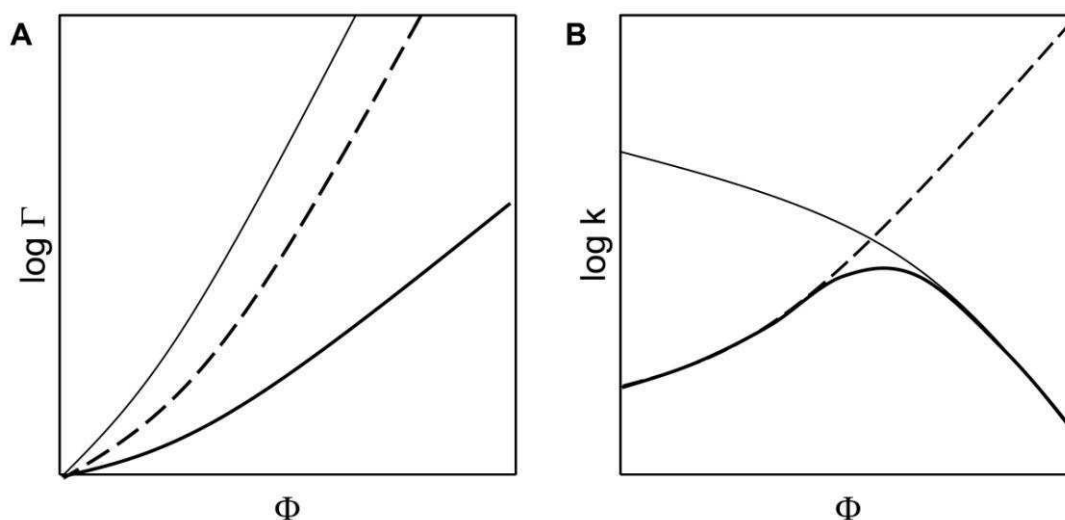
Figure 3: Effect of the fractional volume occupancy Φ on the non-ideality factor Γ (A) for various degrees of association (n=2 solid line; n=3 dashed line; n=4 slight line) and on the reaction rate constant k (solid line) (B), k being transition state limited at low volume occupancy (dashed line) and diffusion limited at high volume occupancy (slight line), courtesy of Susanne Matheus [38].

Another challenge in formulation development of high concentration protein pharmaceuticals is that dilution for analysis may influence the concentration dependent aggregation and might induce artefacts [67]. Therefore, protein pharmaceuticals should be analyzed at their original concentration wherever possible and one should look for alternative analytical tools which enable to measure at high concentration [16; 54; 68]. Matheus et al. studied the influence of protein concentration (2; 10; 50; and 100 mg/mL) and formulation buffer (PBS pH 7.2, citrate pH 5.5) on antibody aggregation upon shaking [69]. Whereas an almost unchanged monomer fraction of more than 99% was observed in SE-HPLC, opalescence was altered depending on protein concentration and formulation buffer. Subvisible protein aggregates quantified by light obscuration analysis did not depend on protein concentration at t=0, whereas after shaking stress the number of particles >10 μm and >25 μm were influenced by protein concentration and formulation buffer. For citrate buffer formulations, the highest number of subvisible particles was measured in the highest concentration (100 mg), whereas for PBS buffer formulations the number of subvisible particles >25 μm decreased with increasing protein

concentration possibly attributed to an increase in large precipitates at the expense of smaller sized subvisible and light scattering particles. An inverse concentration and aggregation relationship seen at lower concentrations might be explained by a reduced ratio of the air/water interface to protein with increasing concentration [34]. The formation of native protein aggregates could also be important with respect to non-native protein aggregation. The aggregates may serve as nuclei, undergo conformational changes, and subsequently grow rapidly to form insoluble precipitates [59; 61; 70]. Irreversible non-covalent aggregates can be detected, qualified and quantified by SE-HPLC. But the native-like aggregates are often overlooked and poorly analyzed [16].

Indeed, the analytical tools for reversible aggregates are not satisfying. Static and dynamic light scattering and analytical ultracentrifugation appear to be more beneficial to monitor the phenomenon of self-association, as the concentration and the primary microenvironment can be maintained during measurement. A new method to rapidly detect protein self-association simultaneously with the determination of the second viral coefficient, a measure of solution non-ideality, using SE-HPLC was described by Bajaj et al. [72] for ß-lactoglobulin. The simultaneous measurement of concentration and scattered light intensity by utilizing a novel flow cell could be a useful tool for high-throughput characterization of protein association during early stages of protein formulation.

6 SPECIAL CHALLENGES IN DRIED PROTEIN PHARMACEUTICALS

Freeze drying is considered the method of choice to stabilize proteins that show substantial stability problems in liquid. About 50% of currently marketed protein drugs are provided in lyophilized form [72]. But lyophilization may induce protein damage due to freezing and drying stress. The effect of freezing and the use of cryoprotectants have been described above. In addition, as water is removed, alternative partners for hydrogen bond formation are considered to be necessary, which is termed water replacement [73]. This is provided by lyoprotectants, mostly

sugars, polyols and amino acids. For lyoprotection, the sugar stabilizers need to be in a proper ratio to the protein to satisfy water binding sites which in practice means that a mass ratio of about 1:1 is usually needed [72; 74; 75].

Protein aggregation can not be assessed directly in the lyophilized formulation, but can be measured after reconstitution with the methods used for analysis of protein solutions. Analytics performed on the lyophilized materials typically focus on material properties such as glass-transition temperature, modification or residual moisture. By Fourier transform infrared spectroscopy (FTIR) the interactions of dried proteins and carbohydrates were observed. It could be shown that hydrogen binding occurs between proteins and carbohydrates and this water replacement is necessary to keep the proteins in the native state during drying [76]. Additionally, these lyoprotectants stabilize the protein by immobilizing them in a glassy matrix which strongly reduces their mobility. Glass formation alone is insufficient as seen e.g. for protein samples freeze dried with dextran, which are completely amorphous and form glasses with high glass transition temperature but show loss of native protein structure [77]. Furthermore, there is evidence by FTIR measurements that only proteins that kept their native state in the dried form, were able to regain most of their biological activity after reconstitution. A loss of native structure during drying seems to be in several cases irreversible and leads therefore to denaturation and aggregation after reconstitution [78; 79] or to poor storage stability.

Protein aggregation involves collisions between protein molecules and is considered to be closely related to molecular mobility [80]. Analysis of the difference between storage temperature and glass transition temperature, as a rough measure for the global mobility, indicated a good correlation between mobility and monomer loss analyzed by SE-HPLC [81; 82]. The solid state chemistry and protein stability was thoroughly elaborated by Pikal in a set of papers studying the structural relaxation of lyophilisates and both the chemical and physical stability of human growth hormone (hGH) [83-86]. The unfolding of hGH in the dried state could be well modeled by a three state kinetic model, which is a two state unfolding model followed by aggregation. Using data for denaturation temperature, heat of denaturation, and heat

17

capacity of denaturation, free energy versus temperature curves were calculated. Even formulations with saccharides added are thermodynamically unstable near ambient temperature but significant denaturation in the solid state is prevented by low mobility. Directly comparing aggregation (SE-HPLC and DLS) of a hydrophobic cytokine in liquid solution in a prefilled syringe vs. lyophilized in a vial in a mannitol-sucrose combination during static storage indicated that for this aggregation prone protein the overall aggregation profile was similar in both dosage forms [19].

Another general point to consider is that the protein also affects its environment e.g. by concentration dependent change in excipients crystallinity and polymorphism [87]. A detailed study on the effect of lyophilisate collapse on antibody stability indicated that protein stability upon storage is still warranted, if not even improved compared to non-collapsed samples. SE-HPLC and AF4 indicated no difference immediately after freeze-drying, but more subvisible and visible particles had formed in partially collapsed lyophilisates. A trend to enhanced stability in the collapsed systems could be shown with a less pronounced storage related increase in soluble aggregates as well as in particle numbers, turbidity values and DLS Z-average diameter and polydispersity index [88].

7 SUMMARY

Typically, available protein and time are limited during formulation development. But in order to thoroughly characterize and understand protein aggregation as a main route of protein instability, different stress tests utilizing a combination of analytical methods are mandatory. Numerous formulation factors like the selection of pH or the addition of surfactants have to be balanced and an optimum has to be found. An additional challenge derives from the fact that aggregation typically does not follow Arrhenius behaviour and extrapolation of static storage stability data to predict aggregation is associated with uncertainties. This applies even more so to mechanical stress study data. Various types of aggregates may be induced by different stress conditions and setups. Frequently, SE-HPLC as the analytical workhorse in small aggregate analysis does not allow adequate conclusions when

used as single method. Especially freeze-thaw and mechanical stress frequently induce no changes in SE-HPLC monomer content but larger aggregates forms, which can only be detected applying another set of analytical methods. Supplemented by characterization of the aggregate structure, such a comprehensive picture allows a better understanding of the underlying mechanism of aggregate formation and a rational formulation approach.

8 ACKNOWLEDGEMENTS

_____

9 REFERENCES

[1]   Mahler, H.C., Friess, W., Grauschopf, U., Kiese, S. (2009). Protein aggregation: Pathways, induction factors and analysis. J. Pharm. Sci. 98(9), 2909-2934.

[2]   Cleland, J.L., Powell, M.F., Shire, S.J. (1993). The development of stable protein formulations: a close look at protein aggregation, deamidation, and oxidation. Crit. Rev. Ther. Drug Carrier Syst., 10 (4), 307-377.

[3]   Capelle, M. A. H., Gurny, R., Arvinte, T. (2007). High throughput screening of protein formulation stability: Practical considerations. European Journal of Pharmaceutics and Biopharmaceutics 65(2), 131-148.

[4]   Hui, Z., Graf, O., Milovic, N., Luan, X., Bluemel, M., Smolny, M., Forrer, K (2008) Formulation Development of Antibodies Using Robotic System and High-Throughput Laboratory (HTL). WO 2008 /157278 A1.

[5]   Grant, Y., Matejtschuk, P., Dalby, P.A. (2009). Rapid optimization of protein freeze-drying formulations using ultra scale-down and factorial design of experiment in microplates. Biotechnology and Bioengineering. 104(5), 957-964.

[6]   Kiese, S., Papppenberger, A., Friess, W., Mahler, H.C. (2008). Shaken, not stirred: mechanical stress testing of an IgG1 antibody. J. Pharm Sci., 97 (10), 4347-4366.

[7]   Colombie, S., Gaunand, A., Lindet, B. (2001). Lysozyme inactivation under mechanical stirring: effect of physical and molecular interfaces. Enzyme Microb. Technol., 28 (9-10), 820-826.

[8]   Cromwell, M.E., Hilario, E., Jacobson, F. (2006). Protein aggregation and bioprocessing. AAPS J., 8 (3), E572-E579.

[9]   Timasheff, S. N. (1993). The control of protein stability and association by weak interactions with water: How do solvents affect these processes. Annual Review of Biophysics and Biomolecular Structure 22 67-97.

[10] Arakawa, T., Prestrelski, S.J., Kenney, W.C., Carpenter, J.F. (2001). Factors affecting short-term and long-term stabilities of proteins. Adv. Drug Deliv. Rev., 46 (1-3), 307-326.

[11] Mahler, H.C., Muller, R., Friess, W., DeLille, A., Matheus, S. (2005). Induction and analysis of aggregates in a liquid IgG1-antibody formulation. Eur. J. Pharm Biopharm, 59 (3), 407-417.

[12] Hawe, A., Kasper, J.C., Friess, W., Jiskoot, W. (2009). Structural properties of monoclonal antibody aggregates induced by freeze-thawing and thermal stress. European Journal of Pharmaceutical Sciences, 38(2), 79-87.

[13] Friess, W, Kiese, S., Mahler, H.C., Pappenberger, A. (2008) Method for stabilizing a protein. (Germany). U.S. Pat. Appl. 2008275220.

[14] Moore, J. M. R., Patapoff, T., W., Cromwell, M. E. M. (1999). Kinetics and Thermodynamics of Dimer Formation and Dissociation for a Recombinant Humanized Monoclonal Antibody to Vascular Endothelial Growth Factor. Biochemistry 38(42), 13960-13967.

[15] Liu, J., Andya, J., Shire, S. (2006). A critical review of analytical ultracentrifugation and field flow fractionation methods for measuring protein aggregation. AAPS Journal 08 (03): E580-E589

[16] Shire, S. J., Shahrokh, Z., Liu, J. (2004). Challenges in the development of high protein concentration formulations. Journal of Pharmaceutical Sciences 93(6), 1390-1402.

[17] Wang, W., Singh, S., Zeng, D.L., King, K., Nema, S. (2006). Antibody structure, instability, and formulation. Journal of Pharmaceutical Sciences 96(1), 1-26.

[18] Gabrielson, J. P., Arthur, K. K., Kendrick, B. S., Randolph, T.W., Stoner, M. R. (2009). Common excipients impair detection of protein aggregates during sedimentation velocity analytical ultracentrifugation. Journal of Pharmaceutical Sciences 98(1), 50-62.

_____

[19] Hawe, A., Friess, W. (2008). Development of HSA-free formulations for a hydrophobic cytokine with improved stability. European Journal of Pharmaceutics and Biopharmaceutics, 68(2), 169-182.

[20] Sek, D., Warne, N.W., Ho, K., Luisi, D.L., Kantor, A. (2008). Use of sucrose to suppress mannitol-induced protein aggregation. PCT/US2008/052115.

[21] Printz, M., Friess, W. (2009). Simultaneous detection of changes in protein tertiary structure and aggregation by SEC with post column addition of Bis-ANS, Poster AAPS National Biotechnology Conference Seattle, USA.

[22] Spencer, D.S., Ke, X., Logan, T.M., Zhou, H.X. (2005). Effects of pH, salt, and macromolecular crowding on the stability of FK506-binding protein: An integrated experimental and theoretical study. Journal of Molecular Biology, 351 (1), 219-232.

[23] Tsai, A.M., van Zanten, J.A., Betenbaugh, M.J. (2000). II Elekcrostatic effect in the aggregation of heat denatured RNase A and implications for protein additive design. Biotechnology and Bioengineering, 59(3), 281-285.

[24] American Society for Testing and Materials (ASTM) Designation: D 999 – 01. (2001). Standard Test Methods for Vibration Testing of Shipping Containers.

[25] American Society for Testing and Materials (ASTM) Designation: D 4169 – 08. (2008). Standard Practice for Performance Testing of Shipping Containers and Systems.

[26] International Safe Transit Association (ISTA); ISTA 1 Series: Non-Simulation Integrity Performance Test; Procedure 1A: Packaged-Products weighing 150lb (68kg) or Less, 2001.

[27] Maa, Y.F., Hsu, C.C. (1997). Protein denaturation by combined effect of shear and air-liquid interface. Biotechnol. Bioeng., 54 (6), 503-512.

[28] Garidel, P., Hoffmann, C., Blume, A. (2009). A thermodynamic analysis of the binding interaction between polysorbate 20 and 80 with human serum albumins

_____

and immunoglobulins: A contribution to understand colloidal protein stabilisation. Biophysical Chemistry, 143(1-2), 70-78.

[29] Bam, N.B., Cleland, J.L., Yang, J., Manning, M.C., Carpenter, J.F., Kelley, R.F., Randolph, T.W. (1998). Tween protects recombinant human growth hormone against agitation-induced damage via hydrophobic interactions. J. Pharm Sci. 87 (12), 1554-1559.

[30] Bam, N.B., Randolph, T.W., Cleland, J.L. (1995). Stability of protein formulations: investigation of surfactant effects by a novel EPR spectroscopic technique. Pharm Res., 12 (1), 2-11.

[31] Katakam, M., Bell, L.N. (1995). Effect of Surfactants on the Physical Stability of Recombinant Human Growth Hormone. Journal of Pharmaceutical Sciences 84(6), 713-16.

[32] Charman, S. A., Mason, K. L., Charman, W. N. (1993). Techniques for assessing the effects of pharmaceutical excipients on the aggregation of porcine growth hormone.   Pharmaceutical Research 10(7), 954-62.

[33] Kreilgaard, L., Frokjaer, S., Flink, J. M., Randolph, T. W., Carpenter, J. F. (1998). Effects of additives on the stability of recombinant human factor XIII during freeze-drying and storage in the dried solid. Archives of Biochemistry and Biophysics 360(1), 121-134.

[34] Treuheit, M. J., Kosky, A. A., Brems, D. N. (2002). Inverse relationship of protein concentration and aggregation. Pharmaceutical Research 19(4), 511-516.

[35] Ha, E., Wang, W., Wang, Y. J. (2002). Peroxide formation in polysorbate 80 and protein stability. Journal of Pharmaceutical Sciences 91(10), 2252-2264.

[36] Donbrow, M., Azaz, E., Pillersdorf, A. (1978). Autoxidation of polysorbates. Journal of Pharmaceutical Sciences 67(12), 1676-81.

[37] Kerwin, B. A. (2008). Polysorbates 20 and 80 used in the formulation of protein biotherapeutics: structure and degradation pathways. Journal of Pharmaceutical Sciences 97(8),2924-2935.

[38] Matheus, S. (2006). Preparation of high concentration cetuximab formulations using ultrafiltration and precipitation techniques. PhD Thesis, University of Munich, Germany, 140-179.

[39] Ziegler, K., Schwartz, D., Frieß, W. (2008). Agitation-Induced Aggregation Behavior of an IgG Antibody: Effect of Protein and Surfactant Concentration. Abstract 6th World Meeting on Pharmaceutics, Biopharmaceutics and Pharmaceutical Technology Barcelona, Spain.

[40] Mahler, H-C., Senner, F., Maeder, K., Mueller, R. (2009). Surface activity of a monoclonal antibody. Journal of Pharmaceutical Sciences 98(12), 4525-4533.

[41] Chilson, O.P., Costello, L.A., Kaplan, N.O. (1965). Effects of freezing on enzymes. Fed Proc., 24, 55-65.

[42] van den Berg, L., Rose, D. (1959). Effect of freezing on the pH and composition of sodium and potassium phosphate solutions; the reciprocal system KH_2PO_4-Na_2-HPO_4-H_2O. Arch. Biochem. Biophys., 81 (2), 319-329.

[43] Gómez, G., Pikal, M.J., Rodríguez-Hornedo, N. (2001). Effect if initial buffer composition on pH changes during far-from equilibrium freezing of sodium phosphate buffer solutions. Pharm. Res. 18, 90–97.

[44] Whittam, J.H., Rosano, H.L. (1973). Effects of the freeze-thaw process on alpha amylase. Cryobiology, 10 (3), 240-243.

[45] Fishbein, W.N., Winkert, J.W. (1977). Parameters of biological freezing damage in simple solutions: catalase. I. The characteristic pattern of intracellular freezing damage exhibited in a membraneless system. Cryobiology, 14 (4), 389-398.

[46] Printz, M., Friess, W. (2009). SEC with UV and fluorescence detection by BisANS and the influence of PS 20. Poster Protein Stability Conference, Breckenridge, USA.

[47] Kiese S. Protein aggregation – Induction, analytical methods and inhibition in biopharmaceutical formulations. [PhD thesis]. University of Munich, Germany; 2009. 227–250.

_____

[48] Chang, B.S., Kendrick, B.S., Carpenter, J.F. (1996). Surface-induced denaturation of proteins during freezing and its inhibition by surfactants. J. Pharm. Sci. 85, 1325–1361.

[49] Natalello, A., Santarella, R., Doglia, S.M., de Marco, A. (2008). Physical and chemical perturbations induce the formation of protein aggregates with different structural features. Prot. Exp. Purif. 58, 356–361.

[50] Carpenter, J.F., Crowe, J.H. (1988). The mechanism of cryoprotection of proteins by solutes. Cryobiology, 25 (3), 244-255.

[51] Bhatnagar, B.S., Pikal, M.J., Bogner, R.H. (2008). Study of the individual contributions of ice formation and freeze concentration on isothermal stability of lactate dehydrogenase during freezing. J. Pharm Sci. 97, 798-814.

[52] Minton, A.P. (2005). Influence of macromolecular crowding upon the stability and state of association of proteins: predictions and observations. J. Pharm Sci., 94 (8), 1668-1675.

[53] Wilf, J., Minton, A.P. (1981). Evidence for protein self-association induced by excluded volume. Myoglobin in the presence of globular proteins. Biochim. Biophys. Acta, 670 (3), 316-322.

[54] Friess, W., Mahler, H.-C., Jörg, S. (2009). Highly concentrated protein formulations. In: Mahler H.C., Luessen H, Borchard G. (Eds.), Protein Pharmaceuticals - Formulation, Analytics and Delivery. Editio Cantor Verlag, Aulendorf, Germany, 192-220.

[55] Rosenberg, E., Hepbildikler, S., Kuhne, W., Winter, G. (2009). Ultrafiltration Concentration of Monoclonal Antibody Solutions: Development of an Optimized Method minimizing Aggregation, Journal of Membrane Science, accepted for publication.

[56] Thomas, C.R., Nienow, A.W., Dunnill, P. (1979). Action of shear on enzymes: studies with alcohol dehydrogenase. Biotechnology & Bioengineering 21(12), 2263-2278.

[57] Watterson, J.G., Schaub, M.C., Waser, G. (1974). Shear-induced protein-protein interaction at the air-water interface. Biochimica et Biophysica Acta 356(2), 133-143

[58] Katayama, D. S., Nayar, R., Chou, D.K., Valente, J. J., Cooper, J., Henry, C.S., Vander Velde, D.G., Villarete, L., Liu, C. P., Manning, M. C. (2006). Effect of buffer species on the thermally induced aggregation of interferon-tau. Journal of Pharmaceutical Sciences 95(6), 1212-1226.

[59] Chi, E. Y., Krishnan, S., Randolph, T. W., Carpenter, J. F. (2003). Physical Stability of Proteins in Aqueous Solution: Mechanism and Driving Forces in Nonnative Protein Aggregation. Pharmaceutical Research 20(9), 1325-1336.

[60] Le Brun, V., Friess, W., Schultz-Fademrecht, T., Muehlau, S., Garidel, P. (2009). Lysozyme-lysozyme self-interactions as assessed by the osmotic second virial coefficient: Impact for physical protein stabilization. Biotechnology Journal 4(9), 1305-1319.

[61] Wang, W. (2005). Protein aggregation and its inhibition in biopharmaceutics. Int. J. Pharm. 289, 1-30.

[62] Hall, D., Minton, A.P. (2003). Macromolecular crowding: qualitative and semiquantitative successes, quantitative challenges. Biochim. Biophys. Acta. 1649, 127-139.

[63] Zimmerman, S.B., Minton, A.P. (1993). Macromolecular crowding: biochemical, biophysical, and physiological consequences. Annu. Rev. Biophys. Biomol. Struct., 22, 27-65.

[64] Dathe, M., Gast, K., Zirwer, D., Welfle, H., Mehlis, B. (1990). Insulin aggregation in solution. Int. J. Peptide Protein Res. 36, 344-349.

[65] Kendrick, B.S., Li, T., Chang, B.S. (2002). Physical stabilization of proteins in aqueous solution. In: Carpenter J.F., Manning M.C. (eds.). Rational design of stable protein formulations: Theory and practice, Kluwer Academic/Plenum Publishers, New York, 2002, 61-84.

[66] Kanai, S., Liu, J., Patapoff, T.W., Shire, S.J. (2008). Reversible self-association of a concentrated monoclonal antibody solution mediated by Fab-Fab interaction that impacts solution viscosity. J. Pharm Sci., 97 (10), 4219-4227.

[67] Shire SJ, Liu J, Friess W, Jörg S, Mahler H-C. High-Concentration Antibody Formulations. In: Jameel F, Hershenson S, editors. Formulation and process development strategies for manufacturing biopharmaceuticals. New York, USA: John Wiley & Sons; 2010. 349-381.

[68] Harris, R. J., Shire, S. J., Winter, C. (2004). Commercial manufacturing scale formulation and analytical characterization of therapeutic recombinant antibodies. Drug Development Research 61(3), 137-154.

[69] Matheus, S., Friess, W., Mahler, H.C. (2005). Liquid high concentration IgG1-antibody formulations. Poster AAPS National Biotechnology Conference, San Francisco, USA.

[70] Brange, J. Physical stability of proteins. In Frokjaer, S., Hovgaard L. (Eds.) Pharmaceutical formulation development of peptides and proteins, Taylor and Francis, London (2000), 89-112.

[71] Bajaj, H., Sharma, V.K., Kalonia, D.S. (2007). A high-throughput method for detection of protein self-association and second virial coefficient using size-exclusion chromatography through simultaneous measurement of concentration and scattered light intensity. Pharm Res., 24 (11), 2071-2083.

[72] Costantino, H.R. (2004). Excipients for use in lyophilized pharmaceutical peptide, protein, and other bioproducts.IN Pikal M.J. Costantino H.R. (Eds.) Lyophilization of Biopharmaceuticals; AAPS Press, Arlington VA, USA, 139-228.

[73] Crowe, J.H., Crowe, L.M., Carpenter, J.F. (1993). Preserving dry biomaterials: the water replacement hypothesis. Part 1. Biopharmacology, 6(3), 28-33.

[74] Andya J.D., Hsu C.C., Shire S.J. (2003). Mechanisms of aggregate formation and carbohydrate excipients stabilization of lyophlized monoclonal antibody formulations. APPS Pharm Sci. 5(2) Article 10, 1- 11.

_____

[75] Cleland, J., Lam, X., Kendrick, B., Yang, J., Yang T.-H., Overcashier, D., Brooks, D., Hsu, C., Carpenter, J.F. (2001). A specific molar ratio of stabilizer to protein is required for storage stability of a lyophilized monoclonal antibody. J. Pharm. Sci. 90 310-321

[76] Carpenter, J.F., Crowe, J.H. (1989). An infrared spectroscopic study of the interactions of carbohydrates with dried proteins. Biochemistry, 28 (9), 3916-3922.

[77] Pikal, M.J., Dellerman, K.M., Roy, M.L., Riggin, R.M. (1991). The effects of formulation variables on the stability of freeze-dried human growth hormone. Pharm Res., 8 (4), 427-436.

[78] Prestrelski, S.J., Tedeschi, N., Arakawa, T. Carpenter, J.F. (1993). Dehydration-induced conformational transitions in proteins and their inhibition by stabilizers. Biophys. J., 65 (2), 661-671.

[79] Prestrelski, S., Pikal, M. J., Katherine A.; Arakawa, T. (1995). Optimization of lyophilization conditions for recombinant human interleukin-2 by dried-state conformational analysis using Fourier-transform infrared spectroscopy. Pharmaceutical Research 12(9), 1250-9.

[80] Yoshioka, S. Molecular mobility of freeze-dried formulations as determined by NMR relasation and its effect on storage stability. Freeze-Drying / Lyophilzation of pharmaceutical and biological products; 2nd Ed., Rey,L.; May,J.C.; Marcel Dekker Inc, New York, USA, 2007, 187-212.

[81] Roy, M. L., Pikal, M. J., Rickard, E. C., Maloney, A. M. (1992). The effects of formulation and moisture on the stability of a freeze-dried monoclonal antibody-vinca conjugate: a test of the WLF glass transition theory. Developments in Biological Standardization 74, 323-40.

[82] Yoshioka, S., Aso, Y., Nakai, Y., Kojima, S. (1998). Effect of High Molecular Mobility of Poly(vinyl alcohol) on Protein Stability of Lyophilized gamma-Globulin Formulations.   Journal of Pharmaceutical Sciences 87(2), 147-151.

_____

[83] Pikal, M. J., Rigsbee, D. R., Roy, M. L. (2007). Solid state chemistry of proteins: I.Glass transition behavior in freeze dried disaccharide formulations of human growth hormone (hGH). Journal of Pharmaceutical Sciences 96(10), 2765-2776.

[84] Pikal, M. J., Rigsbee, D., Roy, M.L., Galreath, D., Kovach, K. J., Wang, B., Carpenter, J. F., Cicerone, M. T. (2008). Solid state chemistry of proteins: II. The correlation of storage stability of freeze-dried human growth hormone (hGH) with structure and dynamics in the glassy solid. Journal of Pharmaceutical Sciences 97(12), 5106-5121.

[85] Pikal, M. J., Rigsbee, D., Roy, M.L. (2008). Solid state stability of proteins III: Calorimetric (DSC) and spectroscopic (FTIR) characterization of thermal denaturation in freeze dried human growth hormone (hGH). Journal of Pharmaceutical Sciences 97(12), 5122-5131.

[86] Pikal, M.J., Rigsbee, D., Akers, M. J. (2009). Solid state chemistry of proteins IV. What is the meaning of thermal denaturation in freeze dried proteins? Journal of Pharmaceutical Sciences 98(4), 1387-1399.

[87] Dixon, D., Tchessalov, S., Barry, A., Warne, N. (2009). The impact of protein concentration on mannitol and sodium chloride crystallinity and polymorphism upon lyophilization. Journal of Pharmaceutical Sciences 98(9), 3419-3429.

[88] Schersch K. (2009). Effect of collapse on pharmaceutical protein lyophilisates. PhD Thesis, University of Munich, Germany, 260-268.

_____

CHAPTER 2

Individual Second Virial Coefficient (B$_{22}$) Determination of Monomer and Oligomers in Heat Stressed Protein Samples using Size Exclusion Chromatography and Light Scattering

ABSTRACT

The objective of this work was to determine the second virial coefficient (B$_{22}$) of monomer and oligomer protein species in heat stressed samples individually and simultaneously. An HP-SEC equipped with a flow-mode detector system enabling to measure light scattering and UV transmission in the same cell was used to separate and analyze the different species. The folded/unfolded nature of the protein was analyzed by extrinsic fluorescence spectroscopy using BisANS. The B$_{22}$ of each species was calculated from the concentration and light scattering data as described in an earlier publication. Upon heat exposure, monomer and formed oligomers yielded more negative B$_{22}$ values reflecting stronger attractive forces as compared to those for the initial monomer. The increased attractive forces are attributed to partial unfolding of the protein species, and were reflected in the extent of aggregation. Based on the B$_{22}$ values the monomer appeared to be the most reactive species after

_____

heat stress. In summary, the presented B_{22} determination technique can be used to analyze and follow the nature of intermolecular interactions for all present protein species (monomer and oligomers) and provide further understanding of the mechanism of protein aggregation and growth of aggregates.

1 INTRODUCTION

In the last two decades, recombinant protein drug products have become an important area of therapeutics in the pharmaceutical industry [1]. A major challenge in bringing these drugs to market is the development and manufacture of stable formulations, specifically with respect to protein aggregation as aggregates are related to activity loss, side effects, and immunogenicity [2]. Various types of protein aggregates can develop, and a number of analytical methods are required to analyze the entire size range and types - native or unfolded, covalent or non-covalent, reversible or irreversible - of protein aggregates and the reader is referred to recently published reviews [3; 4]. High performance size exclusion chromatography (HP-SEC) represents a typical workhorse for aggregate analysis. It allows robust quantification of small aggregates and at the same time providing information on fragmentation. But it still has to be handled with care [5]. The method can be used by utilizing various detectors including UV absorption, fluorescence or light scattering based units.

Protein aggregation is fundamentally driven by protein-protein interactions. Thus, the understanding of protein-protein interactions can provide a means to minimize the physical instability. Protein interactions depend on the net charge of the macromolecule, the extent of hydration of the protein and the resulting interactions such as hydrophobic and electrostatic interactions, hydrogen bonding and van der Waal´s forces [6]. The second virial coefficient B$_{22}$ (also known as A$_2$) is a widely used parameter to study net protein-protein interactions and to describe thermodynamic non-ideality of protein solutions. Derived from the virial expansion of the osmotic pressure term, B$_{22}$ represents the non-ideality in dilute colloid solution and is given by [7]

$$\frac{\prod}{RTc} = \frac{1}{M} + B_{22}c + ...$$ (1)

where $\prod$ represents the osmotic pressure, c the protein concentration, R the gas constant, T the temperature and M the molecular weight. B$_{22}$ reflects the interactions and the intermolecular forces of two solute molecules, e.g., protein molecules in

_____

diluted solutions. The B_{22} value consists of the excluded volume contribution, which is always positive, and the energetic interactions (Van der Waal´s, electrostatic, hydrophobic, etc.), which might be repulsive or attractive [8]. Positive B_{22} values indicate repulsive protein-protein interactions. In contrast, net attractive protein-protein interactions are given by negative B_{22} values, which could reflect a more aggregation prone system. B_{22} could therefore be used as a surrogate parameter for protein stability and might be seen as relevant for the prediction of protein aggregation [9; 10]. Up to now there is only limited information available on the correlation between B_{22} and protein aggregation [11; 12; 13]. A correlation of B_{22} and physical protein stability as analyzed by turbidity was shown by a study on lysozyme [13; 14; 15]. Furthermore, B_{22} analysis showed the same tendency to identify the most stable G-CSF formulation based on turbidity and HP-SEC analysis [16]. Changes in B_{22} values induced by different pH, ionic strength and/or addition of co-solutes (salts, sugars, polymers, etc.) can be explained by changes in the protein net charge or shielding effects [8; 17], and thereby support formulation development.

Currently, different experimental techniques are used to determine B_{22} in protein solutions. However, one should be aware of the differences in B_{22} values obtained via different measurement techniques. The reader is referred to literature [18]. These techniques include (a) membrane osmometry to measure the osmotic pressure at several protein concentrations [19], (b) equilibrium sedimentation measuring protein concentration distribution when equilibrium conditions of sedimentation and diffusion have been achieved [20], (c) self-interaction chromatography determining the retention of protein molecules by columns carrying the very same protein [13; 21] and (d) static light scattering either in batch mode [20] or flow-mode using SEC [22]. The batch-mode light scattering method is limited by its high susceptibility to interference with dust particles and other impurities. In order to overcome this problem, a flow-mode method using an online static light scattering detector combined with SEC has been developed [23]. Hereby, a light scattering (LS) detector and a concentration determination detector (UV or a differential refractometer (RI)) are connected in series. The analysis is based on the principle that each point on the chromatogram of the LS detector has its corresponding data point in the UV chromatogram. When the two chromatograms are overlaid with necessary corrections due to the inter-detector

band broadening and the inter-detector volume, a whole range of concentrations and the corresponding scattering intensities could be obtained and these data could be used to generate the Debye plot. To overcome the potentially erroneous corrections necessary with the series connection of the two detectors, Bajaj et al. established a dual-detector cell for simultaneous measurement of scattered light intensity and concentration [24] which eliminates the need to use empirical correction methods, and forms the basis for the presented study.

Protein unfolding and/or small disturbances in protein structure exposing hydrophobic patches on the surface are supposed to induce the formation of aggregation prone protein species [25-27]. Hence, the chromatographic separation and the B$_{22}$ analysis of aggregated species are important. We analyzed the B$_{22}$ for multiple protein species, such as monomer, dimer, trimer, etc., formed upon thermal stress in order to understand whether the B$_{22}$ values of these diverse protein species are different. The critical question is whether or not protein aggregation could be linked to the B$_{22}$ value. Theoretically, a negative B$_{22}$ value could indicate that dimers and trimers originating from unfolded monomer have a higher tendency to further interact and to form large aggregates on long term storage. This may result in a limited amount of low molecular weight aggregates but in a substantial growth in large aggregates and sub-visible particles. In contrast a positive B$_{22}$ value would suggest colloidally stable low molecular weight aggregates and this very fraction should increase during storage time. A possible correlation between more attractive B$_{22}$ values and more pronounced aggregate-aggregate association and growth of larger particles was mentioned by Li et al [28].

Regarding the term B$_{22}$, it consists of the letter B for the second virial coefficient, and two numbers describing the two interacting solutes observed, e.g., 1 stands for water (the solvent), 2 for the first solute (e.g. protein) and 3 for a second solute (e.g. a salt). In our case the interaction of two monomers, two dimers, or two timers etc. was analyzed. Hence the authors agreed on naming the interaction parameter in the following B$_{22}$.

_____

2 MATERIALS AND METHODS

2.1 Materials

Solutions of two model proteins (Protein X (IgG2, 144 kDa) and Protein Z (IgG1, 148 kDa)) in 10 mM acetate buffer, pH 4, 0.3M NaCl were used. The protein content of the solutions was determined by UV extinction at 280 nm subtracting UV extinction at 320 nm using an extinction coefficient of 1.4 mg mL^{-1} cm^{-1}. The running buffer is identical with the formulation buffer and no unfolding or aggregation effects were observed in the unstressed samples at $t_{(0\ min)}$ and in the initial/bulk material.

2.2 Methods

2.2.1 Thermal stress

Samples were heat stressed at 48°C (temperature stability of 0.1°C) in a water bath (Thermo/Neslab RTE-110 Bath/Circulator, Neslab Instruments, US) for time periods between 5 and 60 min in 2 mL safe-lock tubes.

2.2.2 B$_{22}$ Analysis

In order to characterize protein molecule interaction, B$_{22}$ values were determined using the static light scattering method described by Bajaj et al. [8]. Briefly, proteins were analyzed by HP-SEC on a HP Series 1100 Agilent Instruments (Agilent Technologies, Germany) with two YMC-Pack Diol-300 (YMC Europe GmbH, Germany) columns with lengths of 50 cm and 30 cm for good peak separation. As running buffer, formulation buffer was used. The analytics were performed at a flow rate of 0.8 ml/min, and approximately 60 µg of protein were injected. Samples were stored at 4°C (HP Series 1100, G1329A ALS) and the column temperature was set to 25°C (HP Series 1100, G 1316A). In the triple detector (based on a Differential Refractometer Waters 410) 90° light scattering intensity, UV transmittance at 280 nm and RI data were recorded (Fig.1).

_____
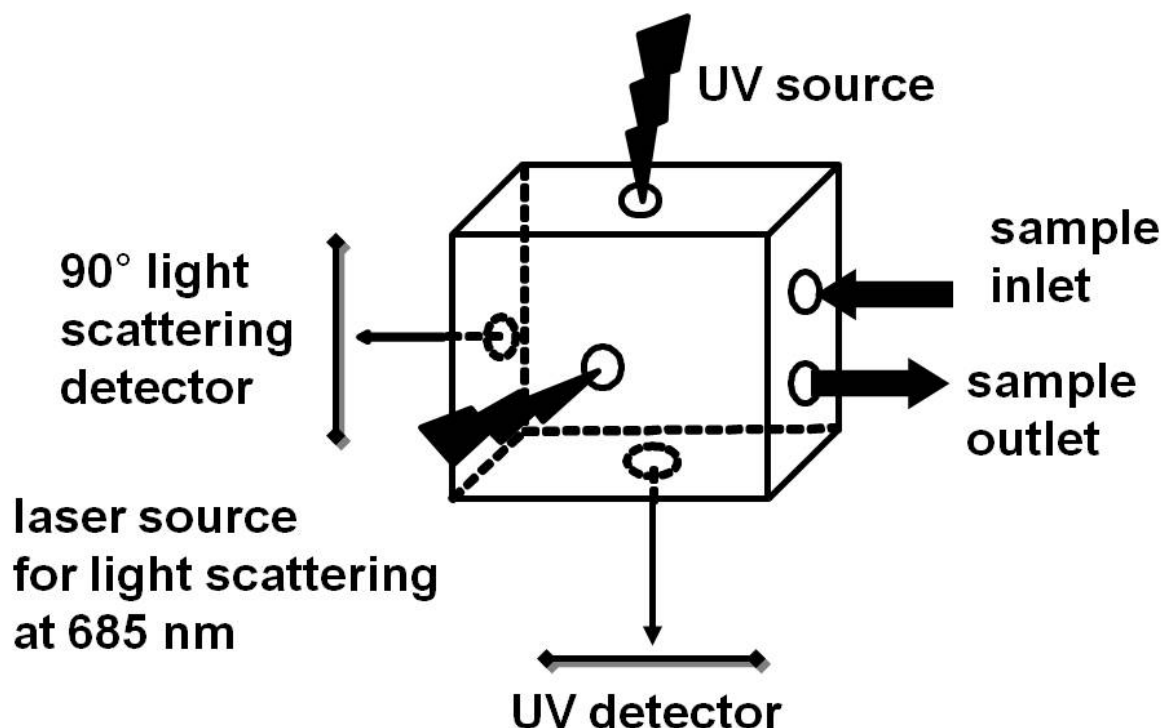
Figure 1: A schematic drawing of the dual-detector cell used for simultaneous measurement of scattered light intensity at a 90° angle and protein concentration by UV detection.

To quantify monomer amounts and formed soluble aggregate quantity, the AUC (area under the curve) was calculated in percent of the total monomer amount recovered in the initial samples as gained by UV transmission data converted to protein concentration. For B$_{22}$ analysis, scattered light intensity at 90° and intensity of transmitted UV light (data between 15 and 85% height of the descending portion of the peak) were converted to RΘ and concentration, respectively. B$_{22}$ was obtained from the slope of the Debye plot Kc/RΘ vs. c, and the average molecular weight was calculated from the inverse of the intercept. As by size separation HMWs could not be baseline separated perfectly, a possible influence of the peak overlay was considered. Therefore, to separate the peaks a deconvolution calculation was used giving the same B$_{22}$ values, and thereby confirming that the method and the calculations based on the original chromatograms are accurate and reliable. Deconvolution calculations were performed using the MathLab software provided by

_____

MathWorks. By fitting a separate function f(x) for each peak and estimating a Gaussian distribution the separation of the peaks was achieved.

2.2.3 Visual Inspection, Turbidity and Fluorescence Chromatography

The existence of visible particles was surveyed by naked eye under gentle container movement. For turbidity measurement UV extinction at 350 nm was analyzed. For analysis of protein unfolding, the fluorescent dye BisANS combined with the SEC method described by Hawe et al. 2008 was applied [29]. Samples were spiked with BisANS to a final dye concentration of 10 µM. Fluorescence analysis was conducted on the HP Series 1100 Agilent Instruments using a TSKgel G3000SWxl column (Tosoh Bioscience, Stuttgart, Germany) and a guard column. The acetate buffer was used as mobile phase at a flow rate of 0.8 mL/min. After size separation the samples were lead through a fluorescence detector (FP 1520, Intelligent Fluorescence Detector, Jasco) with an excitation wavelength set to 385 nm and emission maxima were recorded at 485 nm.

3 RESULTS AND DISCUSSION

3.1 Protein species induced by thermal stress

Thermal stress leads to unfolding and aggregation of proteins [3]. No increase in turbidity was observed by UV measurements at 350 nm and no visible aggregates were observed by naked eye. The total AUC was unchanged for both proteins, which indicated that within the limits of experimental error the total mass balance was maintained. Thus, the formation of insoluble aggregates was negligible. The formation of small soluble aggregates however was observed and is in agreement with literature [3]. The HP-SEC chromatograms were obtained by measuring simultaneously scattered light intensity at a 90° angle and UV transmittance. The UV transmittance was converted into absorbance and the data were used to calculate the B_{22} values and the molecular weight. Selected chromatograms for protein X (Fig. 2) and for protein Z (Fig.3) are provided.
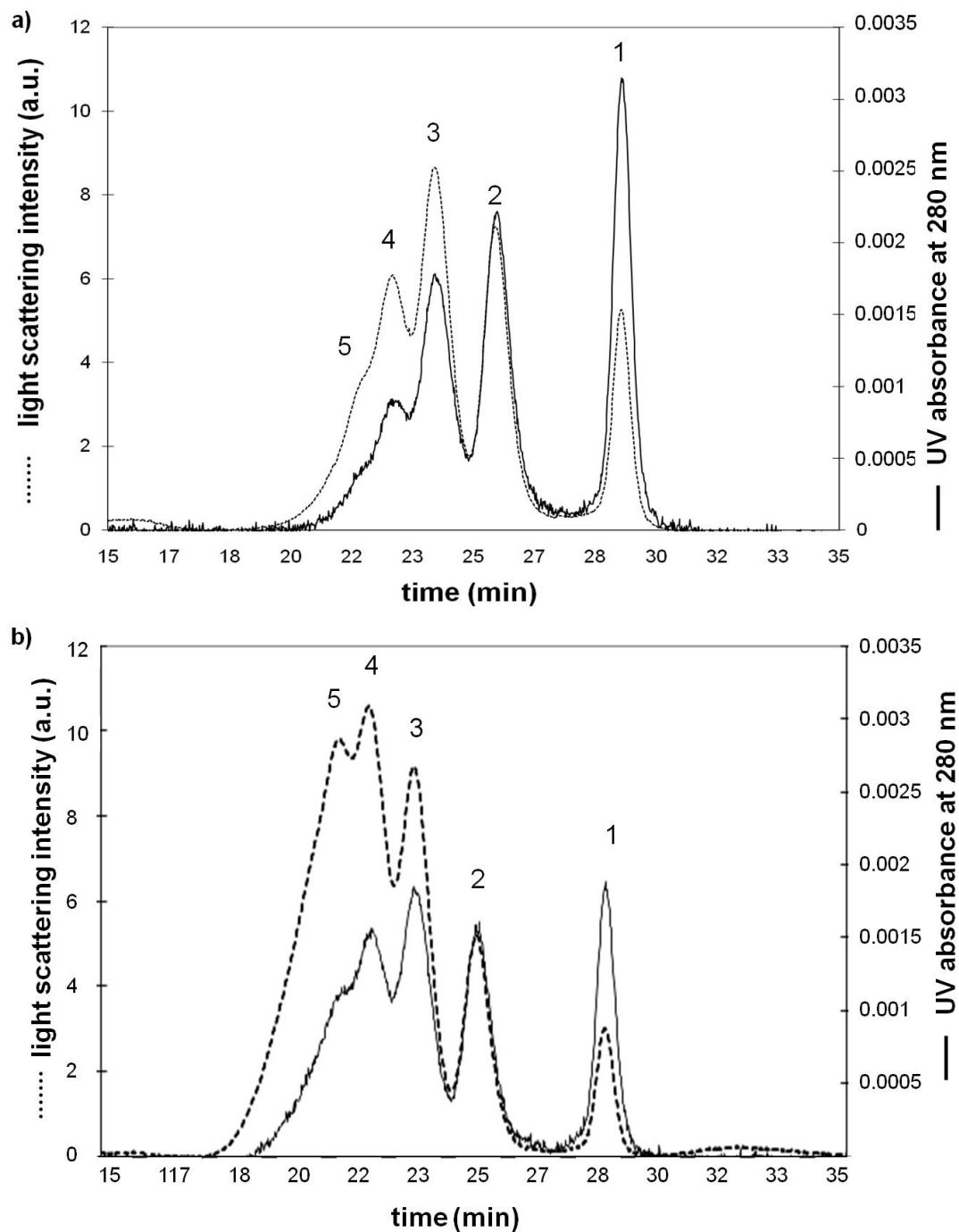
Figure 2: Exemplary chromatograms of protein X stressed for 10 min (a) and 30 min (b) showed a decreasing peak for the remaining monomer (1), and increasing amounts for dimer (2), trimer (3), tetramer (4) and pentamer (5) appearing as shoulder in front of the tetramer peak. Chromatograms were gained by measuring simultaneously scattered light intensity at a 90° angle (dashed line) and UV transmittance converted into absorbance (black line).
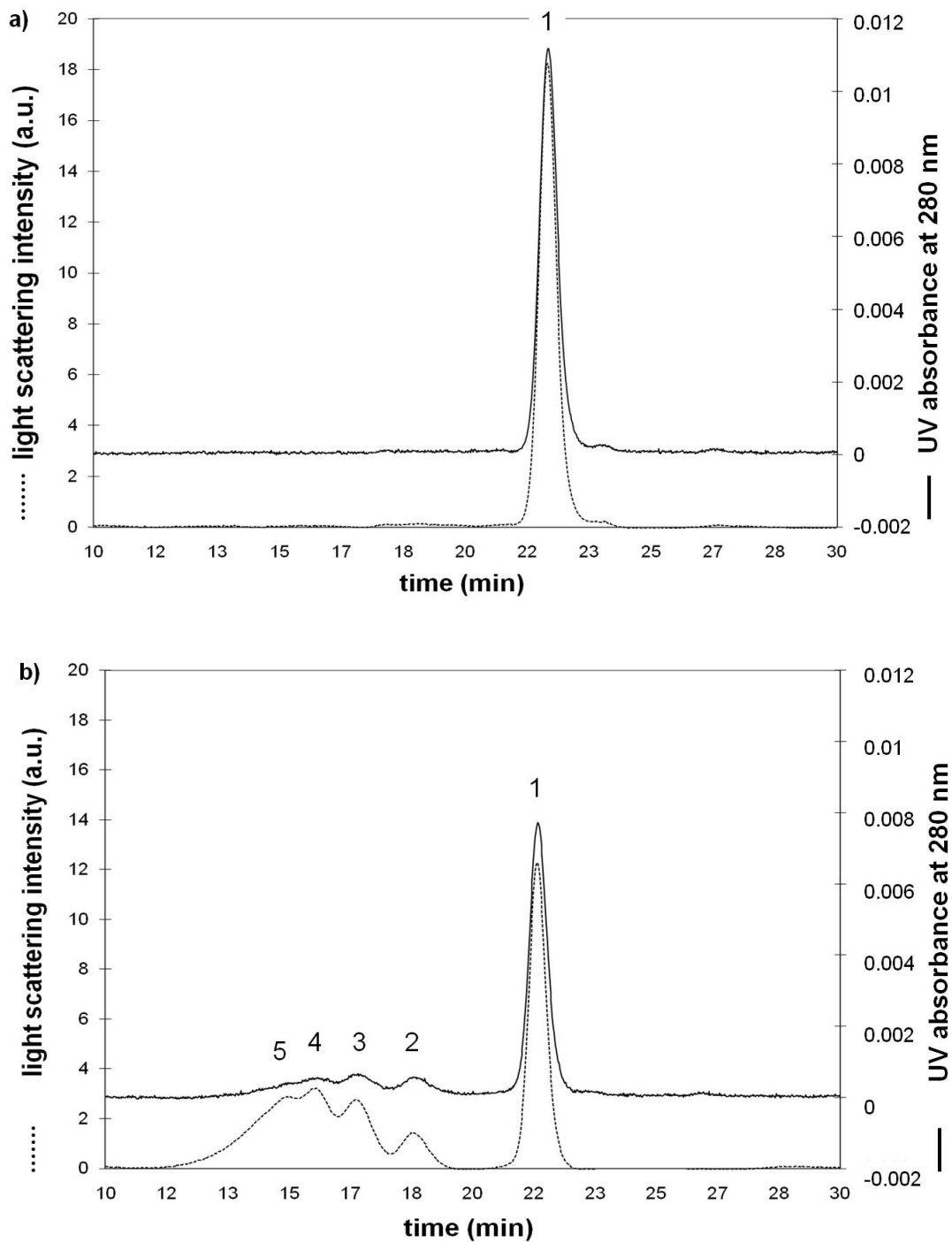
Figure 3: Exemplary chromatograms of protein Z at t = 0 min (a) and after heat stress for 60 min (b) showed peaks for the monomer (1), dimer (2), trimer (3), tetramer (4) and pentamer (5), the latter one was only visible in the light scattering data. The chromatograms were gained by measuring simultaneously scattered light intensity at a 90° angle (dashed line) and UV transmittance converted into absorbance (black line).

The chromatograms of stressed protein X (Fig.2) showed the monomer peak and exhibited four additional peaks. These peaks reflect dimer, trimer, tetramer and pentamer species, as confirmed by molecular weight calculation (see 3.2 and 3.3). In the beginning, the formation of dimers was induced. After further heat exposure the amount of trimers was increased, followed by the formation of tetramers and pentamers. The presence of the pentamer peak could be observed in both proteins X and Z (Fig.2b and 3.b). This peak is the result of the further growth in the oligomer species (dimer, trimer, tetramer and pentamer) over time. As this pentamer species only appeared in the chromatograms as a shoulder and in low amounts, even for protein X, it could not be analyzed further for B$_{22}$ and molecular weight calculations. The data points were insufficient. The Debye plots of the protein after stress exposure showed a negative slope and B$_{22}$, resp. (Fig.4). The average molecular weight was calculated from the inverse of the intercept. In the bulk material, only protein monomer was observed in both protein X and Z samples. The amount of protein oligomers displayed as relative AUC, increased over time. In protein X approximately 17% monomer remained after 30 min heat stress and 83% soluble aggregates were formed (Fig.5a). In contrast, for protein Z a monomer amount of approximately 67% remained after 60 min heat stress and only 7.5% to 9.5% of each soluble aggregate species was generated (Fig.5b). Even at longer time of heat stress, far less aggregates formed in protein Z compared to protein X solution. Therefore, protein Z seemed to be more stable than protein X. However, the amount of the formed aggregates for protein Z remained too low for B$_{22}$ and molecular weight calculations. But the chromatograms of protein Z monomer provided sufficient peak resolution and adequate amount of protein species to gain sufficient data points for B$_{22}$ and molecular weight calculation. In contrast, for protein X the calculation of molecular weight and B$_{22}$ values for monomer, dimer, trimer and tetramer species could be performed. The calculations are described in the following sections (3.2 and 3.3).

_____
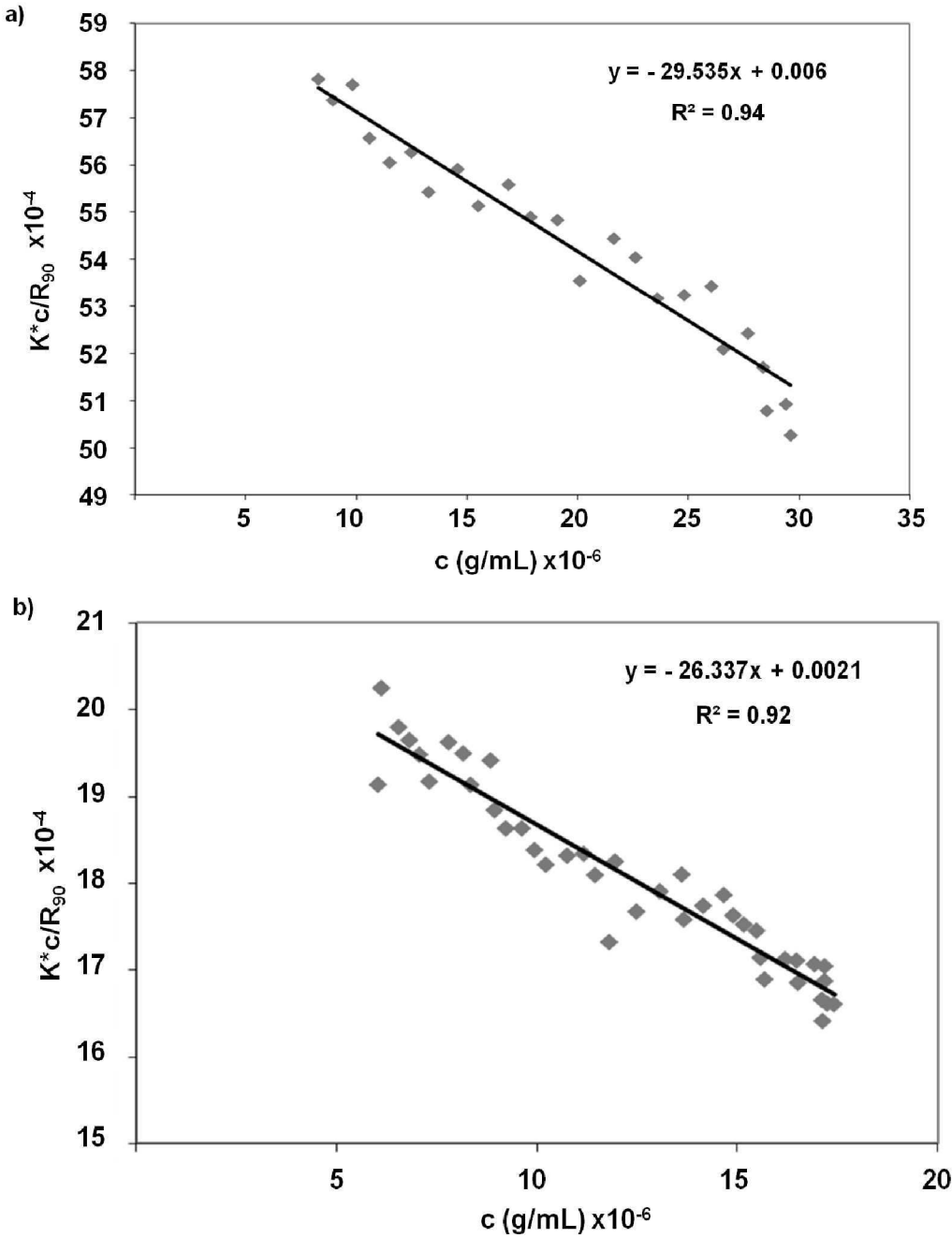
Figure 4: Exemplary Debye plots of protein X for a) monomer after stress exposure for 10 min and b) trimer after stress exposure for 30 min.

_____

a)

b)

Figure 5: Percentage of monomer (black columns), dimer (grey columns), trimer (black and white striped columns), tetramer (white columns) and pentamer (black and white checked) after thermal stress of model protein X (a) and Z (b).

_____

By using BisANS it is possible to observe protein unfolding. Hydrophobic surfaces of the protein become exposed during unfolding and due to the interaction of the dye with the hydrophobic areas the observed fluorescence intensity is increased [29]. The used SEC separation method could demonstrate that the extrinsic fluorescence intensity for both the aggregate peaks and the monomer peak increased with the duration of heat stress (data not shown). Thus, upon thermal stress the proteins became at least partially unfolded, whereby additional hydrophobic regions appeared at the protein's surface. Those hydrophobic areas might however enhance protein-protein interactions and lead to a progress in aggregation.

3.2 Molecular weight of different protein species

Calculating the molecular weight of protein species from the retention time data and molecular weight size standards can yield erroneous results, as the elution time of a protein species depends on the molecular weight, shape, its glycosilation and tendency to interact with the column resin [30]. HP-SEC in combination with a concentration detector, UV or RI and a light scattering detector is a better alternative to SEC alone to determine the protein molecular weight. The light scattering signal is proportional to both concentration and molecular weight and overcomes the limitations of standard SEC [30]. To determine the molecular weight graphically via Debye plot, the inverse of the intercept of the Debye plot was used.

Equation (2) describes the Debye plot,

$$\frac{Kc}{R_\theta} = \frac{1}{MW} + 2B_{22}c \qquad\qquad (2)$$

where K is an optical constant, c is the concentration of the protein, R_θ is the measured excess Rayleigh's ratio of protein solution, MW is the molecular weight, and B_{22} is the osmotic second virial coefficient. The angular dependence of R_θ has been dropped in the following due to the assumption of isotropic scattering and is

written as R$_{90}$, as a 90 degree scattering detector was used. To calculate the weight average molecular weight MW the following equation (3) was used

$$MW = \frac{1}{\dfrac{Kc}{R_{90}} - 2B_{22}c} \qquad (3)$$

The optical constant K is defined as

$$K = \frac{4n\pi(dn/dc)^2}{\lambda^4 N_A} \qquad (4)$$

where n is the refractive index of the solvent, dn/dc is the refractive index increment of the solute in a given solution, λ is the wavelength of the incident light and N$_A$ is Avogadro´s Number. Rayleigh's ratio at 90° scattering angle is defined as

$$R_{90} = \frac{I_S \cdot R^2}{I_0} \qquad (5)$$

where R$_{90}$ is the Rayleigh's ratio at 90° scattering angle, I$_S$ is the intensity of the scattered light, R is the distance of the sample from the detector, and I$_0$ is the intensity of the incident light.

Regarding protein X, sufficient quantities of the three aggregated protein species were formed and ample amounts of monomer was retained to obtain adequate data points to estimate the molecular weights for all these species (Fig.6a). Calculations showed a molecular weight average for the monomer of 144.6 kDa, which is in good accordance with the literature (144 kDa) [8]. Calculating the molecular weight for the induced soluble aggregates confirmed the formation of dimers, trimers and tetramers.

_____

For the first higher molecular weight species eluting prior to the monomer, a molecular weight average of 274.5 kDa was calculated (expected dimer: 288 kDa). The second soluble aggregate showed a molecular weight average of 430.7 kDa (expected trimer: 432 kDa) and for the third aggregate species a molecular weight of 558.5 kDa (expected tetramer: 576 kDa) was observed.

The molecular weight of protein Z monomer was calculated to a value of 145.9 kDa (148 kDa) (Fig.6b). For the induced soluble aggregates the data points were insufficient to calculate their molecular weights.

a)

b)
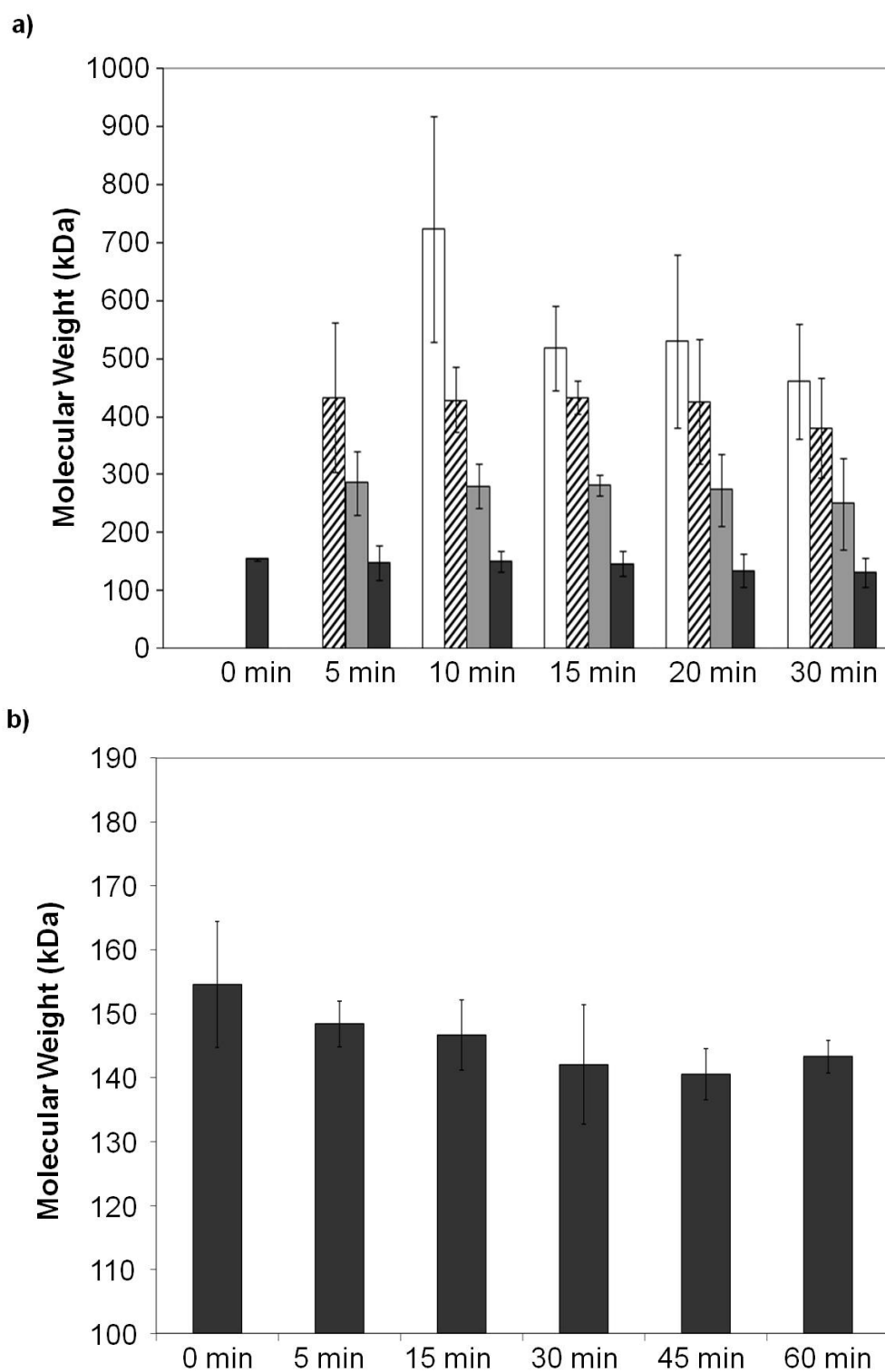
Figure 6: Molecular weight average calculated graphically via the inverse of intercept of Debye plot for monomer (black columns), dimer (grey columns), trimer (black and white striped columns), and tetramer (white columns) of protein X (a) and protein Z (b). For Protein Z only the monomer data is shown.

3.3 B_{22} values of different protein species

B_{22} values were calculated via the method described by Bajaj et al. [8; 24] for protein X monomer and aggregated species formed upon thermal stress. For protein Z only the B_{22} of the monomer could be determined due to insufficient data points in the chromatogram for determination of B_{22}. The B_{22} values differed dependent on the aggregation status. A schematic illustration of the approach to determine B_{22} after size separation for different protein species individually is shown in figure 7. Due to heat stress, the protein monomer gets unfolded and upon further heat stress dimer, trimer, tetramer and higher molecular weight species are formed. Using an SEC, a size separation was achieved and the B_{22} values among the monomer- (B_{22} monomer), dimer- (B_{22} dimer), trimer- (B_{22} trimer) and tetramer- (B_{22} tetramer) species was calculable.
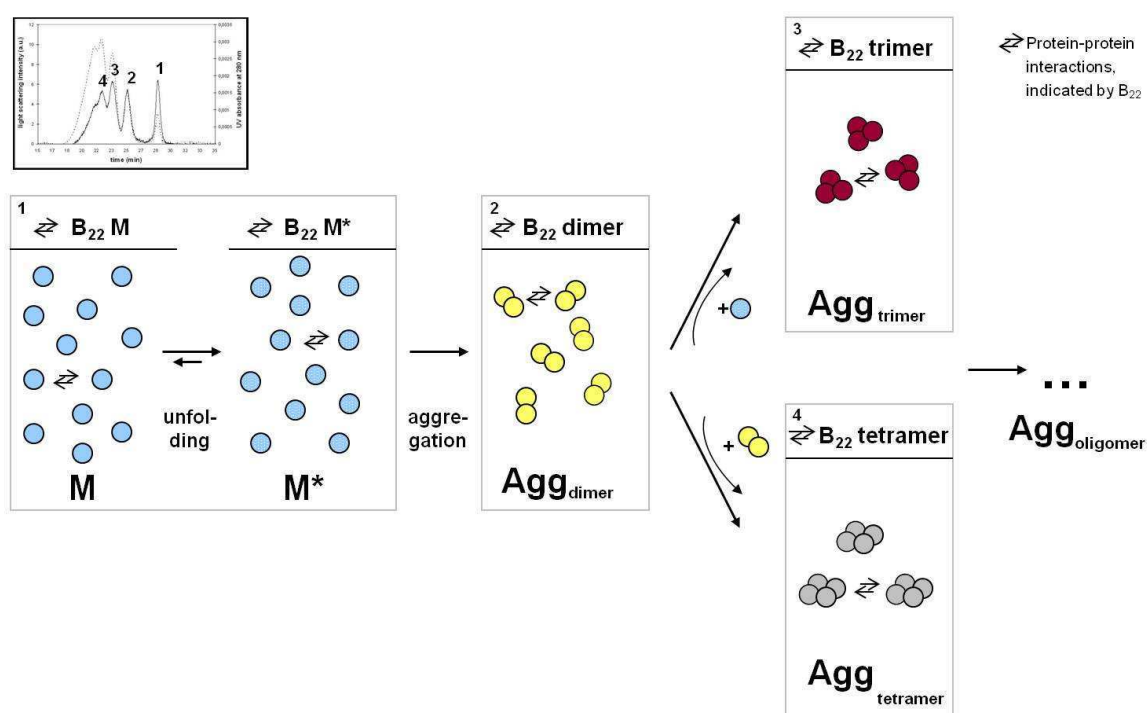
Figure 7: A schematic illustration of the approach to determine B22 after size separation for different protein species individually (M=native monomer, M*=partially unfolded monomer, Agg=aggregated species).

_____

Regarding the non-stressed protein monomers, B$_{22}$ values of -4.88*10^{-4} mol*mL/g² for protein X (Fig.8a), which is in good accordance with literature [8], and -5.87*10^{-4} mol*mL/g² for protein Z (Fig.8b) were obtained. A slightly negative B$_{22}$ value under the given conditions was plausible. At pH 4 the protein molecules carry positive net charge. Due to the charge shielding effect of the 300 mM NaCl the charge-induced repulsive forces between the protein monomer molecules diminish and molecules can approach each other more closely [31; 32]. As the repulsive forces were strongly reduced, the attractive hydrophobic interactions, dipole interactions and hydrogen bonding predominate and result in a negative B$_{22}$ value indicating overall protein-protein attraction. Le Brun et al. also mentioned a significant impact of pH and ionic strength on B$_{22}$ of an IgG1 [33]. Varying relevant formulation parameters they obtained a significantly positive B$_{22}$ value at acidic pH and low buffer and salt concentrations.

_____

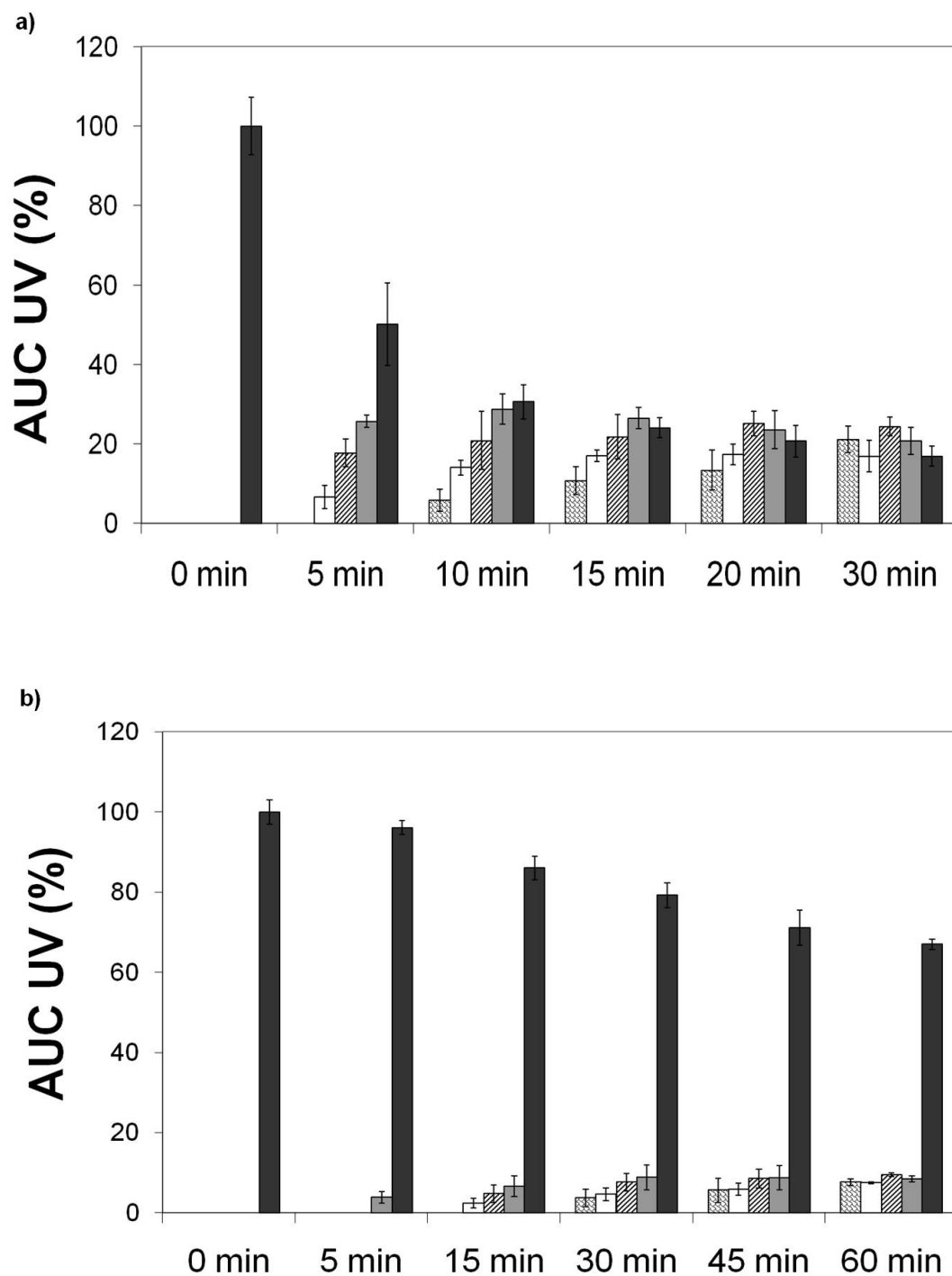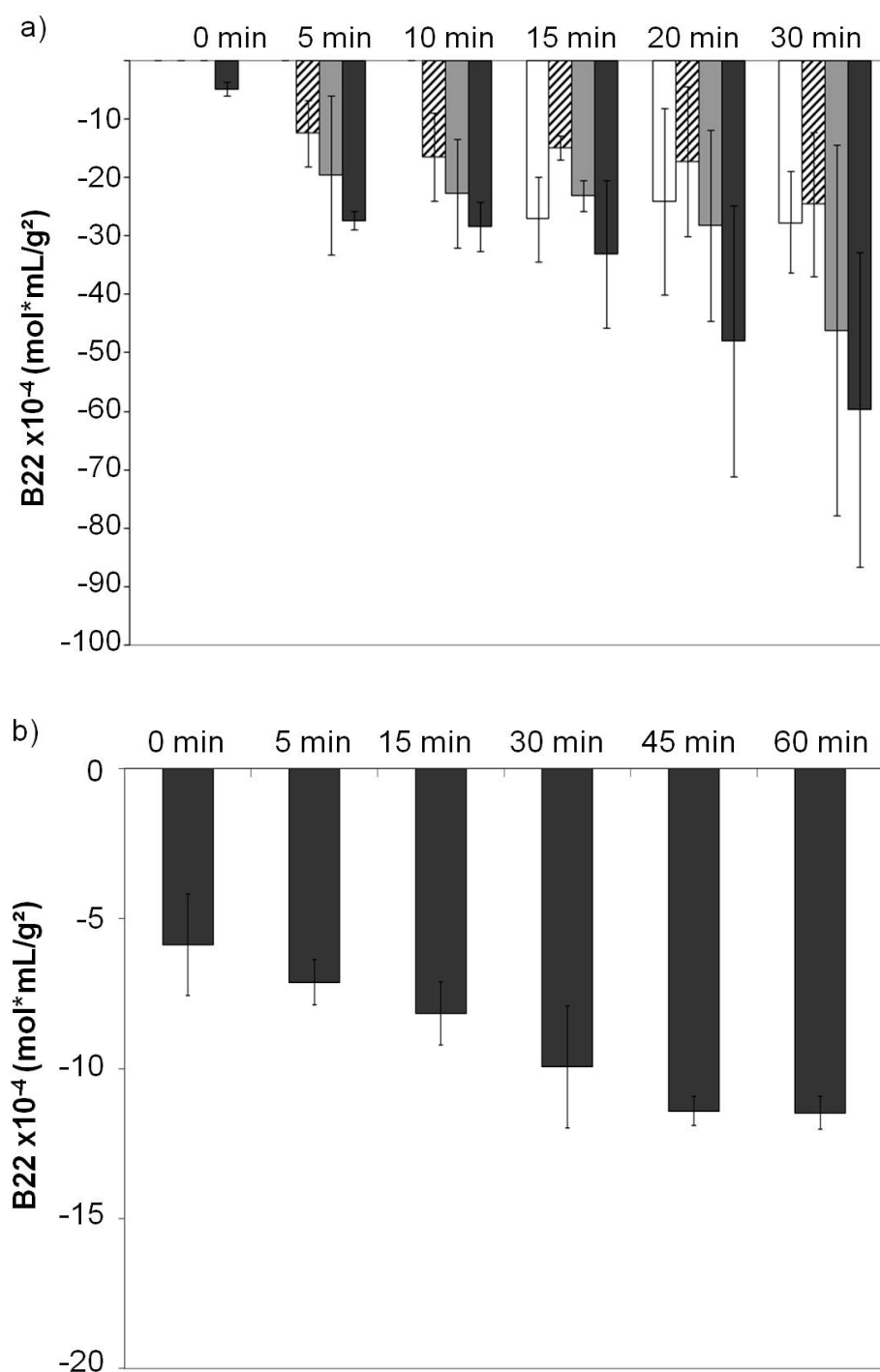**Figure 8:** Determination of the B22 via Debye plot and the slope for monomer (black columns), dimer (grey columns), trimer (black and white striped columns) and tetramer (white columns) of protein X (a) and protein Z (b) using the equation Kc R90-1 = MW-1 + 2B22c [7].

_____

After thermal stress the B$_{22}$ values of the monomers became more negative. This reduction can be explained by protein unfolding confirmed by the fluorescence analysis. The surface exposure of the hydrophobic areas initially hidden in the inner core of the protein molecules enables stronger hydrophobic protein-protein interactions. The B$_{22}$ value for protein X monomer decreased from -4.9*10^{-4} mol*mL/g² to -27.3*10^{-4} mol*mL/g² already after 5 min and after 60 min to -59.6*10^{-4} mol*mL/g². The B$_{22}$ value for protein Z monomer ranged from -5.9*10^{-4} mol*mL/g² to -11.5*10^{-4} mol*mL/g². The difference between the two proteins in the monomer interaction correlates with the higher protein Z stability. The higher stability of protein Z is reflected in the fact that protein X formed approx. 83% aggregates (Fig.5a), whereas protein Z showed soluble aggregate formation of less than 20 % after 30 min (Fig.5b). The tendency of protein Z to aggregate less might be reflected by the less negative B$_{22}$ values between the monomer species representing less attractive protein-protein interactions. Although we were getting pure monomer peaks in the HP-SEC chromatograms, the fluorescence and the B$_{22}$ values of these monomer species had changed. This indicates a change in the monomer conformation and the monomer interaction behavior. This leads to the conclusion that the analysis of protein aggregation should not only focus on the aggregate properties such as size and amount, but orthogonal methods are necessary to study changes of the monomer fraction after separation from aggregated species. By using this orthogonal approach, more detailed information on the quality of the protein monomer is obtained.

Compared to the B$_{22}$ values of the unstressed protein monomer (protein X: -4.9*10^{-4} mol*mL/g²), after thermal stress the B$_{22}$ values of all soluble aggregates and monomers decreased. At the end of the exposure to higher temperature, the B22 values calculated for the dimer were -46.1*10^{-4} mol*mL/g²; for the trimer -24.6*10^{-4} mol*mL/g² and for the tetramer -27.5*10^{-4} mol*mL/g² (Fig.8a). Overall, a significance of the decrease with longer time of heat stress could not be established because of to the marked standard deviations in the results.

_____

The B_{22} values of the induced soluble aggregates were in a similar range as the B_{22} value of the monomer. This corresponds to the fact that these aggregates consisting of low numbers of protein molecules did not further aggregate to form larger aggregates in the higher nm and µm size range. Instead the types of aggregates did stay rather consistent over time. At a pH of 2, lower compared to our study, heat treatment of IgG results in weakly aggregated protein solution because of the repulsive interactions [34]. With increasing heat stress exposure, decreased B_{22} values of the monomer, reflecting increased attractive interactions, were observed. Thereby aggregation was facilitated. Monomers showed the most negative B_{22} values reflecting the highest attractive interactions. This might be a reason why the amount of dimers and other oligomers was increasing, but no larger visible aggregates were detected. The total recovery stayed around 100 %.

Comparing with relevant literature, one notes that the B_{22} values determined in this study are in the rather low range of B_{22} values reported so far. For example in the context of protein crystallization B_{22} values in a range of -2 to $-8*10^{-4}$ mol*mL/g² are mentioned [35]. Solubility studies described B_{22} values under various solvent conditions for lysozyme of +0.2 to $-7.4*10^{-4}$ mol*mL/g² and for ovalbumin form -3.3 to $-4.5*10^{-4}$ mol*mL/g² [35]. But the overall tendency for proteins to aggregate more easily, e.g., while stirring, at a comparable low B_{22} value of $-1.8*10^{-4}$ mol*mL/g² is stated in LeBrun et al. 2010 [27]. Another approach to compare the B_{22} values between different molecules was recently described by Sahin et al. [36] using a normalized B_{22} value. They used the ratio of the apparent second viral coefficient and B_{22} and the hard sphere repulsion contribution to the second virial coefficient by hard sphere repulsion, $B_{22,HS}$. The $B_{22,HS}$ for the monomer, dimer, trimer and tetramer were calculated as $1.94*10^{-5}$, $9.76*10^{-6}$, $6.49*10^{-6}$ and $4.87*10^{-6}$, respectively. These values were calculated using $B_{HS}=uN_A/(2M^2)$ as described by Harding et al. [37]. Here u is the excluded volume, N_A is the Avagadro's number and M is the molecular weight of the species (150kD for a monomer). $B_{22}/B_{22,HS}$ ratios range from -140 to -500 (compared to a value of +2 for the hard sphere) indicating that for all oligomers the magnitude of attraction between molecules is the dominant factor contributing to the aggregation process. On a relative basis, the tetramer had the largest negative value for B_{22}/B_{ex}. While the B_{22} value of the protein X and Z monomer species clearly

_____

changed between unstressed and stressed samples and further decreased with increasing heat stress exposure (Fig.8a and b), the B$_{22}$ values of the oligomers did not follow this trend, but remained constant. This difference between monomers and oligomers became even more pronounced once the excluded volume was incorporated in the calculation (Fig. 9a and b). Here, the relative magnitudes of B$_{22}$/B$_{ex}$ were indistinguishable because of large error bars.
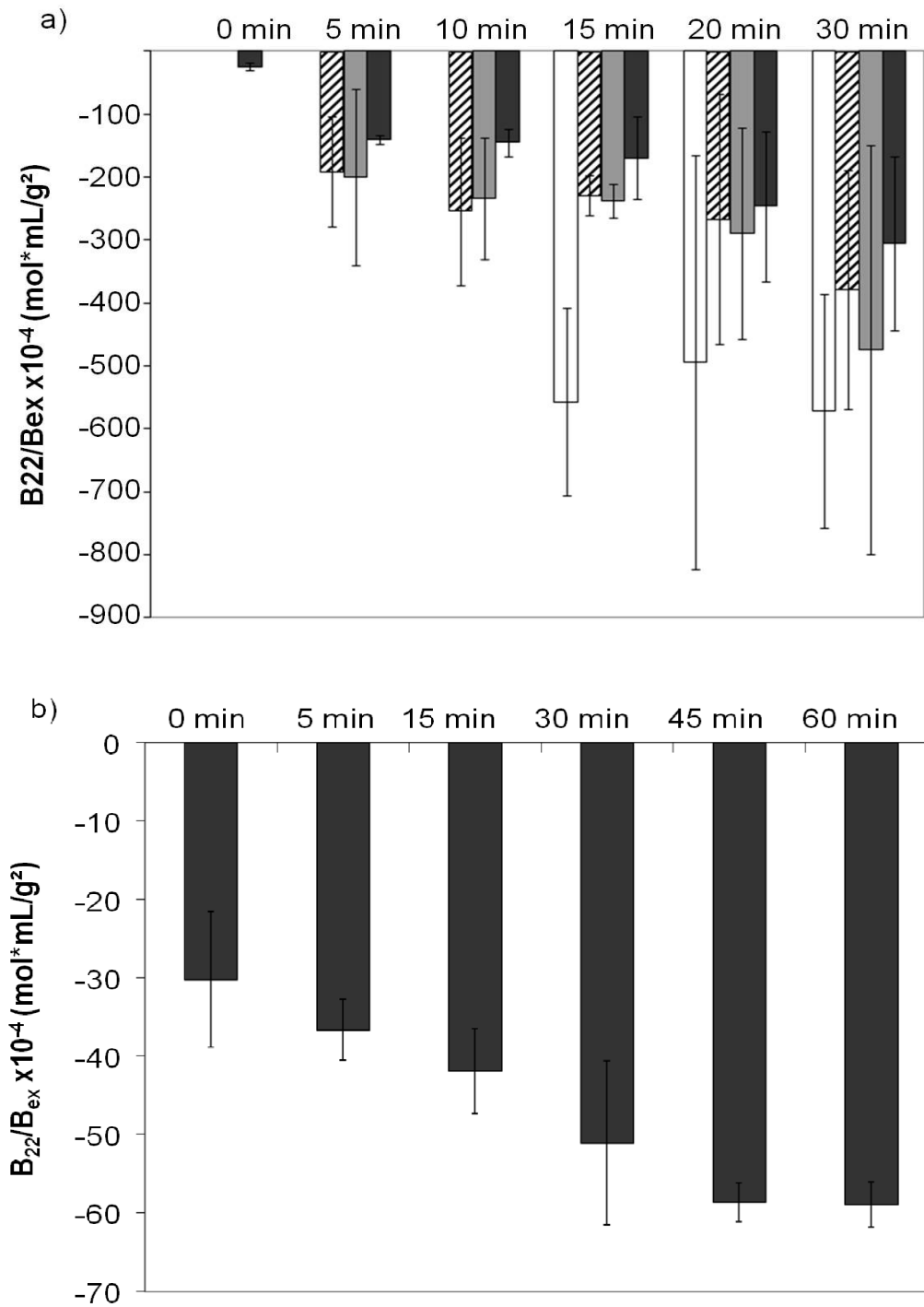
Figure 9: Determination of the ratio of the apparent second viral coefficient B22 and the hard sphere repulsion contribution to the second virial coefficient Bex for monomer (black columns), dimer (grey columns), trimer (black and white striped columns) and tetramer (white columns) of protein X (a) and protein Z (b).

_____

4 CONCLUSION

Protein aggregation is seen as an inherently heterogeneous process and hardly understood at the moment. Monomers may interact with oligomers, and smaller oligomers may interact with larger oligomers forming a very heterogeneous system. Measuring the cross interactions of the species would be a highly valuable tool to learn more about the aggregation pathways and to get deeper insights into the growth of the protein particles. However, at the moment to the best of the authors' knowledge the measurement of these cross interaction in an aggregating antibody formulation has not been achieved. Though, our new technique based on simultaneous measurements of protein concentration and scattered light intensity in a dual-detector flow cell enabled the calculations of B$_{22}$ values of both monomers and soluble aggregates (oligomers, such as dimers, trimers and tetramers) simultaneously and individually due to the size separation on the column prior to the B$_{22}$ analysis. Since B$_{22}$ values of unfolded and aggregated species are difficult to obtain individually, this is one of the few cases in which such data are reported. Another benefit of the HPLC based method is the amenability for high throughput screening. It was observed that the B$_{22}$ values indicated slightly attractive interactions in the native state due to high salt concentration shielding protein charges and prevailing attractive forces. Upon thermal stress exposure, the protein partially unfolds as seen in extrinsic fluorescence data. In addition, the decreased B$_{22}$ values indicate an increase in the attractive protein-protein interactions between the monomer and oligomers. Thus, the decreased B$_{22}$ values might reflect the partial unfolding of the protein as a result of thermal stress, whereby, the hydrophobic attractive interactions of the protein molecules are augmented. Of high importance is the fact that the B$_{22}$ of the protein monomer decreased drastically upon heat stress and appears to be the most reactive species. Simultaneously the fluorescence intensity increased indicating partial unfolding of the monomer. The gained B$_{22}$ data of the stressed monomer as well as the oligomer protein species are more negative than reported data of B$_{22}$ so far, e.g., for crystallisation. Thus, the new method and the obtained data allow for a better understanding of protein interactions and aggregation stability in formulation development.

_____

5 ACKNOWLEDGMENTS

_____

6 APPENDIX

6.1 Calculation of the second virial coefficient (B$_{22}$)

In the following, the method to determine B$_{22}$ by static light scattering using a dual-detector cell evolved and described by Bajaj et al. is explained. Further information can be found in recent publications [8; 24]. A schematic of the dual-detector cell is shown in Figure 1.

The cell volume was 10µL. For light scattering a laser source at 685 nm was used and a fibre optic cable that served as UV source from a MiniDATA UV (Analytical Instrument Systems, Flemington, NJ) hosting a deuterium lamp. The path length for UV measurements was 3 mm [Bajaj et al]. The scattered light intensity at 90° and the intensity of the transmitted UV light are converted to RΘ and concentration, respectively, and B$_{22}$ is gained as the slope of the Debye plot Kc/RΘ vs c, as described in the following.

6.2 Determination of Rayleigh´s ratio (R$_\Theta$) out of scattered light intensity (I$_S$)

The Molecular weight (MW) of the protein samples in diluted solutions and for polarized light is related to intensity of the scattered light from the sample by the equation [8; 24]

$$MW = \frac{NA\lambda^4 R^2 I_S}{4\pi^2 \sin^2 \Phi c (dn/dc)^2 n^2 I_0}$$

(6)

where NA is the Avogadro's number, λ is the wavelength of the incident radiation, R is the distance of the sample from the detector, I$_S$ is the intensity of the scattered light, Φ is the angle between the plane of the incident polarized light and the scattering detector, c is the concentration of protein sample, dn/dc is the refractive index increment of protein solution, n is the refractive index of the solvent and I$_0$ is the intensity of the incident light.

_____

Taking the constants and instrument parameters into the light scattering instrument constant, A90, it can be written as

$$MW = \frac{I_S}{A90 \, c (dn/dc)^2}$$

(7)

where IS is the intensity of the scattered light, A90 is the light scattering instrument constant, c is the concentration of protein sample, and dn/dc is the refractive index increment of protein solution.

Consequently, A90 can be written as

$$A90 = \frac{I_0 * 4\pi^2 n^2}{NA * \lambda^4 * R^2}$$

(8)

Here, A90 is the light scattering instrument constant, I_0 is the intensity of the incident light, n is the refractive index of the solvent, NA is the Avogadro's number, λ is the wavelength of the incident radiation, R is the distance of the sample from the detector.

Since the intensity of the incident radiation, I0, and the distance between the sample and detector, R, is fixed, the ratio of these two parameters can be obtained by rearranging the above equation and is represented as K1.

$$\frac{R^2}{I_0} = \frac{4\pi^2 n^2}{NA \lambda^4 A90} = K1$$

(9)

Hence, K1 can be simply obtained from the instrument constant A90, wavelength of the incident light λ (685 nm), and refractive index of the solution.

Rayleigh's ratio at 90° scattering angle is defined as

$$R\Theta = \frac{I_S R^2}{I_0}$$

(10)

where RΘ is the Rayleigh's ratio at 90° scattering angle, I$_S$ is the intensity of the scattered light, R is the distance of the sample from the detector, and I$_0$ is the intensity of the incident light.

Combining the two above mentioned equations, Rayleigh's ratio can also be written as

$$R\Theta = K1 * I_S$$

(11)

Here RΘ is the Rayleigh's ratio at 90° scattering angle, K1 is the constant of intensity of incident radiation I$_0$ and distance sample/detector, and I$_S$ is the intensity of the scattered light.

6.3 Determination of the protein concentration (c) using the UV transmission data (Ia)

The concentration for each corresponding data point on the UV chromatogram was estimated from the UV signal intensity. In the present instrument configuration, the UV chromatogram represented the intensity of the transmitted light. Hence, the concentration of the injected protein at each data point was estimated using the equation

$$c(g/mL) = \log\left(\frac{I100\%T - I0\%T}{Ia - I0\%T}\right) * \frac{10}{E1\% * b}$$

(12)

where c is the concentration of the protein, I100%T is the intensity of the UV signal at the baseline, I0%T is the signal of the UV detector in off-mode, Ia is the UV signal at

_____

a given time point on the chromatogram, E1% is the extinction coefficient of 1% protein solution, and b is the path length of the UV cell (3 mm).

6.4 Determination of the second virial coefficient (B$_{22}$) using the Debye plot and the slope

According to Bajaj et al. the intensity of the scattered light is related to the osmotic compressibility and B$_{22}$ processing the data by the method of Zimm (1948), using the [7].

$$\frac{Kc}{R\Theta} = \left(\frac{1}{M} + 2Bc\right)\left(1 + \frac{16\pi^2 r^2 \sin^2\left(\Theta/2\right)}{3\lambda^2}\right)$$

(13)

where RΘ is the measured excess Rayleigh´s ratio of protein solution, which is measured as a function of concentration, c, at multiple angles, Θ. M is the weight-average molecular weight, r is the radius, and λ is the wavelength of the incident light.

In case of proteins, equation (9) can be simplified, as proteins are independent of the angle of the incident light in the used wavelength region (400-800 nm). The simplified equation is known as the Debye equation

$$\frac{Kc}{R\Theta} = \frac{1}{M} + 2B_{22}c$$

(14)

B$_{22}$ values are obtained from the slope of the Debye plot (Kc/RΘ vs c). The inverse of the intercept provides the molecular weight. To minimize the contribution from dust particles a 90° angles is chosen for the measurements.

_____

The optical constant K is defined as

$$K = \frac{4\pi^2 (n * dn/dc)^2}{\lambda^4 NA}$$

(15)

where n is the refractive index of the solvent, dn/dc is the refractive index increment of the solute in a given solution, λ is the wavelength of the incident light and NA is Avogadro´s Number.

7 REFERENCE LIST

[1] Walsh G 2005. Biopharmaceuticals: recent approvals and likely directions. Trends Biotechnology 23: 553-558.

[2] Hermeling S, Crommelin DJ, Schellekens H, Jiskoot W 2004. Structure-immunogenicity relationships of therapeutic proteins. Pharmaceutical Research 21: 897-903.

[3] Mahler HC, Friess W, Grauschopf U, Kiese S 2009. Protein aggregation: Pathways, induction factors and analysis. Journal of Pharmaceutical Sciences 98: 2909-2934.

[4]   Li Y, Roberts CJ 2010. Aggregation of therapeutic proteins in Protein Aggregation Pathways, Kinetics, and Thermodynamics. Editors: Mahler, Borchard, Luessen

[5] Carpenter JF, Randolph TW, Jiskoot W, Crommelin D J A, Middaugh CR, Winter G 2010. Potential inaccurate quantitation and sizing of protein aggregates by size exclusion chromatography: Essential need to use orthogonal methods to assure the quality of therapeutic protein products. Journal of Pharmaceutical Sciences 99(5): 2200-2208.

[6] Pace CN 1990. Conformational stability of globular proteins. Trends in Biochemical Sciences 15: 14-7.

[7] Zimm BH 1946. Application of the methods of molecular distribution to solutions of large molecules. Journal of Chemical Physics 14: 164-79

[8] Bajaj H, Sharma VK, Kalonia DS 2007. A high-throughput method for detection of protein self-association and second virial coefficient using size-exclusion chromatography through simultaneous measurement of concentration and scattered light intensity. Pharmaceutical Research 24: 2071-2083.

[9] Weiss WF IV, Young TM, Roberts CJ 2009. Principles, Approaches, and Challenges for Prediction of Protein Aggregation Kinetics and Shelf Life. Journal of Pharmaceutical Sciences 98: 1246

_____

[10] Valente JJ, Payne RW, Manning MC, Wilson WW, Henry CS 2005. Colloidal behavior of proteins: effects of the second virial coefficient on solubility, crystallization and aggregation of proteins in aqueous solution. Current Pharmaceutical Biotechnology 6(6): 427-36.

[11] Katayama DS, Nayar R, Chou DK, Valente JJ, Cooper J, Henry CS, Vander Velde DG, Villarete L, Liu CP, Manning MC 2006. Effect of buffer species on the thermally induced aggregation of interferon-tau. Journal of Pharmaceutical Sciences 95: 1212-1226.

[12] Chi EY, Krishnan S, Randolph TW, Carpenter JF 2003. Physical Stability of Proteins in Aqueous Solution: Mechanism and Driving Forces in Nonnative Protein Aggregation. Pharmaceutical Research 20: 1325-1336.

[13] Le Brun V, Friess W, Schultz-Fademrecht T, Muehlau S, Garidel P 2009. Lysozyme-lysozyme self-interactions as assessed by the osmotic second virial coefficient: Impact for physical protein stabilization. Biotechnology Journal 4: 1305-1319.

[14] George A, Wilson WW 1994. Predicting protein crystallization from a dilute-solution property. Acta Crystallographica Section D. Biological Crystallography 50: 361–365.

[15] George A, Chiang Y, Guo B,Arabshahi A, Cai Z, Wilson WW 1997. Second virial coefficient as predictor in protein crystal growth. Methods in Enzymology 276: 100–110.

[16] Chi E Y, Krishnan S, Kendrick B S, Chang BS, Carpenter JF, Randolph TW 2003. Roles of conformational stability and colloidal stability in the aggregation of recombinant human granulocyte colony-stimulating factor. Protein Science 12(5): 903-913.

[17] Curtis R A, Ulrich J, Montaser A, Prausnitz JM, Blanch HW 2002. Protein-protein interactions in concentrated electrolyte solutions. Hofmeister-series effects. Biotechnological Bioengineering 79: 367–380.

[18] Scott DJ 2008. The shock of the old: hydrodynamics for the masses. Biochemical Society Transactions 36(4): 766-770.

[19] Tombsand M, Peacocke AR 1975. The Osmotic Pressure of Biological Macromolecules. Monographs on Physical Biochemistry. Biochemical Education 3 (2): 37-37.

[20] Tanford C, De PK 1961. The unfolding of beta-lactoglobulin at pH 3 by urea, formamide, and other organic substances. Journal of Biological Chemistry 236: 1711-1715.

[21] Tessier PM, Lenhoff AM, Sandler SI 2002. Rapid measurement of protein osmotic second virial coefficients by self-interaction chromatography. Biophysical Journal 82(3): 1620-1631.

[22] Bloustine J, Berejnov V, Fraden S 2003. Measurements of protein-protein interactions by size exclusion chromatography. Biophysical Journal 85: 2619-2623.

[23] Wyatt PJ 2002. Method for measuring the 2nd virial coefficient of a protein monomer (Wyatt Technology Corporation, USA). Application: US, 2002, p 19.

[24] Bajaj H, Sharma VK, Kalonia DS 2004. Determination of second virial coefficient of proteins using a dual-detector cell for simultaneous measurement of scattered light intensity and concentration in SEC-HPLC. Biophysical Journal 87: 4048-4055.

[25] Cromwell M, Hilario E, Jacobson F 2006. Protein aggregation and bioprocessing. AAPS Journal 8: E572-E579.

[26] Wang W 2005. Protein aggregation and its inhibition in biopharmaceutics. International Journal of Pharmaceutics 289: 1-30.

[27] Le Brun V, Friess W, Bassarab S, Garidel P 2010. Correlation of protein-protein interactions as assessed by affinity chromatography with colloidal protein stability: A case study with lysozyme. Pharmaceutical Development and Technology 15: 421-430.

_____

[28] Li Y, Ogunnaike BA, Roberts CJ 2010. Multi-variate approach to global protein aggregation behavior and kinetics: Effects of pH, NaCl, and temperature for alpha-chymotrypsinogen A. Journal of Pharmaceutical Sciences 99(2): 645-662.

[29] Hawe A, Friess W, Sutter M, Jiskoot W 2008. Online fluorescent dye detection method for the characterization of immunoglobulin G aggregation by size exclusion chromatography and asymmetrical flow field flow fractionation. Analytical Biochemistry 378: 115-122.

[30] Wen J, Arakawa T, Philo JS 1996. Size-exclusion chromatography with online light-scattering, absorbance, and refractive index detectors for studying proteins and their interactions. Analytical Biochemistry 240: 155-166.

[31] Tsumoto K, Ejima D, Senczuk AM, Kita Y, Arakawa T 2007. Effects of salts on protein-surface interactions: applications for column chromatography. Journal of Pharmaceutical Sciences 96: 1677-1690.

[32] Yadav S, Liu J, Shire SJ, Kalonia DS 2010. Specific interactions in high concentration antibody solutions resulting in high viscosity. Journal of Pharmaceutical Sciences 99: 1152-1168.

[33] Le Brun V, Friess W, Bassarab S, Muehlau S, Garidel P 2010. A critical evaluation of self-interaction chromatography as a predictive tool for the assessment of protein-protein interactions in protein formulation development: a case study of a therapeutic monoclonal antibody. European Journal of Pharmaceutics and Biopharmaceutics 75: 16-25.

[34] Vermeer AWP, Norde W 2000. The thermal stability of immunoglobulin: unfolding and aggregation of a multi-domain protein. Biophysical Journal 78: 394-404.

[35] Guo B, Kao S, McDonald H, Asanov A, Combs LL, Wilson WW 1946. Correlation of second virial coefficients and solubilities useful in protein crystal growth. Journal of Crystal Growth 196: 424-433.

[36] Sahin E, Grillo AO, Perkins MD, Roberts CJ 2010. Comparative effects of pH and ionic strength on protein-protein interactions, unfolding, and aggregation for IgG1 antibodies. Journal of Pharmaceutical Sciences 99(12): 4830–4848

_____

[37] Harding E, Horton JC, Jones S, Thornton JM , Winzor DJ 1999. COVOL: An interactive program for evaluating second virial coefficients from the triaxial shape or dimensions of rigid macromolecules. Biophysical Journal 76: 2432-2438.

CHAPTER 3

Simultaneous Detection and Analysis of Protein Aggregation and Protein Unfolding by Size Exclusion Chromatography with Post Column Addition of the Fluorescent Dye BisANS

ABSTRACT

For development and optimization of protein formulations sensitive analytical tools are required to follow both aggregation and changes in protein-structure. The latter can be seen as the beginning of physical instability leading to aggregation. The focus of this work laid on the development of a novel analysis simultaneously detecting changes in protein conformation and the formation of oligomers. By adding the extrinsic fluorescent dye BisANS after SEC and UV-detection, it was possible to separate protein monomer and oligomers by size, to analyze the amount of formed oligomers quantitatively using UV-detection, and to observe changes in protein structure of different protein species by fluorescence detection. This enabled to distinguish between native-like and denatured oligomers and monomers formed under different stress-conditions. Correspondingly, increased fluorescence reflecting partial unfolding was assigned specifically to monomer, oligomer or both. The

_____

unfolding of monomer is not traceable by commonly used detection methods, but its monitoring may provide important information about activity and long-term stability. By adding the dye after SEC and UV-detection, interferences with prior detectors are precluded, excipients are separated avoiding interferences with the protein-dye interaction and additionally, the dye-protein interaction cannot impact the aggregation formation, as added after the separation of monomer and aggregates.

1 INTRODUCTION

Biopharmaceuticals, specifically recombinant proteins and antibodies have become an important factor in the pharmaceutical industry. One major challenge in protein formulation development is their stability. Biopharmaceuticals may easily form aggregates during various steps of manufacturing, such as fermentation, purification, formulation and during storage [1]. The aggregation of the protein compromises the stability as well as the product quality and may lead to a reduced activity of the product. Furthermore, the safety of the biopharmaceutical product may be at risk due to potential immune responses [2, 3]. Therefore the control of the protein aggregate formation and its minimization is highly necessary. Protein aggregates, as defined by Mahler et al. are a universal term of all kinds of not further defined multimeric (oligomers, multimers) protein species that are formed by covalent bonds or non-covalent interactions leading to soluble and/or insoluble aggregates [1]. Several factors are described which induce protein aggregation during manufacturing and storage, including temperature (elevated temperature, freezing and/or thawing), mechanical stress (shaking, stirring, pumping) [4-6], surface interactions and formulation parameters (protein concentration, pH, general composition) [6-9]. The different stress factors may lead to different patterns of protein aggregates with respect to size, degree of unfolding or covalent/non-covalent nature [4, 5, 10, 11]. This was recently shown by Joubert et al. [10] and Luo et al. [11]. Joubert et al. applied various stress methods on eight monoclonal antibodies (IgG1 and IgG2 subtypes as well as intravenous IgG) and observed a similar mechanism of aggregation of the different IgG molecules under the same stress exposure. Furthermore, a dependency on the nature of the stress was claimed for the chemical modifications tested for IgG2 aggregates [11]. Higher temperature typically directly induces the unfolding resulting in aggregates of highly non-native character [5, 6, 10, 11]. Freezing and drying induces complex physical stresses due to, e.g., pH changes, cryo-concentration of the protein and solutes, and newly evolving ice-liquid interfaces, frequently resulting in larger aggregates of only partially unfolded protein molecules [12-19]. Changes in the secondary and the tertiary structure of the protein molecules are seen as one possibility for the beginning of protein denaturation and the formation of non-native, irreversible aggregates. Partially unfolded states, also

_____

described as molten globule state or "A" state, if acid denatured [20], might promote aggregation. Conformationally altered or aggregated protein molecules are supposed to function as nuclei or enhance aggregation, although this is discussed controversially in literature [21-24].

In general the use of orthogonal, complementary analytical methods is recommended to analyze the complex pattern of the potential formed protein aggregates [1, 4, 10]. For quantitative protein analysis and for size estimation SEC, SDS-PAGE, field flow fractionation, flow imaging analysis, static and dynamic light scattering, light obscuration and turbidity measurements are used. SEC analysis with the possibility of applying various detectors, such as UV, fluorescence, light scattering, and RI detector, is one of the most frequently used analytical methods in protein analytics [1]. Standard methods characterizing protein structure are fluorescence spectroscopy, circular dichroism (CD), Fourier-transformed infrared spectroscopy (FTIR) [1, 25] and to a lesser extent Raman spectroscopy. Fluorescence spectroscopy in particular can be employed as a highly sensitive method for protein quantification as well as for conformation characterization [25-30]. Intrinsic protein fluorescence deriving from the naturally fluorescent amino acids tryptophan, tyrosine and phenylalanine, can provide information on conformational changes of proteins [29-30]. For extrinsic fluorescence a fluorescent dye is needed. Typically, extrinsic dyes enter non-covalent interactions with proteins and protein degradation products via, e.g., hydrophobic, ionic or electrostatic interactions [25, 31]. The fluorescence properties of these extrinsic dyes can be explained by solvent relaxation processes and (twisted) intra-molecular charge transfer reactions, which are affected by the environment and by the interactions of the dyes with protein molecules [25]. Consequently, extrinsic fluorescence dyes are used in various fields of protein analytics, e.g., to characterize unfolding and denaturation, measure surface hydrophobicity and detect aggregation or fibrillation, e.g., via fluorescence spectroscopy and fluorescence microscopy [25, 27]. Commonly used dyes for protein characterisation are 1-anilinonaphthalene-8-sulfonate (ANS) and 4,4′-Dianilino-1,1′-binaphthyl-5,5′-disulfonic acid dipotassium salt (BisANS), Nile Red, Congo Red, 9-(Dicyanovinyl)julolidine (DCVJ), Thioflavin T and Sypro Orange/Red. Their use increases, as sensitivity, suitability, and versatility make them suitable for high-

throughput screening [25]. ANS and its dimeric analogon BisANS show hardly any fluorescence in aqueous solutions, but are highly fluorescent in organic and apolar solvents and upon interaction with hydrophobic surfaces, e.g., on protein molecules [25]. For several proteins a higher affinity and a stronger fluorescence enhancement has been described for BisANS as compared to ANS [25], and BisANS was therefore chosen in this study. Using fluorescent dyes it is possible to observe changes in protein tertiary structure. Due to protein unfolding, hydrophobic surfaces become exposed and by their interaction with the dye an increase in fluorescence intensity is observed [25-28]. Compared to other fluorescent dyes, the use of BisANS provides the advantage that only very small quantities are needed. Additionally, as it is water soluble, BisANS also helps avoiding potentially harmful effects of other solvents, e.g., of DMSO (dimethyl sulfoxide) or ethanol, which are needed to dissolve Nile Red.

Given the broad patterns of protein aggregation, it would be advantageous to have analytical tools to detect the formed aggregates quantitatively and to observe protein unfolding in the different species individually at the same time. Understanding the coherence and the sequence of events in protein interaction, unfolding and aggregation could be useful in the effort to control and minimize protein aggregation. Hence, our approach was the development of a method to simultaneously detect changes in protein conformation with high sensitivity based on extrinsic fluorescent dye interaction and to separate and quantify the aggregate species, namely the formed oligomers, such as dimers, trimers and tetramers using SEC. As different stress methods lead to diverse aggregate species with patterns varying quantitatively and qualitatively, we selected five different stress methods, i.e., pH, temperature, freeze/thaw, light, and shaking stress to demonstrate the benefits of the new method and to understand the aggregate pattern resulting from the different stress factors. A broad range of stress methods, including an extremely low pH value of 1.1 was chosen to trigger conformational changes. Instead of using the SEC and the fluorescence spectroscopy separately, the idea was to combine them on the basis of the method described by Hawe et al. 2008 [26]. In our approach, the fluorescent dye BisANS was added to the eluting protein sample after column separation and UV detection via post column module (PCM). Subsequently, the sample was led through the fluorescence detector. Instead of adding the fluorescent dye directly to the

_____

sample or to the mobile phase as described previously [26], the dye was added after size separation and UV detection, but prior to fluorescence detection. The application of the PCM entails the advantage of its minimized contact time between the fluorescent dye and the protein [32]. The approach enables the removal of other excipients such as surfactants present in the protein formulation from the protein prior to dye addition. This reduces the risk of dye-surfactant interactions affecting dye-protein interaction both below and above the surfactant's critical micelle concentration (CMC). Additionally, micelles are formed at high surfactant concentrations and an interference with the correct analysis might be observed, as micelles show about the same retention time as the protein monomer. Furthermore, by using the PCM, artifacts originating from different elution behavior of the dye-protein complex compared to pure protein cannot occur. Interactions of the dye with the column resin were eliminated, which due to hydrophobic interactions might influence the protein elution [33]. The obtained SEC results were compared to the results from turbidity, sub-visible and visible particle analysis and SDS-PAGE. Furthermore, the formation of larger aggregates was monitored by AF4 in combination with MALLS detection.

2 MATERIALS AND METHODS

2.1 Materials

A glycosylated IgG1 (148 kDa) at 2 mg/ml in 10 mM phosphate buffer containing 140 mM NaCl at pH 7.2 (further called PBS) was donated by Merck Serono, Germany. The protein content of the solution was determined by UV absorption at 280 nm (e_1 = 1.4 $(mg/mL)^{-1}cm^{-1}$). BisANS powder (SIGMA, Sigma-Aldrich Chemie GmbH, Germany) for extrinsic fluorescence detection was dissolved in PBS for further use as a stock solution with a concentration of 23.5 µM. Final solution concentration was measured by UV absorption at 385 nm (e_2 = 16750 $(mol)^{-1}cm^{-1}$). For heat-, freeze thaw-, light- and shaking stressed samples both the stress exposure and the analysis of the protein were conducted in 10 mM PBS, 140 mM NaCl, pH 7.2. Analyses of pH-stressed protein samples in the batch mode were performed under the changed pH conditions within 24h, whereas the flow mode

analyses (SEC, AF4) were performed in 10 mM PBS, 140 mM NaCl, and pH 7.2. For statistics, three sub-runs of the same stressed sample were analyzed. The average and standard deviations are provided. Samples were stressed and stored in 6R vials closed with rubber stoppers respectively in falcon tubes 15mL. For HPLC analysis, 1mL HPLC vials were used. All other chemicals used were of analytical grade unless stated otherwise.

2.2 Stress Methods

2.2.1 pH Stress

The IgG1 was stressed changing the pH of the formulation by adding the required amount of HCl 1M or NaOH 1M. The actual pH was measured by a MP 220 pH meter (Mettler Toledo). Final pH values of 9.1, 5.1, 3.1 and 1.1 were adjusted. Analysis was done shortly after pH values were adjusted.

2.2.2 Thermal Stress

The IgG1 (10 mL) was stressed at 60°C in a water bath for 20 and 40 minutes and cooled back to room temperature.

2.2.3 Freeze/Thaw Stress

The IgG1 was stored in a freezer at -80°C for 30 min and then thawed at 25°C in a water bath for 30 min. This cycle was performed 10 or 20 times resp. in 15 mL falcon tubes with a filling volume of 10 mL.

2.2.4 Light Stress

The IgG1 (10 mL) was stressed in a SUNTEST CPS (Heraeus, Original Hanau) at 54 W/m² by a Xenon lamp for 24 or 48 hours in 15 mL falcon tubes. The chamber was not cooled and sample temperatures of 35°C were observed, which is however far below T_m of the protein (71°C).

_____

2.2.5 Shaking Stress

The IgG1 was shaken in vertically standing 6R vials for 72 and 168 hours on a horizontal shaker at 900 rpm while being protected from day light.

2.3 Analytical Methods

2.3.1 Visual Inspection

The existence of visible particles was surveyed after gently swirling the illuminated sample.

2.3.2 Turbidity Measurements

For turbidity measurements a NEPHLA turbidimeter (Dr Lange, Germany) was used. Light (= 860 nm) was sent through the samples and the scattered light was measured at a 90° angle. The results were given in formazine nephelometric units (FNU). Turbidity was also characterized via UV absorbance at 350 nm in a UV VIS Spectrophotometer (Agilent Technologies) and compared to the nephlometry results.

2.3.3 Sub-visible Particle Counting

Sub-visible particle counting based on light obscuration was performed on a PAMAS device (Rutesheim, Germany) equipped with a laser diode and a photodiode detector for size distribution analysis. Three measurements of a volume of 0.5 ml for each run were analyzed with a forerun volume of 0.3 ml. Results refer to a sample volume of 1.0 ml. Between measurements the device was cleaned with water until particle counts correspond to the acceptance criteria of the European Pharmacopoeia (Pharm.Eur. 2.9.19; number of particles >10µm less then 25 particles in 25 mL).

2.3.4 Asymmetrical Flow Field Flow Fractionation (AF 4)

The formation of oligomers and fragments as well as the molecular weight of the different protein species were determined by AF4 on an Eclipse 2 Separation

Systems (Wyatt Technology Europe GmbH). A 10 kDa regenerated cellulose membrane with a 350 µm spacer, a 10 mM phosphate buffer at pH 7.2 (140mM NaCl) as mobile phase, an injection volume of 20 µL respectively 40 µL, and a detector flow of 1 mL/min in combination with UV (MVD Agilent 1100Serie) and light scattering (Dawn EOS, Wyatt Technology Cooperation) detectors were used. The percentage of monomer and oligomer AUC was calculated as the ratio of the AUC compared to the AUC of the initial sample. Samples were stored in the sample holder at 4°C. Protein quantification and molecular weight calculations were conducted using the ASTRA software.

2.3.5 Sodium Dodecyl Sulfate - Polyacryl Amide Gel Electrophoresis (SDS-PAGE)

The formation of covalent aggregates and fragments was analyzed by SDS-PAGE under reducing and non-reducing conditions in an electrophoresis chamber with a power supply using Bis-Tris gels and Bis-Tris SDS-Running buffer (Invitrogen GmbH, Germany). Samples were diluted to a final concentration of 0.025 mg/mL with SDS buffer or, when using reducing conditions, with a 10% DDT solution. The samples were heated at 95°C for 20 minutes and a sample load of 10 µL was used. A standard silver staining protocol following the manufacturer´s instructions including washing, fixing, staining, de-staining and drying was employed for the detection of the protein bands.

2.3.6 Fluorescence Spectroscopy

Extrinsic fluorescence spectroscopy in batch mode was conducted on a Varian Eclipse Fluorescence Spectrometer (Darmstadt, Germany). 1 mL protein sample was spiked with BisANS stock solution (23.5 µM) to a final concentration of 1 µM in Eppendorf tubes 1.5 mL and analyzed in white 96 well plates (NUNC) shortly after the dye was added. The spectra were corrected by subtracting the dye containing buffer spectrum. The excitation and the emission range were set to 385 nm and 390-600 nm respectively, the excitation and emission slits were adjusted to 5 nm each, the PMT detector voltage was regulated to 700 V, and a scanning speed of

120 nm/min was used. The fluorescence of the protein solutions prior and after filtration via a 5 µm syringe filter was compared.

2.3.7 High Performance Size Exclusion Chromatography (SEC) with a Post Column Module (PCM) for Fluorescence Detection

SEC was performed on an Agilent 1100 (Agilent Technologies, Germany) using a 500 mm YMC-Pack Diol-300 column (YMC Europe GmbH, Germany) with 100 µL injection volume. A 10 mM PBS at pH 7.2 mobile phase at a flow rate of 0.7 mL/min was used. After protein size separation and UV detection at 280nm (Agilent variable wavelength UV detector G1314A) but prior to the fluorescence detection, a BisANS stock solution of 23.5 µM in PBS was pumped into the system at a flow rate of 0.25 mL/min via a post column module (PCM). The PCM was based on a pump (Merck-Hitachi L6200A) and a connecting chamber (T-connector, G1820-80512, Agilent Technologies, Germany). The fluorescence spectra (Agilent fluorescence detector G1321A) were recorded at an excitation wavelength of 385 nm and the maximum emission wavelength of 485 nm. Thereby, it was possible to size-separate the protein by SEC and oligomers and monomer were quantified by UV detection. The fluorescence analysis after dye addition allowed to analyze unfolding individually for monomer and oligomers.

In a different setting, samples were spiked with BisANS prior to SEC to a final concentration of 10µM as described by Hawe [24]. The samples were analyzed using a TSKgel G3000SWxl column (Tosoh Bioscience, Stuttgart, Germany) equipped with a guard column on the Agilent 1100 (Agilent Technologies, Waldbronn, Germany). A 10 mM PBS at pH 7.2 mobile phase eluted at 0.5 mL/min and the same detectors as mentioned above were used. The percentage of monomer and oligomer AUC was calculated as the ratio of the AUC compared to the AUC of the initial sample. The second set up was used to be as close as possible to method described earlier [26] to tell the benefits of the novel post column addition method. The 500 mm YMC-Pack Diol-300 column was used as it resulted in improved peak resolution.

3 RESULTS AND DISCUSSION

3.1 Visual Inspection and Turbidity

All samples were first analyzed by naked eye to observe any appearance of visible particles. Whereas the pH, temperature- and light- stress samples remained free of any or showed only very few visible particles (similar to the starting material), the freeze/thaw (F/T) stressed samples showed a higher number of particles. Samples which underwent shaking stress for several hours became turbid with severe formation of visible particles. These observations were proven by turbidity measurements. Shaking stress led to a pronounced increase in turbidity (40.6 FNU), whereas only a slight increase in turbidity was observed for pH 1.1, heat, F/T and light stressed samples (< 10 FNU) (Fig.1a). The data of the turbidity measurements in UV absorbance at 350 nm showed the same trends (data not shown).

3.2 Sub-visible Particle Counting

The number of sub-visible particles detected by light obscuration particle counting revealed an increase in particles >1 µm for all stressed samples by a factor of a least 10 (Fig.1b). IgG initial samples showed around 5,500 particles larger than 1 µm; 200 particles >10 µm and only few particles > 25 µm. Shaken stress samples revealed the highest formation of particles with 200,000/mL >1 µm; 5000/mL >10 µm; and 300/mL > 25 µm. F/T stressed samples showed a pronounced increase especially in particles > 10 µm and > 25 µm. Regarding the other stressed samples, the number of particles > 10 µm stayed well below 1000/mL and for particles > 25 µm below 100/ml. These results are in good accordance to previously published work [4, 5, 24].

3.3 AF 4

To analyze the formation of soluble aggregates and fragments AF4 was used as this technique is known to be suitable for larger protein aggregates. Thereby, the AF4 analysis showed the time- and stress- dependent formation of diverse oligomer species and fragments with the same tendency as seen in the SEC analysis discussed later (Fig.1c). The monomer content dropped down to 4 % for pH 1.1

_____

stressed samples. This might be due to the formation of larger insoluble aggregates or to the formation of soluble aggregates, which may be absorbed to the regenerated cellulose membrane utilized due to marked hydrophobic interactions. For heat stressed samples the monomer amount was decreased from 97.3 % initially, to approx. 60 % (60°C 20min/40min), to 84 % (F/T 20 cycles) and to 48 % (light 2d) (Fig.1d). The amount of oligomers was increased and reached the highest extent for light 2d stressed samples with an amount of 38 %. Temperature stressed samples showed an amount of 26 % oligomers after 40 min. In pH 1.1 stressed samples approx. 4 % of oligomers were found, which was quantitatively as much as the remaining monomer. F/T stressed samples showed hardly any oligomer formation (1 %). The amount of fragments was consistent at approx. 1.5 – 2 %.

A molecular weight for the initial monomer of 149.73 kDa was calculated from the MALLS data. Oligomers appearing in the initial and the F/T stressed sample showed a molecular weight of approximately 270 – 300 kDa, which reflects a dimeric state. The oligomers induced in the thermal and light stressed samples showed a higher molecular weight of 500 and 560 kDa respectively indicating the formation of trimers and higher multimeric species. The fragments were calculated to have a molecular weight of approx. 45 kDa to 65 kDa for initial and heat stressed samples. The fragments appearing in the light stressed samples showed a molecular weight of 115 kDa.

3.4 SDS-PAGE

The reducing SDS-PAGE showed for all samples the light and the heavy chain. For light stressed samples also aggregates of approx. 300 – 450 kDa could be detected (data not shown) indicating the formation of covalently linked aggregates.

3.5 Fluorescence Spectroscopy

In batch mode extrinsic dye fluorescence intensity was increased for all stressed samples. The highest increase occurred in pH 3.1, pH 1.1, thermal and shaking stressed samples. In addition, it could be shown that larger particles (> 5 μm)

contribute to the fluorescence intensity since after filtration the intensity for all tested stressed samples dropped down by approx. 50 % (Fig.1e). The fluorescence intensity observed in the F/T stressed samples was almost only due to larger particles as it could be reduced to starting material level by filtration. This is in good accordance to the data obtained in the SEC (see 3.7), where no fluorescence signal increase in monomer and soluble aggregates was observed for F/T and shaken stressed samples. The pH, heat and light stressed samples, however, also showed a fluorescence signal in the SEC analysis due to their conformationally altered oligomers and monomer. To avoid loss of BisANS due to adsorption to the filters, BisANS was added after the filtration step. Substantial adsorption of BisANS binding protein species can be ruled out due to the high protein concentrations used and the low protein binding of the filters of 5 µm pore size used.

_____

a)

b)

c)

d)

_____

e)
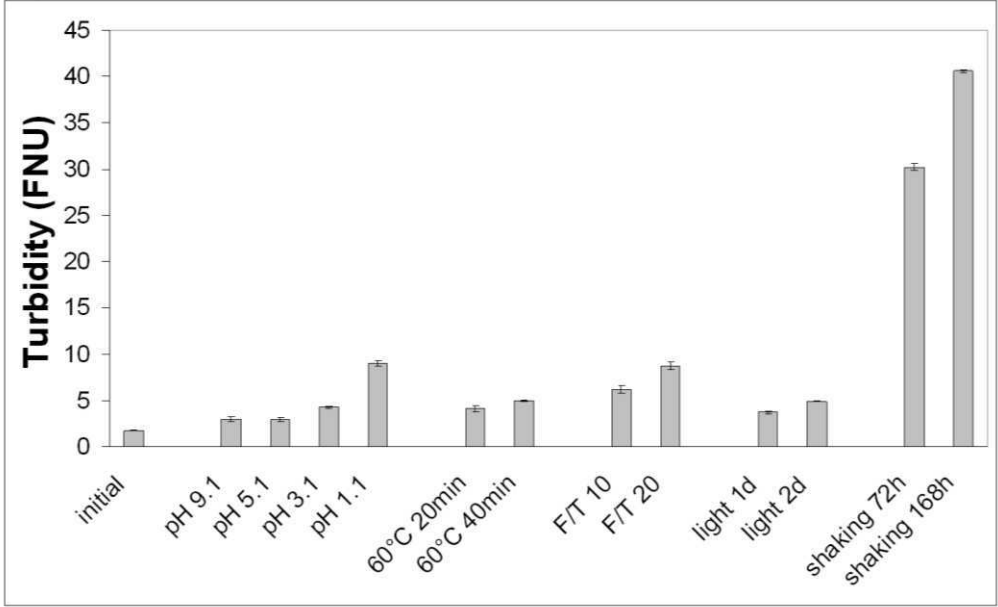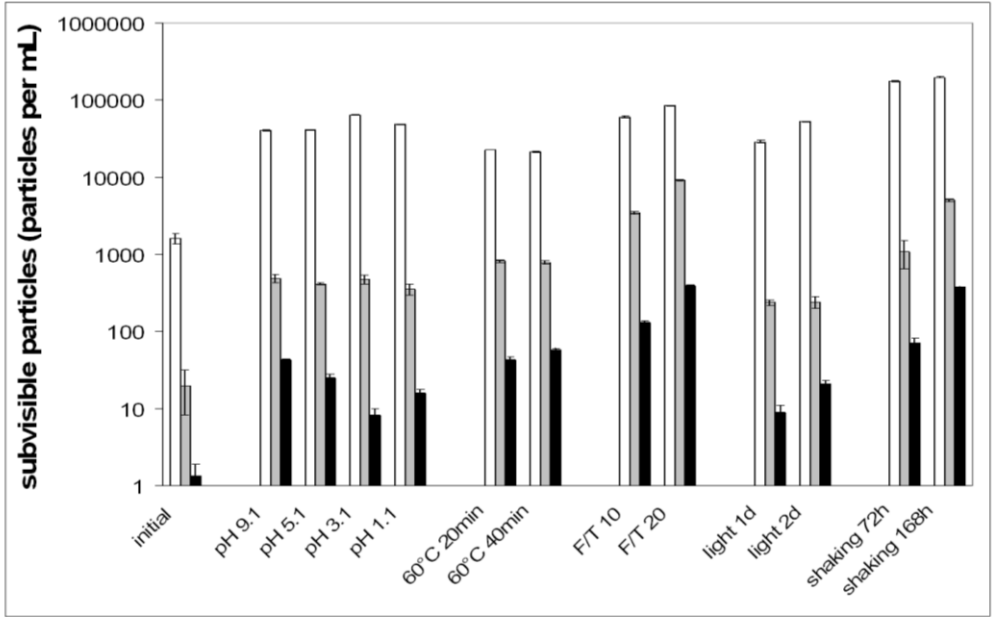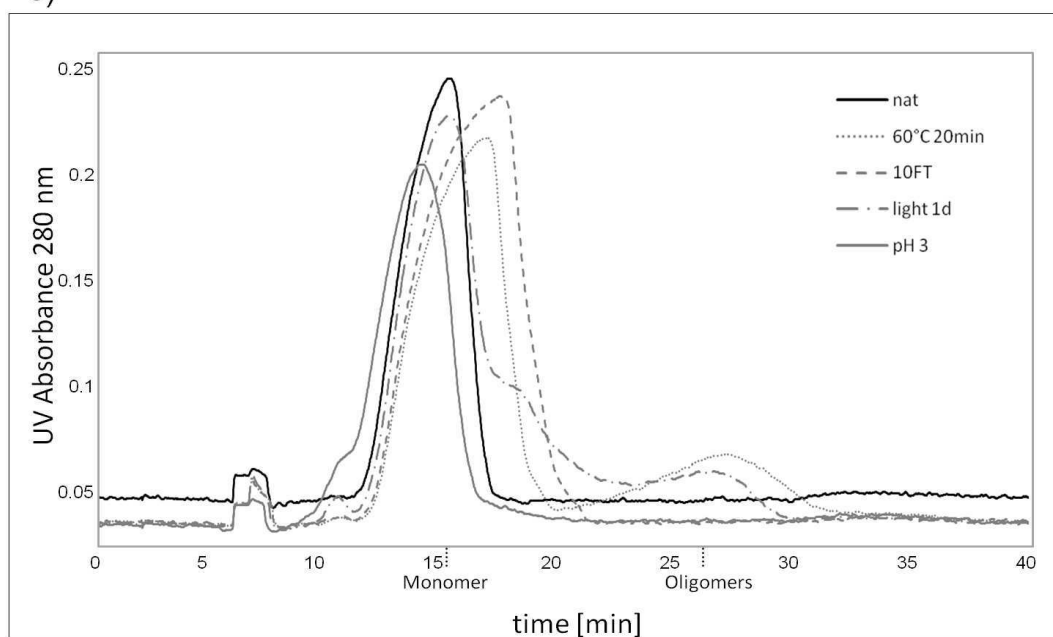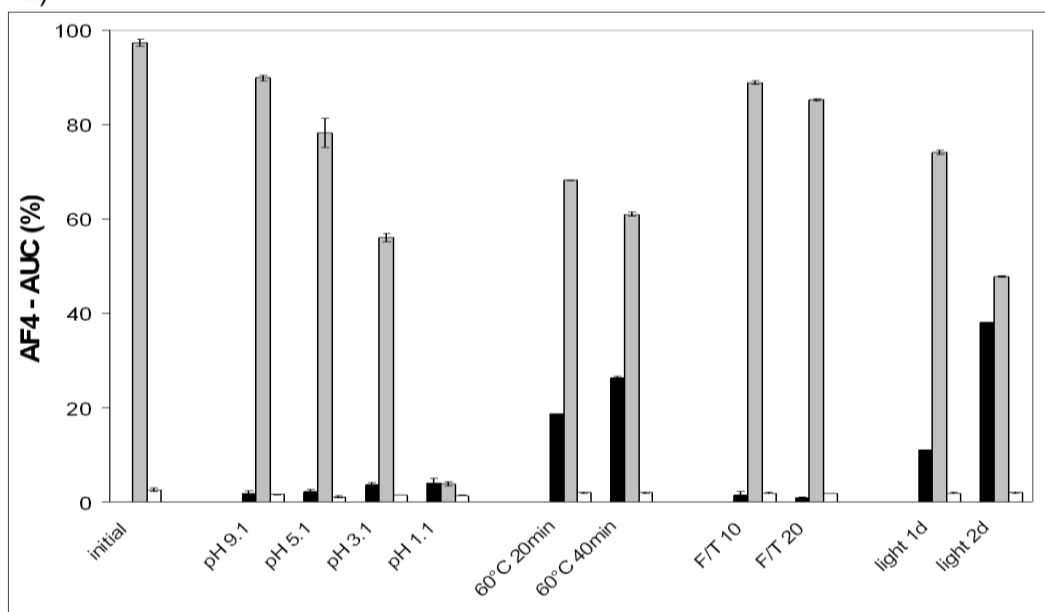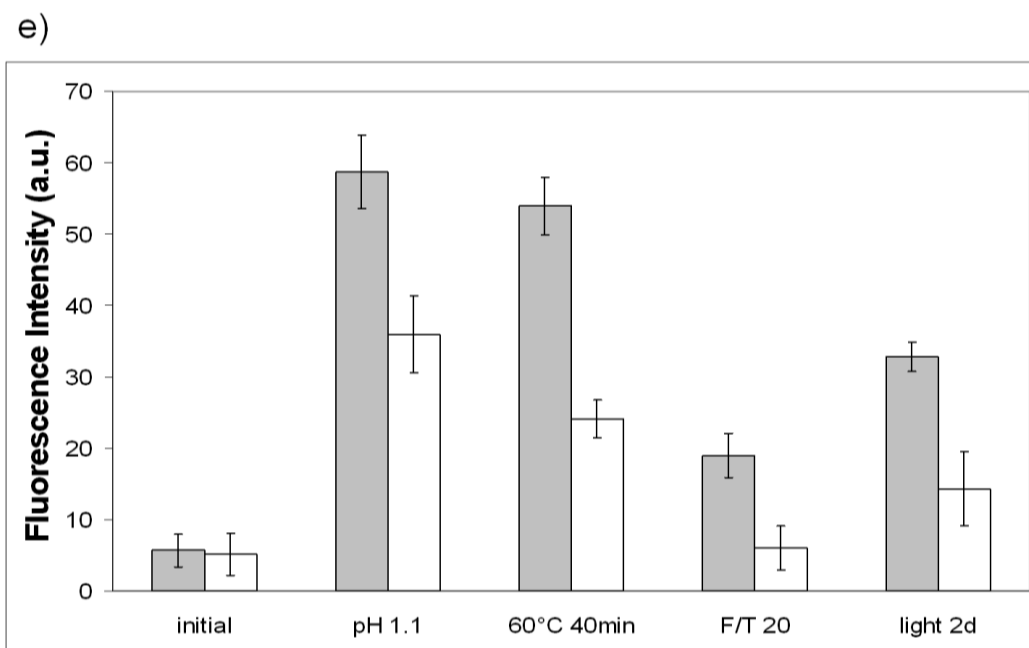
Figure 1: a) Turbidity as measured in IgG samples after stress exposure in batch mode. b) Sub-visible particles per mL > 1 µm (white), > 10 µm (grey) and > 25 µm (black) as measured in IgG samples after stress exposure showing an average of three measurements and standard deviations. c) Exemplary AF4-UV chromatograms of IgG samples for the initial solution, and after temperature (20min 60°C), F/T (10 cycles), light (24h), and pH (pH 3) stress exposure at λ=280 nm and d) Percentage of oligomers (black), monomer (grey) and fragments (white) in IgG samples after stress exposure as analyzed by AF4 separation and UV detection. e) Extrinsic fluorescence spectroscopy in batch mode for IgG samples after stress exposure (black) and after 5 µm filtration (white).

3.6 SEC with UV detection

To detect and quantify oligomers, fragments and monomers after stress, SEC with UV detection at 280 nm was used. In the bulk material a small amount of < 1 % oligomers and fragments was present. The chromatograms obtained after stress exposure of the protein samples differed significantly. As seen in the exemplarily given chromatograms in Figure 2a the obtained peaks showed qualitative and quantitative differences which were stress dependent. Whereas the heat stressed samples showed only one induced oligomer peak, the induction of several different oligomer peaks was observed for pH and light stressed samples. Oligomers were not

detected in F/T and shaking stressed samples, which is in good accordance to previously published work [4, 5]. In the pH stressed samples a decrease of remaining monomer from 98.8 % for pH 9.1 to 9.2 % for pH 1.1 (91.2 % / pH 5.1, 88.5 % / pH 3.1) was observed (Fig.2b). The monomer amount in the temperature stressed samples dropped down to 64.7 % after 40 min. For the F/T stressed samples a remaining monomer amount of 80.9 % after 20 cycles was obtained. Light stressed samples showed a remaining monomer amount of 40.0 % after 2 days of light exposure. In shaken stressed samples a monomer amount of 88.6 % after 168h of shaking remained. The oligomer amount of the F/T and shaken stressed samples was hardly increased, whereas the oligomer amounts of the pH stressed samples (61.6 % for pH 1.1), temperature stressed samples (37.1 % after 40 min) and light stressed samples (61.5 % after 2 days of light exposure) were significantly increased. Substantial formations of fragments were observed in pH 1.1 (14 %), F/T 20 (1.3 %), and light 2 days (4.2 %) samples. The other samples showed less than 1 % fragments. A total recovery > 90% was observed for most samples, only for F/T and shaking stressed samples a total recovery < 90% resulted due to the formation of insoluble particles.

Thus, the stress methods induce the formation of protein aggregates to a different extent and in various size ranges. Whereas, F/T and shaking lead to pronounced formation of sub-visible particles but remain essentially free of oligomers, pH, heat and light stress induced different quantities and qualities of oligomers. The results regarding amount, size and conformation are in accordance to previous published work by Kiese et al. who also describe the rather native like appearance of particles after shaking stress [4] and Hawe et al. who described conformational differences between particles induced by heat and by freeze thaw stress [5]. Whether the samples also differ in their degree of unfolding was to be analysed further.
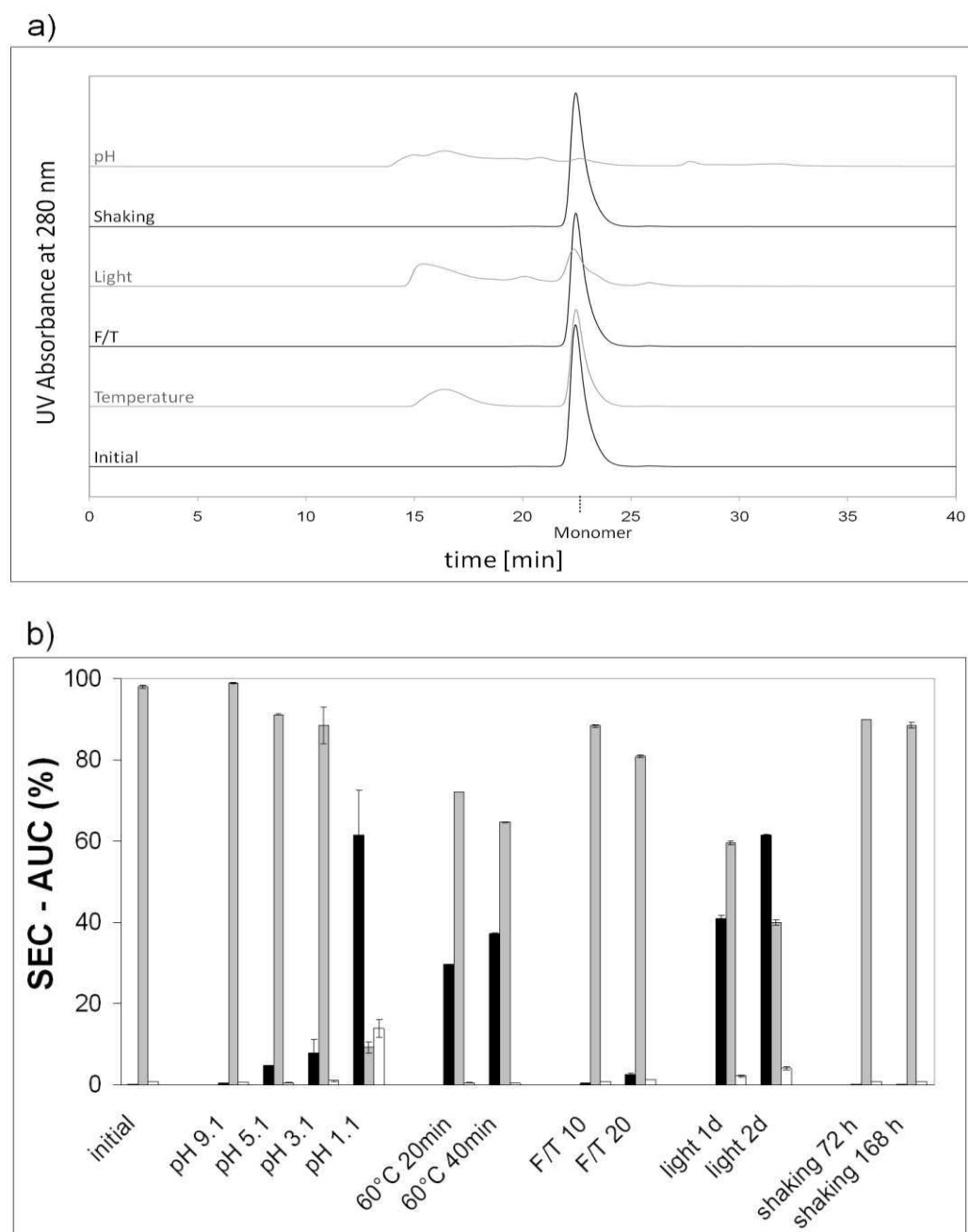
Figure 2: a) Exemplary SEC-UV chromatograms of IgG samples for the initial solution, and after temperature (40min 60℃), F/T (20 cycles), light (48h), shaking (168h) and pH (pH 1.1) stress exposure at λ=280 nm and b) AUC % of IgG oligomers (black), monomer (grey) and fragments (white) as measured after stress exposure.

3.7 SEC-PCM with fluorescence detection

Protein conformational changes were observed by bulk fluorescence analysis (see 3.5). Conformational changes in the protein structure were also confirmed by a study on the same protein which demonstrated that FTIR, although not sensitive enough to pick up changes after storage for 24h at 55 °C, detected structural changes and unfolding after thermal treatment for 1 h at 70 ° [34]. Thus the method appers to be more sensitive than FTIR with respect to pick of conformational changes.

Looking at the fluorescence chromatograms gained simultaneously with the SEC-UV data, the PCM method revealed fluorescence peaks for oligomers formed in the temperature, light and pH stressed samples (Fig.3a). Additionally, an increase in the monomer fluorescence peak of these samples was observed. The highest fluorescence increase was observed for the oligomers present in the pH 1.1 sample showing a total AUC of 7660 a.u. (pH 3.1 / 362 a.u., pH 5.1 / 87.9 a.u.) (Fig.3b). No oligomer fluorescence was observed at pH 9.1 as well as for F/T and shaking stressed samples. This is in accordance with literature, which also described the formation of native like oligomers after the exposure of protein to these types of stresses [4, 5, 6]. Oligomers in the temperature stressed samples showed an AUC of 1591 a.u. after 20 min and 2148 a.u. after 40 min at 60°C. Oligomers induced by light stressed also showed substantial fluorescence (633 a.u. / 1 day, 2087 a.u. / 2 days). These observations correspond to Matheus et al. who proofed conformational changes after thermal stress by FTIR [34] and to the fluorescence spectroscopy data. Here, the fluorescence of the F/T sample after filtration was at the level of the starting material indicating that only larger particles induced the fluorescence increase in the F/T samples prior to filtration and the monomer remained unchanged. Whereas the monomers in the initial, F/T and shaken samples gave fluorescence peaks with an AUC of approx. 27 a.u., the monomer fluorescence peaks in the temperature, light and pH stressed samples were increased, which is again in accordance with previously published work [4, 5, 6]. Temperature stressed samples showed a moderate increased monomer fluorescence peak (20 min / 40.7 a.u., 40 min / 53.7 a.u.). The monomer fluorescence peak of the light stressed samples was increased to an AUC of 180.8 a.u. after 1 day and 345.3 a.u. after 2 days of light

_____

exposure. The highest increase in monomer fluorescence was again observed in the pH stressed samples. The pH 1.1 sample showed a monomer peak AUC of 2345.9 a.u. (pH 9.1 / 34.4 a.u., pH 5.1 / 117.5 a.u., pH 3.1 /1043.6 a.u.).

The UV quantification and the corresponding fluorescence data did not correlate linearly. The highest degree of protein-dye interaction leading to fluorescence intensity is seen for pH 1 stressed samples (approx. 60 % oligomers resulting in 7660 a.u. fluorescence) followed by the temperature stress samples with 30 % and 36 % oligomers after 20 and 40 min resp. with a fluorescence intensity of 1592 a.u. and 2148 a.u and finally the light stressed samples (approx. 40 % oligomers day 1 and 60 % day 2 with fluorescence of 633 a.u. and 2087 a.u. resp.). A strong discrepancy between UV and fluorescence signal was also observed for the remaining monomer in the pH 1.1 stressed samples, where < 10 % gave the highest fluorescence signal of 2346 a.u. This indicates that monomer and oligomers differ in their conformational change stressing the fact of the diversity of inducible protein aggregates, which was traceable with our SEC-PCM method. With this additional fluorescence data set we were able to provide supplementary information about protein structure of monomers and oligomers simultaneously without the need of any further separate analytical tools. Furthermore, compared to batch mode fluorescence spectroscopy, due to prior size separation in our PCM approach, an increase in fluorescence intensity could be assigned to the different protein species and partial unfolding of protein monomers as well as the change of conformation in formed oligomers were sensitively detected. Other methods to determine the conformation change of the aggregates would at first require a separation process followed by sampling and further analysis. The quantities of aggregates yielded would not allow for adequate standard FTIR-, Raman- or CD-analysis and furthermore all three methods are limited with respect to their sensitivity to detect only a low percentage of structural change [5, 34]. The unfolding effect of the monomer, similarly is not traceable by any other commonly used detection method, but it indicates that monomer species do partially denature without aggregating, which may be overlooked with the typical bunch or analytical methods used. Monomer unfolding is important information which should be routinely gathered in protein formulation studies.

In general, SEC elution profiles are affected by the eluent and its salt concentration. The dye protein interaction is considered to be unaffected in the typically used ionic strength range. But overall, the potential general effect of SEC, the eluent and the interaction with the column material on protein aggregate analysis has to be considered [35], but the post column module is not expected to add to these concerns. Fluorescent dyes might interfere with protein aggregation. Literature shows examples for both inhibition and promotion of protein aggregation and the effect is even more dramatic when dye is present during stress exposure [32]. Thus, it is therefore beneficial adding the dye after size separation and UV detection to the protein sample. For post column addition a final concentration of 6 µM BisANS is required. This compares well to the concentration used by Hawe et al. and applied in other extrinsic dye protein fluorescence analysis [5, 26]. For establishing the new approach of the dye addition after column separation we focused on BisANS. However, by adding other dyes via our presented PCM method to the size separated protein such as Thioflavin T and Congo Red, which are used in protein amyloidal fibrils analysis, DCVJ and CCVJ, which are sensitive to protein viscosity, or SYPRO Orange and SYPRO Red, which are used for fluorescence based thermal shift assays, further new insights in protein behavior could be gained. In addition, the user might also consider adding further detectors such as RI or MALLS prior to the PCM fluorescence detection, where the dye might interfere with correct analysis. As the dye is added prior to the fluorescence detection, the PCM does not interfere with any necessary prior detection method.

a)

b)
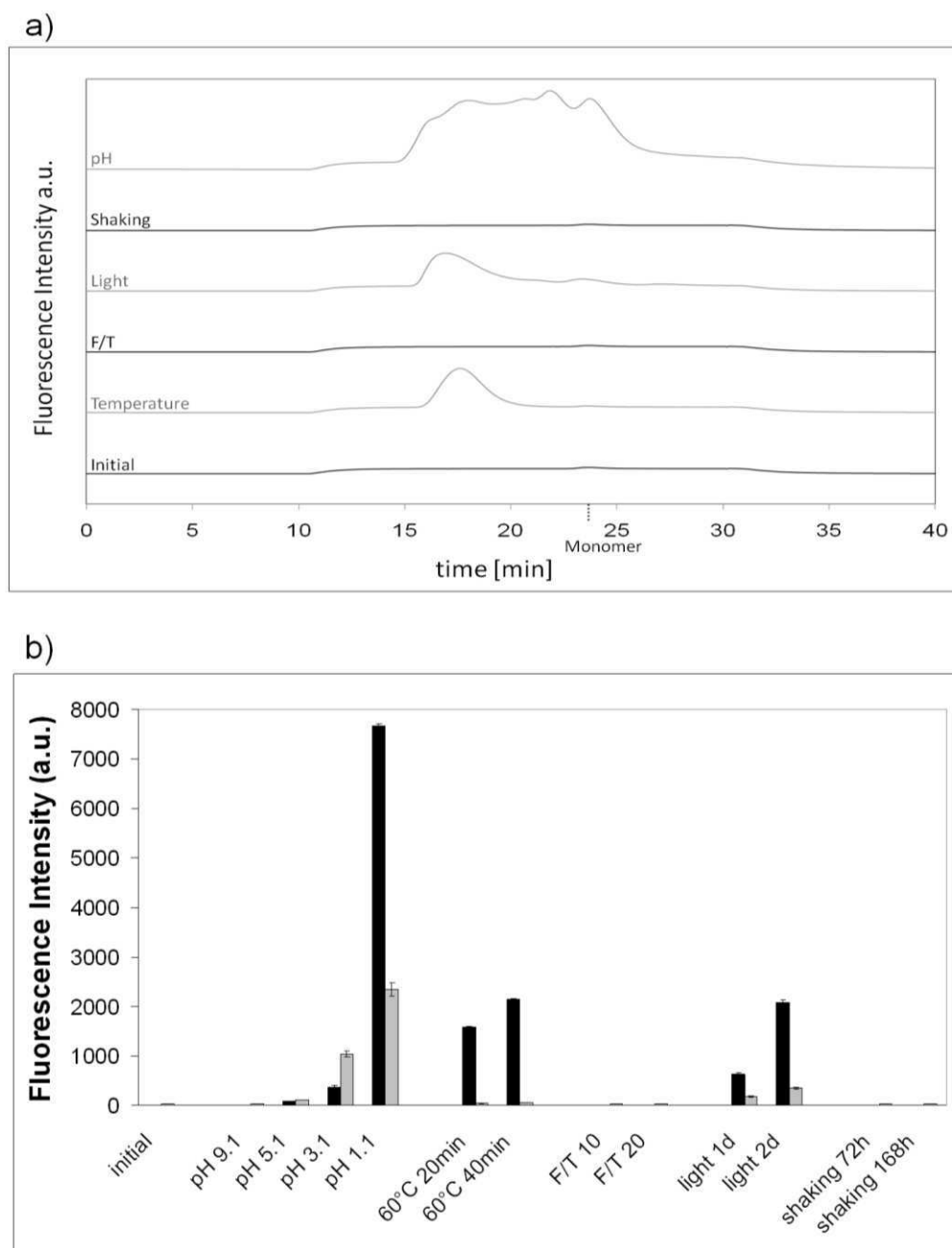
Figure 3: a) Exemplary SEC-PCM fluorescence chromatograms of IgG samples for the initial solution, and after temperature (40min 60°C), F/T (20 cycles), light (48h), shaking (168h) and pH (pH 1.1) stress exposure at the excitation λ=385 nm and the emission λ=485 nm and b) Fluorescence intensity of protein oligomers (black) and unfolded monomer (white) as measured after stress exposure of the protein and the addition of the fluorescence dye BisANS.

3.8 SEC-PCM with fluorescence detection of samples containing PS20

To investigate a possible effect of PS20 on our fluorescence analytics and to test whether the SEC-PCM method would be superior to spiking the samples prior to SEC analytics, we compared both approaches. At first, placebo buffer samples were analysed. In both setups, PCM and prior spiking, PS20 micelles could be visualized at 0.1% and 0.5% PS20. Via fluorescence detection a strong signal was obtained due to incorporation of BisANS into the micelles. The UV detector observed a weak signal, which resulted from light scattering and UV absorption.

In samples containing heat stressed protein, fluorescence signals of both monomer and oligomers were detected in both approaches (Fig.4). Thus, both approaches enable to simultaneously gain and combine the information on size and denaturation state of the different protein species. Due to the dye loss and dilution effects of the dye spiked into the samples prior to the run during SEC, the intensities were higher in the PCM method. Clearly, the oligomers signals in the samples spiked with BisANS prior to SEC decreased with increasing surfactant concentrations. This points to an interference of higher surfactant concentrations with correct analysis. Consequently, the high PS20 concentration affects the BisANS-protein interaction most likely due to dye binding. In contrast, the oligomer signal did stay consistent in the PCM setup for PS20 concentrations between 0.001 % and 0.1 %. Only for samples with a 0.5% PS20 concentration, which is above the concentration typically used in protein formulation, a slight decrease of the oligomer signal and an overlap of the monomer fluorescence signal by the PS20 micelle peak were observed. Figure 5 exemplarily shows the SEC fluorescence chromatograms and demonstrates that at a concentration of 0.05% PS20, which is relevant for formulation development, the spiking method clearly renders erroneous data.

_____
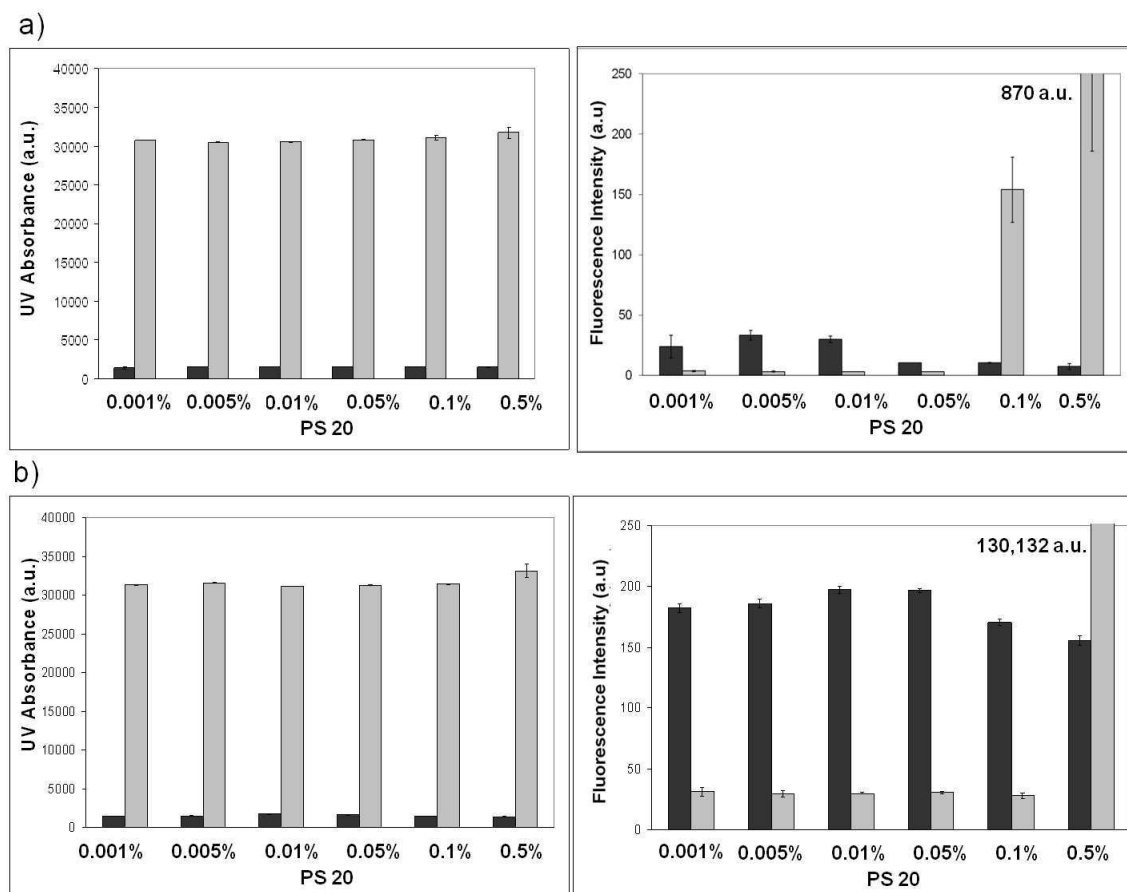
Figure 4: UV absorbance (λ=280 nm) and fluorescence intensities (excitation λ=385 nm, emission λ=485 nm) given in arbitrary units (a.u.) for oligomers (black) and monomer / micelles (grey) in IgG formulations containing PS20 gained after stress exposure (60 °C 15min) and by a) spiking the sample prior to SEC with the fluorescent dye BisANS and b) adding the fluorescent dye BisANS via PCM after size separation.

This is in accordance with other literature, where dyes are used to determine the CMC, as they are incorporated starting at CMC [36-38]. Another approach to avoid the dye-surfactant interaction was shown by Hawe et al. where fluorescent molecular rotors (DCVJ and CCVJ) were suitable dyes to detect aggregation in polysorbate containing IgG formulations [39]. However, the post column addition of the fluorescent dye enables the use of BisANS, which is still considered to be the most sensitive dye in protein aggregation analysis [25].

Interestingly, in the UV detection the monomer AUC and its standard deviation increased at PS20 concentrations of 0.1 and 0.5% (Fig.4). This effect can clearly be attributed to the formed micelles overlaying with the monomer peak potentially leading to an underestimation of the relative oligomer amount in the sample.

Thus, long interaction times of BisANS with protein as well as with other formulation components such as surfactants have to be avoided as they potentially lead to artifacts in, e.g., UV and fluorescence detection. Therefore, it is recommended to use the PCM method and add BisANS after SEC column separation and UV detection prior to fluorescence detection.

_____
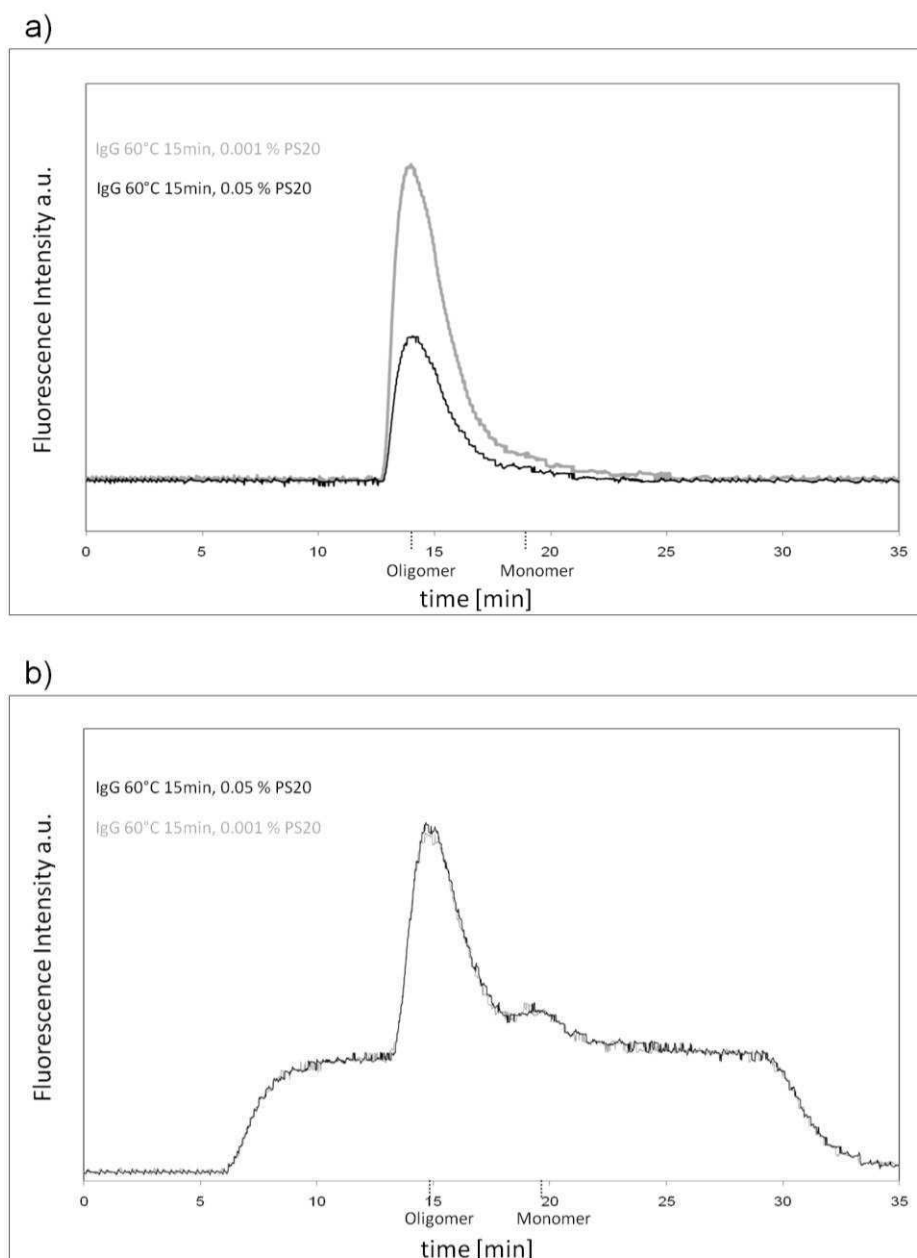
Figure 5: Exemplary SEC fluorescence chromatograms (excitation λ=385 nm, emission λ=485 nm) of the IgG solution after stress exposure (60°C 15min) containing 0.001% (grey line) or 0.05 % (black line) PS20 gained by a) spiking the sample prior to SEC with the fluorescent dye BisANS and b) adding the fluorescent dye BisANS via PCM after size separation.

4 CONCLUSION

The presented novel SEC based approach of using the combination of UV and fluorescence detection with post column addition of BisANS allows an easy monitoring of protein unfolding simultaneously with size analysis and quantification. The assignation of fluorescence increase and thereby unfolding became possible to monomer and/or oligomers specifically. The presented post column addition of the fluorescence dye avoids i) long interaction times of BisANS with protein as well as with other formulation components, such as surfactants, and ii) interferences with size separation and prior detectors potentially leading to artifacts. The aggregates formed upon the chosen different stress methods differed quantitatively and qualitatively, which is in good accordance with previously published literature [10, 11, 34]. For pH, temperature and light stressed samples the formation of oligomers was detected and via PCM an increase in fluorescence for both oligomers and monomer were observed. Whereas acidic pH, temperature and light stress resulted mostly in the formation of unfolded oligomers, F/T and shaking stress induced only few native-like soluble aggregates, but a large number of particles > 1 µm. By assigning increased fluorescence specifically to the monomer or the oligomers, the fluorescence signal revealed partial unfolding of the monomer fraction of pH, temperature and light stressed antibody formulation and allowed to differentiate the degree of unfolding. This effect is not traceable by the commonly used detection methods. But its monitoring might provide important information, which still needs to be linked to long term stability.

5 ACKNOWLEDGEMENT

6 REFERENCES

[1]   Mahler HC, Friess W, Grauschopf U, Kiese S. Protein aggregation: Pathways, induction factors and analysis. Journal of Pharmaceutical Sciences (2009), 98(9), 2909-2934.

[2]   Schellekens H. Factors influencing the immunogenicity of therapeutic proteins. Nephrology, Dialysis, Transplantation (2005), 20(Suppl. 6), vi3-vi9.

[3]   Rosenberg AS. Effects of protein aggregates: an immunologic perspective. AAPS Journal (2006), 8(3).

[4]   Kiese S, Papppenberger A, Friess W, Mahler H-C. Shaken, not stirred: mechanical stress testing of an IgG1 antibody. Journal of Pharmaceutical Sciences (2008), 97(10), 4347-4366.

[5]   Hawe A, Kasper JC, Friess W, Jiskoot W. Structural properties of monoclonal antibody aggregates induced by freeze-thawing and thermal stress. European Journal of Pharmaceutical Sciences (2009), 38(2), 79-87.

[6]   Mahler HC, Mueller R, Friess W, Delille A, Matheus S. Induction and analysis of aggregates in a liquid IgG1-antibody formulation. European Journal of Pharmaceutics and Biopharmaceutics (2005), 59(3), 407-417.

[7]   Sharma VK, Kalonia DS. Temperature- and pH-Induced Multiple Partially Unfolded States of Recombinant Human Interferon-alpha 2a: Possible Implications in Protein Stability. Pharmaceutical Research (2003), 20(11), 1721-1729.

[8]   Saluja A, Badkar AV, Zeng DL, Kalonia DS. Ultrasonic rheology of a monoclonal antibody (IgG2) solution: implications for physical stability of proteins in high concentration formulations. Journal of Pharmaceutical Sciences (2007), 96(12), 3181-3195.

[9]   Yadav S, Liu J, Shire SJ, Kalonia DS. Specific interactions in high concentration antibody solutions resulting in high viscosity. Journal of Pharmaceutical Sciences (2010), 99(3), 1152-1168.

[10] Joubert MK, Luo Q-Z, Nashed-Samuel Y, Wypych J, Narhi LO. Classification and Characterization of Therapeutic Antibody Aggregates. Journal of Biological Chemistry (2011), 286(28), 25118-25133.

[11] Luo Q, Joubert MK, Stevenson R, Ketchem RR, Narhi LO, Wypych J. Chemical Modifications in Therapeutic Protein Aggregates Generated under Different Stress Conditions. Journal of Biological Chemistry (2011), 286, (28), 25134-25144.

[12] Abdul-Fattah AM, Lechuga-Ballesteros D, Kalonia DS, Pikal MJ. The impact of drying method and formulation on the physical properties and stability of methionyl human growth hormone in the amorphous solid state. Journal of Pharmaceutical Sciences (2007), 97(1), 163-184.

[13] Piedmonte DM, Summers C, McAuley A, Karamujic L, Ratnaswamy G. Sorbitol Crystallization Can Lead to Protein Aggregation in Frozen Protein Formulations. Pharmaceutical Research (2007), 24(1), 136-146.

[14] Bhatnagar BS, Pikal MJ, Bogner RH. Study of the individual contributions of ice formation and freeze-concentration on isothermal stability of lactate dehydrogenase during freezing. Journal of Pharmaceutical Sciences (2007), 97(2), 798-814.

[15] Kueltzo LA, Wang W, Randolph TW, Carpenter JF. Effects of solution conditions, processing parameters, and container materials on aggregation of a monoclonal antibody during freeze-thawing. Journal of Pharmaceutical Sciences (2008), 97(5), 1801-1812.

[16] Strambini GB, Gabellieri E. Proteins in frozen solutions: evidence of ice-induced partial unfolding. Biophysical Journal (1996), 70(2), 971-6.

[17] Strambini GB, Gonnelli M. Protein stability in ice. Biophysical Journal (2007), 92(6), 2131-2138.

_____

[18] Gabellieri E, Strambini GB. Perturbation of protein tertiary structure in frozen solutions revealed by 1‑anilino‑8‑naphthalene sulfonate fluorescence. Biophysical Journal (2003), 85(5), 3214‑3220.

[19] Chang BS, Kendrick BS, Carpenter JF. Surface-induced denaturation of proteins during freezing and its inhibition by surfactants. Journal of Pharmaceutical Sciences (1996), 85(12), 1325-30.

[20] Serno T, Carpenter JF, Randolph TW, Winter G. Inhibition of agitation-induced aggregation of an IgG-antibody by hydroxypropyl-.beta.-cyclodextrin. Journal of Pharmaceutical Sciences (2010), 99(3), 1193-1206.

[21] Chi EY, Weickmann J, Carpenter JF, Manning MC, Randolph TW. Heterogeneous nucleation-controlled particulate formation of recombinant human platelet-activating factor acetylhydrolase in pharmaceutical formulation. Journal of Pharmaceutical Sciences (2005), 94(2), 256-274.

[22] Tyagi AK, Randolph TW, Dong A, Maloney KM, Hitscherich C Jr, Carpenter JF. IgG particle formation during filling pump operation: a case study of heterogeneous nucleation on stainless steel nanoparticles. Journal of Pharmaceutical Sciences (2009), 98(1), 94-104.

[23] Frokjaer S, Otzen DE. Protein drug stability: a formulation challenge. Nature reviews. Drug Discovery (2005), 4(4), 298-306.

[24] Kiese S, Pappenberger A, Friess W, Mahler HC. Equilibrium studies of protein aggregates and homogeneous nucleation in protein formulation. Journal of Pharmaceutical Sciences (2010), 99(2), 632-644.

[25] Hawe A, Sutter M, Jiskoot W. Extrinsic Fluorescent Dyes as Tools for Protein Characterization. Pharmaceutical Research (2008), 25(7), 1487-1499.

[26] Hawe A, Friess W, Sutter M, Jiskoot W. Online fluorescent dye detection method for the characterization of immunoglobulin G aggregation by size exclusion chromatography and asymmetrical flow field flow fractionation. Analytical Biochemistry (2008), 378(2), 115-122.

[27] Demeule B, Gurny R, Arvinte T. Detection and characterization of protein aggregates by fluorescence microscopy. International Journal of Pharmaceutics (2007), 329(1-2), 37-45.

[28] Gabellieri E, Strambini GB. ANS fluorescence detects widespread perturbations of protein tertiary structure in ice. Biophysical Journal (2006), 90(9), 3239-3245.

[29] Kumar V, Sharma VK, Kalonia DS. Second derivative tryptophan fluorescence spectroscopy as a tool to characterize partially unfolded intermediates of proteins. International Journal of Pharmaceutics (2005), 294(1-2), 193-199.

[30] Jiskoot W, Crommelin DJ A. Methods for Structural Analysis of Protein Pharmaceuticals. Biotechnology: Pharmaceutical Aspects. (2005)

[31] Matulis D, Lovrien R. 1-Anilino-8-naphthalene sulfonate anion-protein binding depends primarily on ion pair formation. Biophysical Journal (1998), 74(1), 422-429.

[32] Fu X, Zhang X, Chang Z. 4,4-Dianilino-1,1-binaphthyl-5,5-sulfonate, a novel molecule having chaperone-like activity. Biochemical and Biophysical Research Communications 329 (2005), 1087–1093.

[33] Arakawa T, Ejima D, Li T, Philo JS. The critical role of mobile phase composition in size exclusion chromatography of protein pharmaceuticals. Journal of Pharmaceutical Sciences (2010), 99(4), 1674-1692.

[34] Matheus S, Mahler H-C, Friess W. A Critical Evaluation of T m(FTIR) Measurements of High-Concentration IgG1 Antibody Formulations as a Formulation Development Tool. Pharmaceutical Research (2006), 23,(7), 1617-1627.

[35] Carpenter JF, Randolph T, Jiskoot W, Crommelin DJA, Middaugh CR, Winter G. 2010. Potential Inaccurate Quantitation and Sizing of Protein Aggregates by Size Exclusion Chromatography: Essential Need to use Orthogonal Methods to Assure the Quality of Therapeutic Protein Products. Journal of Pharmaceutical Science (Commentary). 99(5): 2200-2208.

_____

[36] Moore A, Harris AA, Palepu RM. Spectroscopic investigations on the binding of ammonium salt of 8-anilino-1-naphthalene sulfonic acid with non-ionic surfactant micelles in aqueous media. Fluid Phase Equilibria (2007), 251(2), 110-113.

[37] Joshi HD. A study of CMC and λmax values of binary systems of cationic surfactants and dyes: Part- 1. Journal of the Institution of Chemists (India) (1999), 71(1), 26-27.

[38] Zhang P, Wu Y, Li L, Zheng H. Estimation of critical micelle concentration of nonionic surfactants based on fluorescence mutation of a near-infrared hydrophobic cyanine dye. Anhui Shifan Daxue Xuebao, Ziran Kexueban (2005), 28(1), 68-71.

[39] Hawe A, Filipe V, Jiskoot W. Fluorescent Molecular Rotors as Dyes to Characterize Polysorbate-Containing IgG Formulations. Pharmaceutical Research (2010), 27(2), 314-326.

CHAPTER 4

Kinetics of Protein Aggregates during Storage

ABSTRACT

Protein formulations tend to aggregate, especially while being exposed to stress. It was shown earlier (Chapter 3) that different stress methods lead to the formation of aggregates which differ with respect to size, amount and conformation. The question addressed in this chapter is whether or not these induced protein aggregates are stable over time or change in number and/or size. Formed protein aggregates are discussed to function as possible nuclei in the protein solution and thereby enhance protein aggregation over time. In this work the focus was on the aggregates formed from an IgG1 in 10mM phosphate buffer, 140 mM NaCl, pH 7.2. Induced by different stress methods, possible changes in the protein aggregates were traced quantitatively and qualitatively while being stored at 4-6°C over three months. Different analytical methods were employed to cover a broad protein aggregate size range. The formation of oligomers, fragments and the remaining monomer as well as changes in protein tertiary structure were monitored using SEC with UV and SEC-PCM (post column derivatisation module) with fluorescence detection after dye addition. Light obscuration particle counting and nephelometric measurements provided insights into the alterations of sub-visible protein particles larger than 1 μm. The aggregates formed under the different stress methods were distinctly different quantitatively and qualitatively. A continuation of the unfolding or aggregation process over time was not observed for any of the induced aggregates. In case of pH, heat, freeze-thaw and light stressed samples the amount of visible particles increased over time.

---

1 INTRODUCTION

The control of protein aggregation is challenging. A better understanding of aggregation behavior is desired, as protein aggregates are supposed to be less active and might affect the immune responses in the patient [1; 2]. Given the wide range of causes and impact of protein aggregation and the variety of induction factors, aggregation pathways [3] are of particular interest. Discovering, quantifying and qualifying aggregation behavior and possible changes in the protein aggregates over time might provide further insight. Especially for long term storage, it would be relevant to discover reasons and induction factors for protein aggregation and particle growth. Whether aggregation induction factors stem from the formulation conditions itself (pH, ionic strength, surfactants) or appear during the fill and finish process (contact to diverse surfaces, mechanical stress during filtration and pumping, sheds from heterogeneous material), is still questioned.

Exogenous surfaces/particles might function as nuclei or enhance aggregation [4-7]. Chi et al. [4] observed the induction and growth of protein aggregates in a recombinant human platelet-activating factor acetylhydrolase (rhPAF-AH) by exogenous nano-sized hydrophilic silica particles through a heterogenous nucleation-controlled mechanism. The induction and progress in the formation of protein aggregates was not observed after filtration or by adding aggregated rhPAF-AH. As driving force the protein-surface interaction was identified. Tyagi et al. [5] identified heterogeneous particles, such as stainless steel nanoparticles shed from filling pumps, as nuclei for the formation of protein aggregates. Frokajaer et al. [6] postulate anionic surfaces to enhance protein aggregation and fibrillation through negatively charged phospholipid vesicles, anionic surfactants and carboxylate-modified polystyrene beads.

In addition, Chang et al. [7] as well postulated a rather surface induced denaturation of protein during freezing, which could be inhibited by adding a surfactant. Hence, foreign surfaces like air or nanoparticles out of foreign, non-proteineous materials, such as hydrophilic silica or stainless steel or other anionic surfaces, are supposed to function as nuclei and induce protein aggregation.

However, aggregated protein molecules did not show any nucleation or aggregation enhancement effect in a study by Kiese et al. [8]. Moreover, the insoluble protein aggregates induced by shaking stress were considered to be reversible and to dissociate over time. However, there is evidence that protein itself might function as nucleus [9], since non-native aggregate nucleation and growth under acidic conditions for samples of alpha-chymotrypsinogen A both seeded with aggregates and un-seeded were observed.

Thus, the analysis of the kinetics of protein aggregates during long term storage was of interest to answer the question, whether protein aggregates once formed during a manufacturing process in small quantities have the ability to grow and increase in number and in size until the biopharmaceutical product reaches the patient. Hence, our approach was the monitoring of IgG1 aggregates over time. The aggregates were induced by various stress methods in a 2 mg/mL IgG1 solution in 10 mM phosphate buffer, 140 mM NaCl, pH 7.2. The aggregate amount and size distribution was analyzed during storage at 4-6°C up to 3 months. As different stress methods lead to diverse aggregate species varying quantitatively and qualitatively we selected four different stress methods, namely pH, thermal, freeze/thaw, and light stress. For quantification and size estimation of oligomers, fragments and remaining monomer, SE-HPLC was employed. Light obscuration measurements were used to observe changes in larger protein aggregates > 1 µm [3; 10]. Unfolding of monomer and soluble aggregates was studied via the post-column-module method with fluorescence detection after Bis-ANS addition

_____

2 MATERIALS AND METHODS

2.1 Materials

A glycosylated IgG1 (148 kDa) at 2 mg/ml in 10 mM phosphate buffer containing 140 mM NaCl at pH 7.2 (further called PBS) was donated by Merck, Germany. The protein content of the solution was determined by UV absorption at 280nm (e_1 = 1.4 $(mg/mL)^{-1}cm^{-1}$). BisANS powder (SIGMA, Sigma-Aldrich Chemie GmbH, Germany) for extrinsic fluorescence detection was dissolved in PBS for further use as a stock solution with a concentration of 23.5 µM. Final solution concentration was measured by UV absorption at 385 nm (e_2 = 16750 $(mol)^{-1}cm^{-1}$). Samples were stored and stressed in 6R vials closed with rubber stoppers respectively in falcon tubes 15mL. For HPLC analysis, 1mL HPLC vials were used. All other chemicals used were of analytical grade unless stated otherwise.

2.2 Stress Methods

2.2.1 pH Stress

The IgG1 was stressed changing the pH of the formulation by adding the required amount of HCl 1M. The actual pH was measured by a MP 220 pH meter (Mettler Toledo). Final pH value of 1 was adjusted by adding 1 mL HCl 1M. The first analysis at t_0 was done shortly after pH value was adjusted. The sample was handled in 15 mL Falcon tubes.

2.2.2 Thermal Stress

The IgG1 was stressed at 60 °C in a water bath for 20 and 40 minutes and cooled back to room temperature in 15 mL Falcon tubes.

2.2.3 Freeze/Thaw Stress

The IgG1 was stored in a freezer at -80 °C for 30 min and then thawed at 25 °C in a water bath for another 30 min. This cycle was performed 10 (F/T 10) or 20 (F/T 20) times resp. in 15 mL falcon tubes with a filling volume of 10 mL.

2.2.4 Light Stress

The IgG1 (10 mL) was stressed in a SUNTEST CPS (Heraeus, Original Hanau) at 54 W/m² by a xenon lamp for 1 day (light 1d) and 2 days (light 2d) in 15 mL falcon tubes. The chamber was not cooled and sample temperatures of 35°C were observed, which is however far below T_m of the protein (71°C).

2.2.5 Aggregation Kinetics of Protein During Storage

To detect changes in the induced protein aggregates and the remained monomer fraction quantitatively and qualitatively over storage time, the stressed samples were stored in a fridge at 4-6°C over 3 months in 15 mL Falcon tubes. At various time points (t_0 = directly after stress exposure; after 1 month = t_{1month}; after 2 months = $t_{2months}$ and after 3 months = $t_{3months}$) the samples were analyzed again and results were compared to the accordant t_0 and the IgG1 initial sample. Always a PBS buffer control was stored and analyzed as well. No noticeable issues were detected and therefore the PBS data are not presented in the data shown here.

2.3 Analytical Methods

2.3.1 Visual Inspection

The existence of visible particles was surveyed by shaking and illumining the sample to fluff settled particles and bring them into movements to be better visible for the naked eye.

2.3.2 Turbidity Measurements

For nephlometry measurements a NEPHLA turbidimeter (Dr Lange, Germany) was used. Light (= 860 nm) was sent through the samples and the scattered light was measured at a 90° angle. The results were given in formazine nephelometric units (FNU).

_____

2.3.3 Sub-visible Particle Counting

Sub-visible particle counting based on light obscuration was performed on a PAMAS device (Rutesheim, Germany) equipped with a laser diode and a photodiode detector for size distribution analysis. Three measurements of a volume of 0.5 ml for each run were analyzed with a forerun volume of 0.3 ml. Results refer to a sample volume of 1.0 ml. Between measurements the device was cleaned with water until particle counts corresponded to the acceptance criteria of the European Pharmacopoeia (Pharm.Eur. 2.9.19; number of particles >10µm less then 25 particles in 25 mL).

2.3.4 High Performance Size Exclusion Chromatography (SEC) with a Post Column Module (PCM) for Fluorescence Detection

SEC using 100 µL injection volume was performed on an Agilent 1100 (Agilent Technologies, Germany) using a 500 mm YMC-Pack Diol-300 column (YMC Europe GmbH, Germany). As mobile phase PBS at a flow rate of 0.7 mL/min was applied. After column separation and UV detection at 280nm, BisANS solution with a concentration of 23.5 µM in PBS at a flow rate of 0.25 mL/min was pumped into the system via the PCM as described in chapter 3 and fluorescence detection was conducted at an excitation wavelength of 385 nm and maximum emission wavelength of 485 nm. An illustration of the system of SEC with PCM is shown in figure 1 in chapter 3.

3 RESULTS

3.1 Visual Inspection and Turbidity

All samples were firstly analyzed by the naked eye. Whereas at t_0 the samples IgG1 initial, pH 1, temperature and light stress remained free of any or showed only a few visible particles, the F/T stressed samples showed already many small particles, but still appeared as clear solutions. The light stressed samples turned slightly yellowish indicating covalent linkage resulting in chromophores in the protein. After 1 and 2 months storage at 4-6℃ the pH 1, temperature and light stressed samples showed few visible particles as well. After 3 months, the IgG1 initial and the pH 1 samples

_____

showed few smaller visible particles. In contrast, the temperature stressed samples showed many relatively large visible particles. The F/T stressed samples showed many but small particles. The light stress samples as well showed small particles, but less compared to the F/T stress.

Regarding the turbidity, the highest turbidity resulted for pH 1 treated protein with ~ 9 FNU and F/T stressed samples at t_0 with 8.7 FNU (Fig.1). The turbidity for the bulk material stored under the same conditions as the stressed samples remained unchanged at a lower value of < 2 FNU. The turbidity was observed to be almost unchanged for the IgG1 samples after stress exposure during the analyzed time range of 3 months.

Figure 1: Turbidity in IgG1 samples after stress exposure and storage time (t_0 = black, t_{1month} = grey, $t_{2months}$ = grey/white striped, $t_{3months}$ = white).

_____

3.2 Light Obscuration Particle Counting

The number of particles detected by light obscuration particle counting revealed a slight increase in particles $> 1\mu m$ at t_0 for all stressed samples (Fig.2). At t_0, IgG1 initial samples showed 1,611 particles larger than $1\mu m$. This number increased over storage time up to 6,472 particles $> 1\,\mu m/mL$ possibly due to handling and filling process, as it was equally handled and filled as the stressed samples. Regarding the pH 1 stressed sample an enormous increase in particles $> 1\,\mu m$ was observed directly after stress exposure at t_0 showing 48,706 particles/mL. This number was even increased after 1 and 2 months to 51,038 and 58,552 particles $> 1\,\mu m/mL$, but interestingly decreased after 3 months down to 42,144 particles/mL. Temperature stressed samples showed after stress exposure at t_0 21,688 particles $> 1\,\mu m$.

This number was slightly increased after one month to 27,858 particles/mL, but decreased over time again to a number of particles $> 1\,\mu m$ of 16,870 /mL at $t_{3months}$. This decrease in particles went along with the appearance of large visible particles and an increase in particles $> 10\,\mu m$ and $> 25\,\mu m$, as presented later possibly indicating a formation of larger particles at the expense of smaller ones. The highest amount of particles $> 1\,\mu m$ was measured in the F/T stressed sample with ~ 84,000 particles/mL. This number was consistent over 3 months storage time. A clear increase in particles $> 1\,\mu m$ was observed in the light stressed sample. Here the number increased from t_0 52,000 to t_{3month} 65,000 particles/mL.
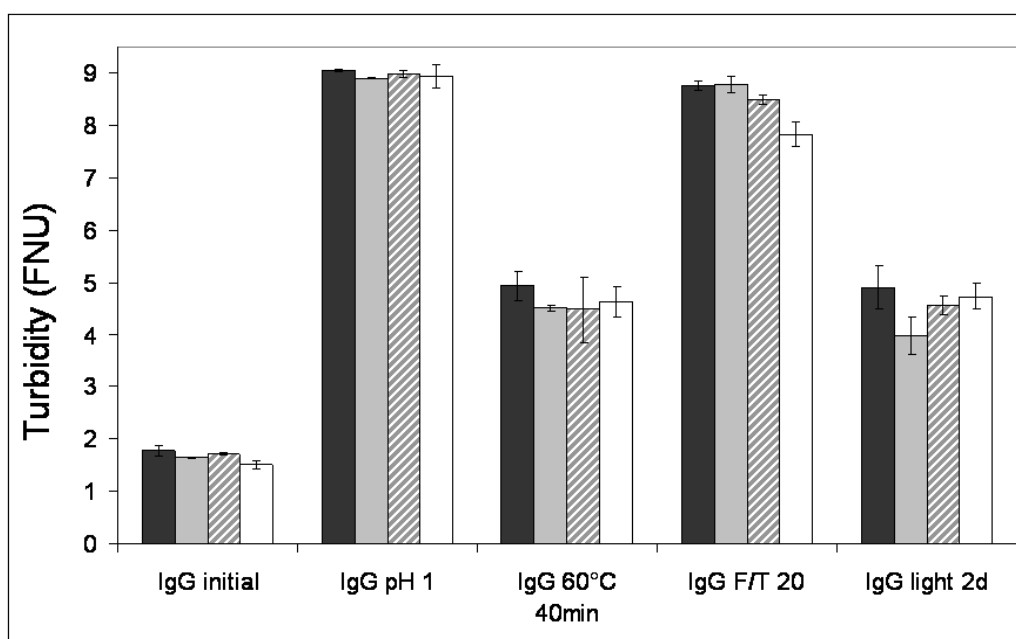
_____

Figure 2: Sub-visible particles > 1 μm in IgG1 samples after stress exposure and storage time (t_0 = black, t_{1month} = grey, $t_{2months}$ = grey/white striped, $t_{3months}$ = white).

The number of particles > 10 μm was increased after stress exposure as well (Fig.3). Whereas the initial sample showed ~ 20 particles > 10 μm, ~ 340 particles of this size range were detected in the pH 1 stressed sample, ~ 800 in the temperature stressed one, ~ 9,200 in the F/T stressed and ~ 240 in the light stressed sample. Although a slight increase in the initial and light stressed sample or slight alterations in the pH 1 stressed sample could be observed over storage time, the number of particles > 10 μm stayed well below 1000/mL. However, an increase in particles > 10 μm was observed for the temperature stressed sample as ~ 4,100 particles were detected after 3 months. The highest number of particles > 10 μm was observed in the F/T stressed samples. The number increased over 1 and 2 months to ~ 25,300 particles/mL, but then a decreased number of ~ 20,200 particles/mL was observed after 3 months of storage at 4-6°C.

_____
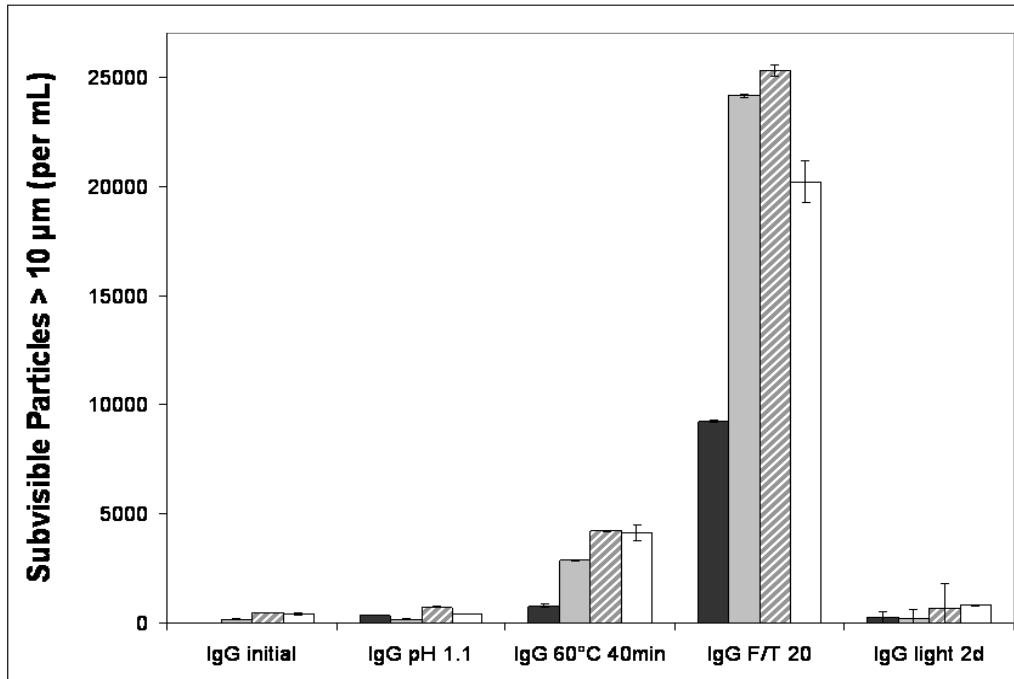
Figure 3: Sub-visible particles > 10 µm in IgG1 samples after stress exposure and storage time (t_0 = black, t_{1month} = grey, $t_{2months}$ = grey/white striped, $t_{3months}$ = white).

Whereas the number of particles > 25 µm remained < 100/mL in the IgG1 initial, pH 1 and light stress samples both after stress exposure and during storage time, the number of particles > 25 µm increased for temperature stressed samples from ~ 60/mL at t_0 to ~ 800/mL at $t_{3months}$ (Fig.4). Even more particles were induced in the F/T stressed sample. Here the number increased from 390 particles > 25 µm/mL at t_0 to ~ 1600/mL at $t_{3months}$. These results are in good accordance to previously published work, where the induction of particles in this size range after stress exposure was observed as well [8; 11; 12].
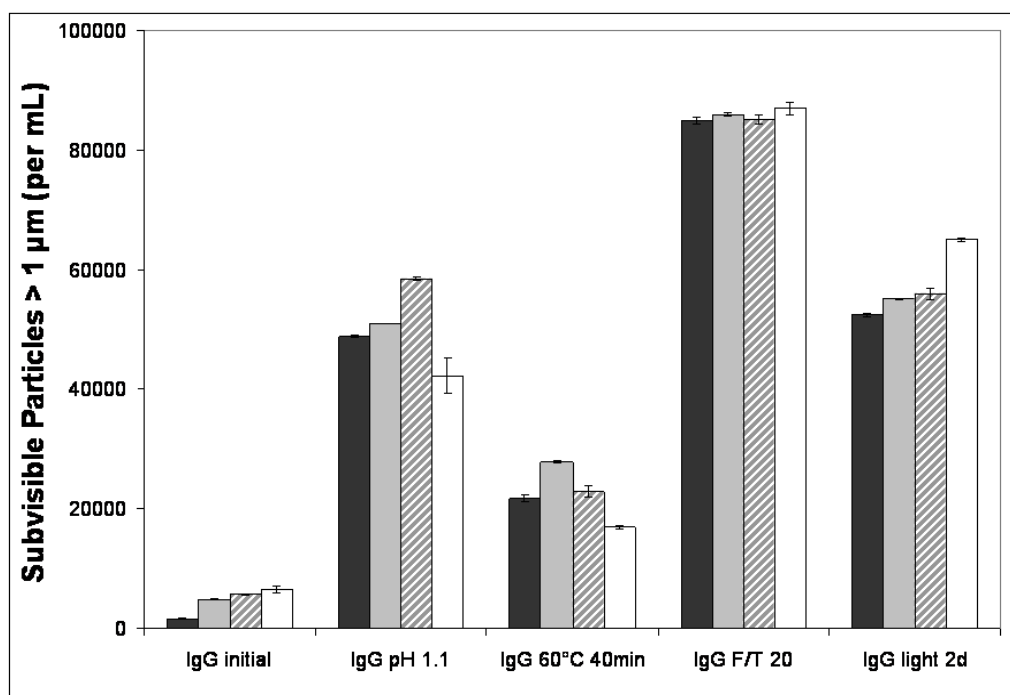
_____
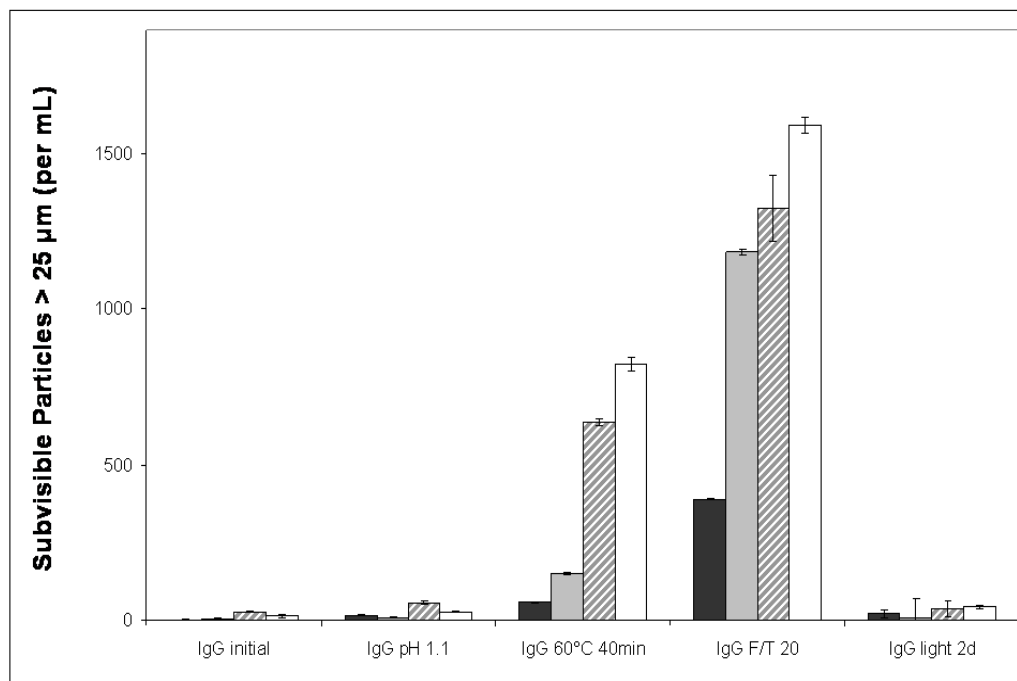
Figure 4: Sub-visible particles > 25 µm in IgG1 samples after stress exposure and storage time (t_0 = black, t_{1month} = grey, $t_{2months}$ = grey/white striped, $t_{3months}$ = white).

3.3 SEC with UV detection

The SEC with UV detection, calculated as a percentage of the AUC of the according peak, where 100% is based on the total recovery of IgG1 initial sample, showed the stress dependent induction of protein oligomers and fragments as well as changes in the protein species over storage time (Fig.5). In the initial sample a small amount of oligomers of 0.3 % was already present. This amount of oligomers in the initial sample did not change over storage time. Also in the F/T stressed sample the amount of oligomers was < 1 %, except the F/T 20 sample at t_0, which showed 2.6 % of oligomers, which over storage time seemed to re-dissolve as the detected amount of oligomers after 3 months was reduced to 0.4 %. High amounts of oligomers were observed in the pH 1 sample at t_0 of 62%. But the amount decreased to 44 % at $t_{3months}$. Due to the column resin interactions with the pronounced unfolded protein after acidic pH exposure, a very large standard deviation was observed for pH 1 stressed samples, which is in line with recent publications [14]. The tendency of a

_____

reduction of the oligomer amount over storage time was also observed in the temperature stressed samples. At t_0 30 % (20 min/60°C) and 37 % (40 min/60°C) oligomers were observed, whereas after storage of 3 months the oligomer amounts were reduced to 21 % and 30 % respectively. The light 1d sample showed approx. 40 % oligomers, which remained consistent during storage at 4-6°C. A slight increase in the amount of oligomers was instead observed for light 2d stressed samples from 61 % at t_0 to 65 % at $t_{3months}$.

Figure 5: AUC % of IgG1 oligomers after stress exposure and storage time (t_0 = black, t_{1month} = grey, $t_{2months}$ = grey/white striped, $t_{3months}$ = white).

Regarding the monomer amount no change was observed in the unstressed IgG1 material (Fig.6). The percentage stayed stable around 99 %. The monomer amount in the pH 1 stressed sample was reduced to 9 % at t_0. This value also remained consistent over storage time. However, the monomer amount in the temperature stressed sample, showing at t_0 72 % (20 min/60°C) and 65 % (40 min/60°C) resp., increased to 78 % and 70 %, respectively after three months. Also the monomer content of the F/T stressed samples increased over time. At t_0 88 % (F/T 10) and

_____

80 % (F/T 20) resp. were observed, whereas at $t_{3months}$ 102 % (F/T 10) and 94 % (F/T 20) resp. monomer could be detected. The same tendency was observed in the light 1d stressed sample, where at t_0 60 % monomer were detected, which increased to 65 % after 3 months. For the light 2d stressed sample at t_0, a monomer content of 40 % was detected, which was more or less consistent over three months.

Figure 6: AUC % of IgG1 monomer after stress exposure and storage time (t_0 = black, t_{1month} = grey, $t_{2months}$ = grey/white striped, $t_{3months}$ = white).

For the unstressed, the temperature-, and the F/T stressed samples the fragment content was rather stable at approx. 0.5 to 1 %. An enormous formation of 14 % fragments was observed in the pH 1 stressed sample at t_0, which even increased over storage time to 16 % after 3 months (Fig.7). But the data showed a high standard deviation. At t_0 for the light stressed samples 2.1 % (light 1d) and 4.2 % (light 2d) fragments were detected, however the percentage of fragments was reduced at $t_{3months}$ to 1.8 % resp. 3.2 %.

_____
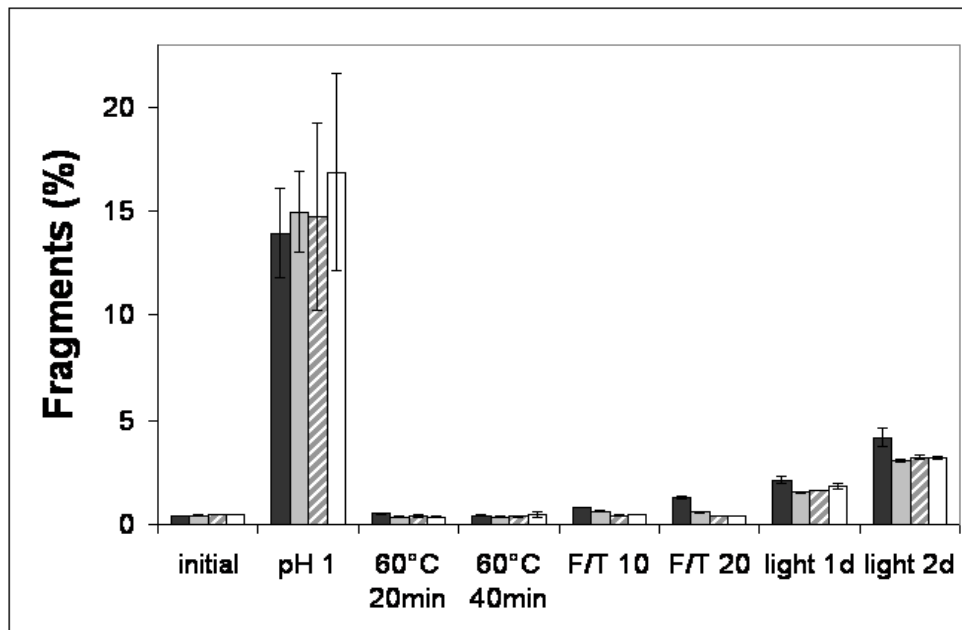
Figure 7: AUC % of IgG1 fragments after stress exposure and storage time (t_0 = black, t_{1month} = grey, $t_{2months}$ = grey/white striped, $t_{3months}$ = white).

Looking at the total recovery, it became obvious that for the unstressed and the temperature stressed sample ~ 100% were recovered consistently (Fig.8). For pH 1 stressed samples, the total recovery dropped from 85 % at t_0 to 70 % at $t_{3months}$, pointing out the poor stability of the protein at this low pH and the tendency to form larger aggregates over time, which were excluded from SEC column. Interestingly, an increase in the total recovery of F/T and light stressed samples become obvious during storage of the samples. The total recovery of the F/T stressed samples at t_0 of 90 % (F/T 10) resp. 85 % (F/T 20) increased during 3 months up to approx. 100 % and 95 % resp. These data points are in good accordance to literature, where freeze/thaw stressed protein is suggested to form native-like, and at least partially reversible aggregates [8; 12]. The same tendency was observed in the light stressed samples, where the total recovery at t_0 of 103 % (light 1d) resp. 106 % (light 2d) was increased at $t_{3months}$ to 106 % resp. 107 %, which might however also be related to a continuing change of chromophoric moieties.

_____

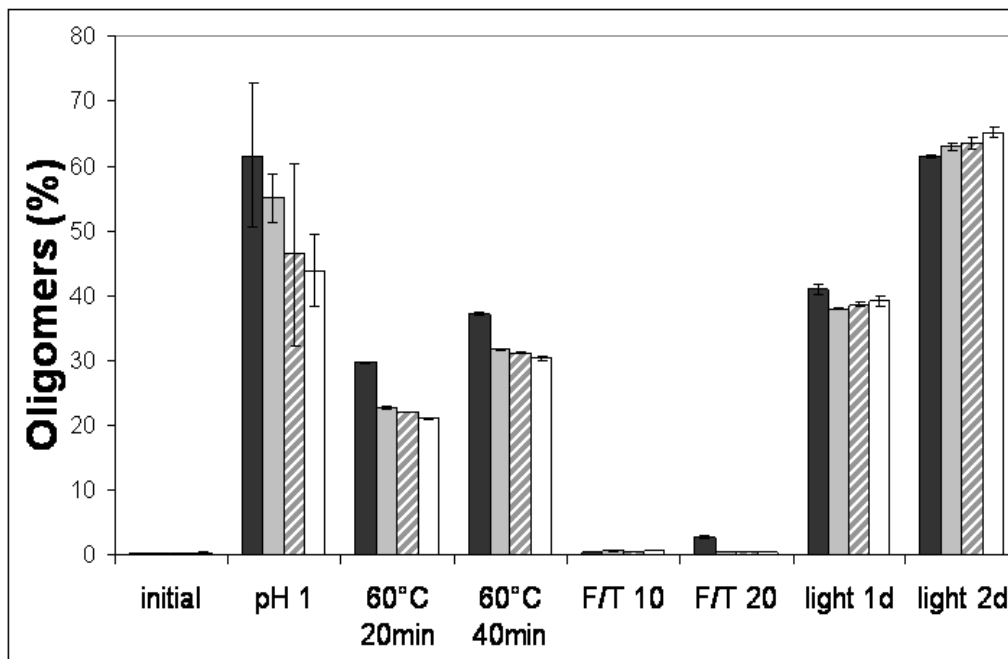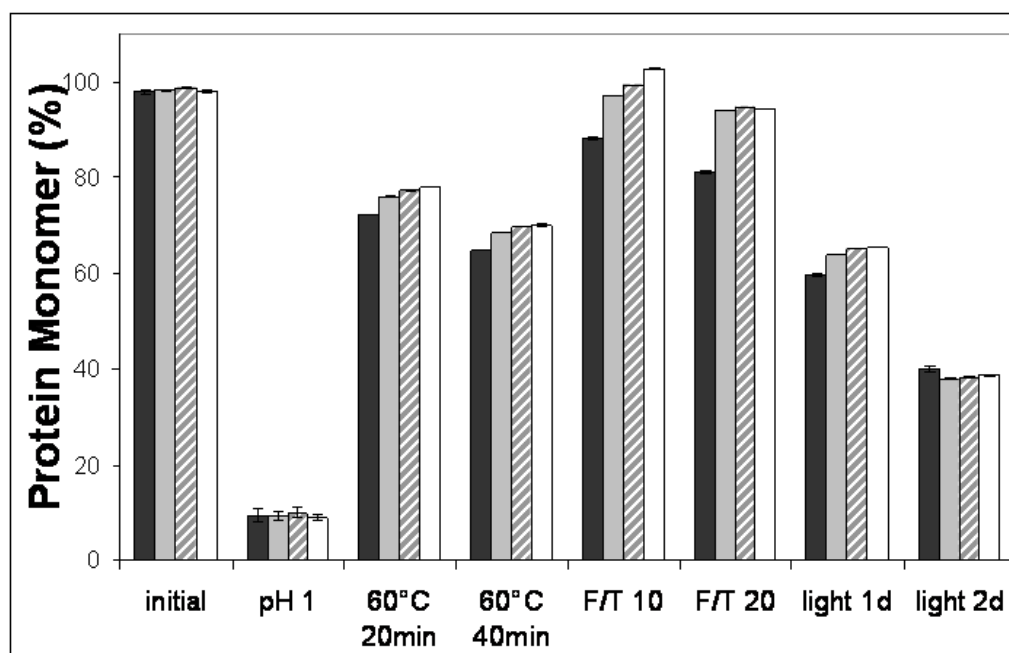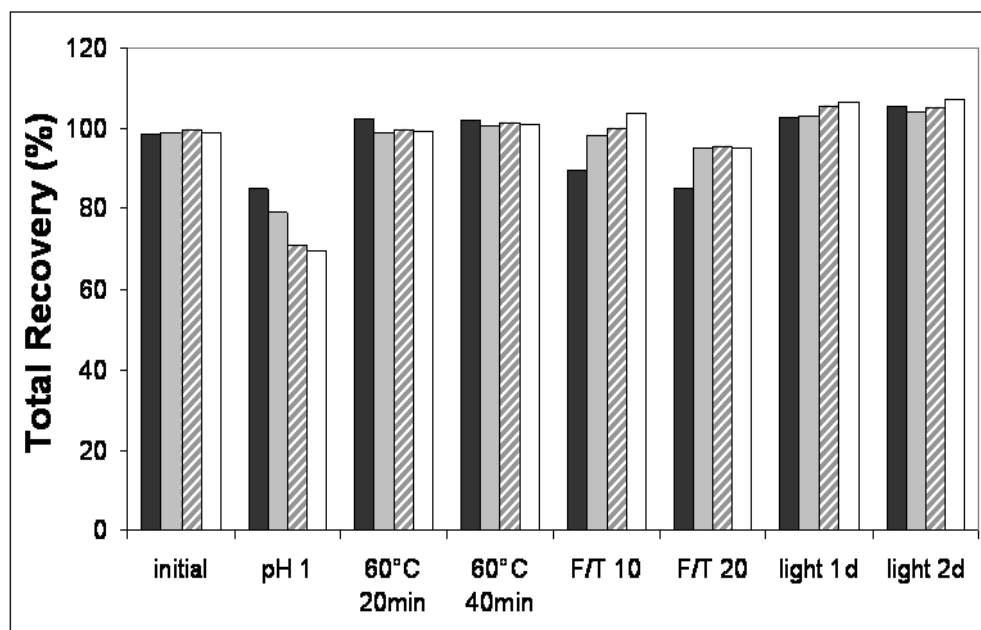**Figure 8:** AUC % of total recovery after stress exposure and storage time (t_0 = black, t_{1month} = grey, $t_{2months}$ = grey/white striped, $t_{3months}$ = white).

3.4 SEC PCM with fluorescence detection

Looking at the extrinsic fluorescence data gained simultaneously via post-column addition of Bis-ANS, the highest increase in the fluorescence signal was observed in the formed oligomers of the pH 1 stressed samples reaching a maximum of 11,963 a.u. at t_{3month} (Fig.9). Over storage time the fluorescence intensity increased in the pH 1 stressed samples from a starting intensity at t_0 of 7,660 a.u. Standard deviations were again high possibly due to the interaction of the column resin and the unfolded molecules. For the temperature stressed samples, a fluorescence intensity AUC of 1,591 a.u. (20 min/60°C) resp. 2,148 a.u. (40 min/60°C) was observed at t_0, which remained more or less stable or over storage time with a slight trend to lower values.

The stable or slightly diminished fluorescence intensity went along with a slight decrease in the UV signal for the oligomers. No oligomer fluorescence peak could be detected for the unstressed IgG1 and the F/T stressed samples although a small quantity of oligomers was observed in the UV spectra. This suggests the presence of

_____

a rather native-like structure of the oligomers. This native-like pattern of the aggregates induced by freezing and thawing is also discussed in literature [8; 12]. Regarding the oligomers induced by light stress, fluorescence peaks covered an AUC of 633 a.u. (light 1d) and 2,087 a.u. (light 2d) at t_0. Whereas the fluorescence intensity remained almost the same for light 1d, the fluorescence intensity of light 2d was slightly increased to 2,785 a.u. At the same time a slight increase in the oligomer amount was detected (from 61.5 % to 65 %) in the UV detection indicating a progression in unfolding.

Comparing the amounts of present oligomers and their fluorescence intensity, it becomes obvious that in the light stressed samples the 41 % (light 1d) resp. 61,5 % (light 2d) oligomers along with a fluorescence intensity of 633 a.u. respectively 2,087 a.u., seem to be different from those oligomers obtained after pH and temperature stress. Here, the fluorescence intensity of 62 % oligomers in the pH 1 stressed samples showed a fluorescence intensity of 7,660 a.u. and the 30 % (20 min/60°C) resp. 37 % (40 min/60°C) a fluorescence intensity of 1,592 a.u. resp. 2,148 a.u. at t_0. The same holds true for other time points, e.g. at $t_{3months}$ in the pH 1 stressed sample 44 % oligomer were detected giving a fluorescence signal of 11,963 a.u., whereas in the light 2d sample at the same time point 65 % oligomers only gave a fluorescence signal of 2,784 a.u.. However, this would suggest that oligomers formed by different stress methods were unfolded to a different extent highlighting again the vast differences and diversity that exist in protein aggregates.

_____
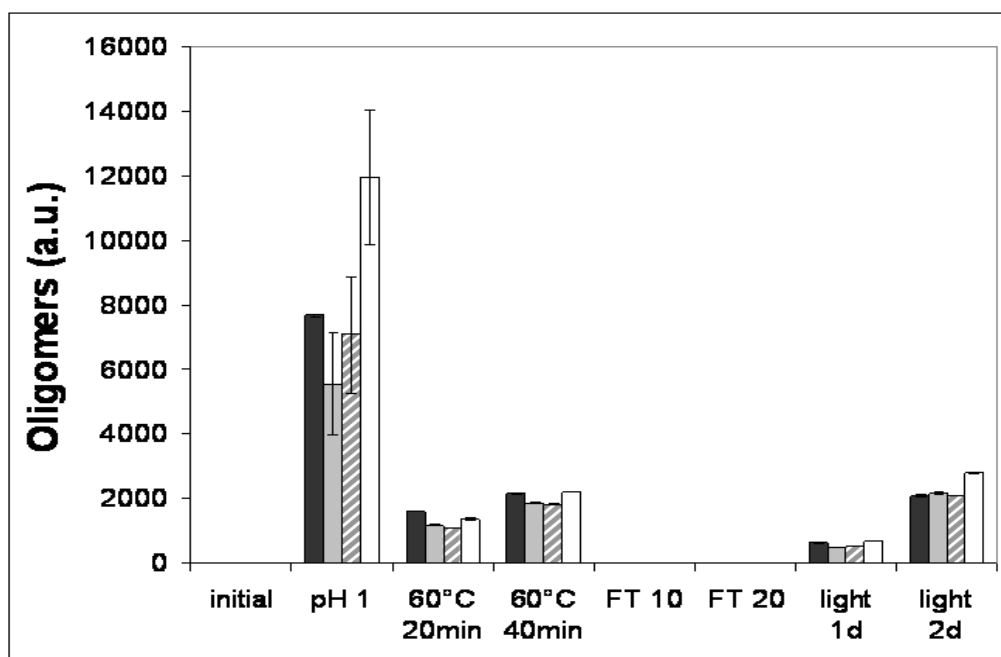
Figure 9: Fluorescence intensity of IgG1 oligomers after stress exposure and storage time (t_0 = black, t_{1month} = grey, $t_{2months}$ = grey/white striped, $t_{3months}$ = white).

Regarding the stress effects on the monomer, the highest increase in fluorescence intensity was again observed in the pH 1 stressed sample (Fig.10). At t_0 an AUC of 2,345 a.u. was obtained, which did not change significantly over storage time. The monomer amount as seen in the UV data stayed constant.

_____
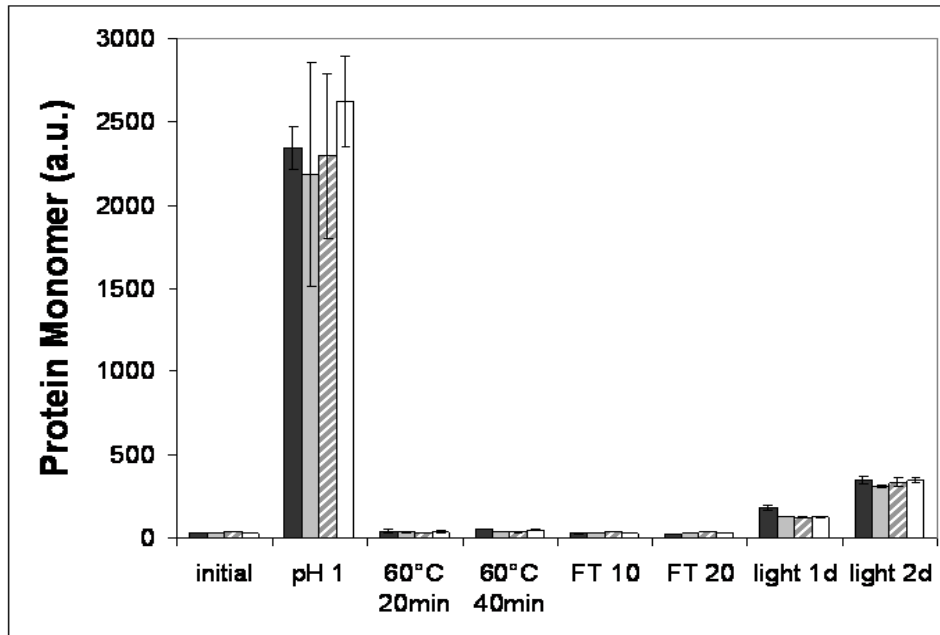
Figure 10: Fluorescence intensity of IgG1 monomer after stress exposure and storage time (t_0 = black, t_{1month} = grey, $t_{2months}$ = grey/white striped, $t_{3months}$ = white).

4 DISCUSSION

The unstressed IgG1 samples showed few visible particles and did not change over time. However, the chosen stress methods differed in one major aspect in their impact on the samples, namely in the duration of the applied stress. While the stress stopped for temperature, F/T and light stressed samples after a given time period, the inferior conditions were kept in the pH 1 samples also during storage, exposing these samples much longer to stress. The outcome of the stress and the subsequent storage are summarized in Figure 11.

All stressed IgG1 samples showed visible particles after three months. This indicates the formation of large aggregates > 100μm in the IgG1 samples during storage, but is reflective of only a very small protein amount.

For samples stressed at pH 1, the inferior conditions were kept during the storage time. SEC with UV detection showed a quantitative decrease in oligomers (-18 %), along with a decrease in total recovery (-15 %). This could indicate that the loss of oligomers might be due to the formation of larger protein aggregates, which were excluded form SEC analysis. Alternatively, the loss in oligomer in SEC could be caused by adsorption of the unfolded species to the chromatographic beads. By light obscuration particle counting, hardly any change could be detected in the size range > 1, > 10 and > 25 µm disproving the formation of sub-visible particles in this size range during storage. Interestingly in samples stressed at pH 1, a slight increase in fluorescence intensity of the oligomers went along with a decrease in their UV signal. This could indicate that the remaining oligomers proceeded in unfolding at acidic pH.

In heat stressed samples the number of sub-visible particles > 10 and > 25 µm increased during storage. The oligomer amount decreased (-7 %), whereas the amount of monomer increased (+5 %). The fluorescence intensity remained unchanged. This could indicate that oligomers either further agglomerated to larger protein particles (> 10 and > 25 µm) and/or re-dissolved into monomer species.

Looking at the F/T stressed samples, the number of particles > 25 % increased during storage, as well as the monomer amount (+13 %) and the total recovery (+10 %). Oligomers were hardly detected (< 3 %). These observations lead to the conclusion, that particles induced by F/T either form larger particles (> 25 % and visible particles) and/or re-dissolve into monomer species. Analysing the light (2days) stressed samples, slight increases in particles > 1 µm and in oligomer amount (+4 %) were observed. This marginal progress in aggregation could possibly reflect an ongoing aggregation due to chemical reactions. But, as no loss in monomer or number of particles for other size ranges was observed neither in light nor in F/T stressed samples, the question remains open, where these newly formed aggregates originate from. In addition, it has to be kept in mind that sub-visible and visible particles represent only very low protein quantities.

_____

Hence, neither a reversible protein aggregation along with a possible re-dissolution to monomer species nor a progress in aggregation forming protein aggregates > 1 µm due to some kind of nucleation effect, were clearly verified in this study. Therefore, induced protein particles were considered to be stable and used in our analytics without further considerations regarding alterations in size and amount distribution over time.

5 CONCLUSION

A nucleation or a progression of unfolding and aggregation during storage followed by an augmentation of protein aggregates were not detected. Only the amount of visible particles increased slightly over time. A trend was observed to a marginal regain of monomer for temperature and F/T stressed samples over time leading to the assumption of a slight re-dissolving of oligomers and protein particles resp.. These observations are in good accordance to literature, where also the nucleation presumption was refuted [8]. The aggregates formed upon the different stress methods were distinctly different quantitatively and qualitatively.

6 ACKNOWLEDGEMENTS

Changes in protein species during storage — Induced by	Visual Inspection — Visible Particles >100 µm[3]	Turbitity — Soluble / Insoluble Aggregates 50 nm – 1 mm[3]	Subvisible Particle Counting — Soluble Aggregates >25 µm	>10 µm	>1 µm	HP-SEC — Oligomers / Monomer / Fragments — Oligomers ~20–200 nm[3]	Oligomers ~10 nm	Monomer ~10 nm	Fragments <10 nm	Total Recovery
pH	↑	–	–	–	–	↑ F	–	↑	↑	→
Temperature	↑	–	⇈	⇈	–	→	↑	–	–	–
F/T	↑↑↑	–	⇈	–	–	–	↑	↑	–	↑
Light	↑	–	–	–	↑	↑	–	–	–	–
for comparison: unstressed bulk material	–	–	–	–	–	–	–	–	–	–
analysed parameters	Number of visible particles	FNU	Number of subvisible particles			Amount of monomer and oligomer / Fluorescence intensity				

Figure 11: A summary of the changes in protein species over time after stress exposure as observed by different analytical methods, where F represents the fluorescence signal, ↑ corresponds to an increase, ↓ shows a decrease and – indicates no change.

7 REFERENCES

[1] Schellekens, Huub. Factors influencing the immunogenicity of therapeutic proteins. Nephrology, Dialysis, Transplantation (2005), 20(Suppl. 6), vi3-vi9.

[2] Rosenberg, Amy S. Effects of protein aggregates: an immunologic perspective. AAPS Journal (2006), 8(3), No pp. given.

[3] Mahler, Hanns-Christian; Friess, Wolfgang; Grauschopf, Ulla; Kiese, Sylvia. Protein aggregation: Pathways, induction factors and analysis. Journal of Pharmaceutical Sciences (2009), 98(9), 2909-2934.

[4] Chang B S; Kendrick B S; Carpenter J F. Surface-induced denaturation of proteins during freezing and its inhibition by surfactants. Journal of pharmaceutical sciences (1996), 85(12), 1325-30.

[5] Chi, Eva Y.; Weickmann, Joachim; Carpenter, John F.; Manning, Mark C.; Randolph, Theodore W. Heterogeneous nucleation-controlled particulate formation of recombinant human platelet-activating factor acetylhydrolase in pharmaceutical formulation. Journal of Pharmaceutical Sciences (2005), 94(2), 256-274.

[6] Tyagi, Anil K.; Randolph, Theodore W.; Dong, Aichun; Maloney, Kevin M.; Hitscherich, Carl, Jr.; Carpenter, John F. IgG particle formation during filling pump operation: a case study of heterogeneous nucleation on stainless steel nanoparticles. Journal of Pharmaceutical Sciences (2009), 98(1), 94-104.

[7] Frokjaer Sven; Otzen Daniel E. Protein drug stability: a formulation challenge. Nature reviews. Drug discovery (2005), 4(4), 298-306.

[8] Kiese, Sylvia; Pappenberger, Astrid; Friess, Wolfgang; Mahler, Hanns-Christian. Equilibrium studies of protein aggregates and homogeneous nucleation in protein formulation. Journal of Pharmaceutical Sciences (2010), 99(2), 632-644.

[9] Andrews, Jennifer M.; Weiss, William F., IV; Roberts, Christopher J. Nucleation, Growth, and Activation Energies for Seeded and Unseeded Aggregation of alpha-Chymotrypsinogen A. Biochemistry (2008), 47(8), 2397-2403.

_____

[10] Newsletter of the AAPS Aggregation and Biological Relevance Focus Group October 2010 2 (2)

[11] Kiese, Sylvia; Papppenberger, Astrid; Friess, Wolfgang; Mahler, Hanns-Christian. Shaken, not stirred: mechanical stress testing of an IgG1 antibody. Journal of Pharmaceutical Sciences (2008), 97(10), 4347-4366.

[12] Hawe, Andrea; Kasper, Julia Christina; Friess, Wolfgang; Jiskoot, Wim. Structural properties of monoclonal antibody aggregates induced by freeze-thawing and thermal stress. European Journal of Pharmaceutical Sciences (2009), 38(2), 79-87.

[13] Hawe, Andrea; Sutter, Marc; Jiskoot, Wim. Extrinsic Fluorescent Dyes as Tools for Protein Characterization. Pharmaceutical Research (2008), 25(7), 1487-1499.

[14] Arakawa, Tsutomu; Ejima, Daisuke; Li, Tiansheng; Philo, John S. The critical role of mobile phase composition in size exclusion chromatography of protein pharmaceuticals. Journal of Pharmaceutical Sciences (2010), 99(4), 1674-1692.

_____

CHAPTER 5

Fluorescence Microscopy of Protein Particles on Filter Surfaces

ABSTRACT

In this study, fluorescence microscopy (FM) is presented as a method to detect protein aggregates (> 1 μm) on the basis of a combination of the methods described by Demeule et al [1] and Li et al. [2]. Shape, apparent size and number of protein aggregates, as counted on fluorescent gridded Cellulose Acetate (CA) filter surfaces, could be successfully visualized by fluorescence illumination of the aggregates after staining with the extrinsic fluorescent dye BisANS. FM was used as a complementary method to, e.g., turbidity and light obscuration particle counting as well as to bright-field microscopy working with a protein detection kit on a digital microscope VHX 500F (Keyence, Germany) to cover larger protein aggregates of 1 – 200 μm. Advantages of FM are the convenient handling and a high sensitivity. Protein aggregates were induced by applying typical stress methods, such as acidic pH, elevated temperature, freeze/thaw and light. Depending on the applied stress methods, we observed different appearances of protein aggregates. A slightly higher sensitivity for FM especially for particles < 10 μm compared to the bright-field microscope was observed due to the higher contrast.

_____

1 INTRODUCTION

In general, the use of orthogonal, complementary analytical methods is recommended [3] for protein stability studies as every technique has its limitations to analyse protein aggregation characteristics. Instabilities, however, may reduce the efficacy of the protein and increase immunogenicity [4; 5]. For quantitative protein analysis and for size estimation SE-HPLC, asymmetrical flow field flow fractionation (AF4), SDS-PAGE, light obscuration, static and dynamic light scattering and turbidity are used. HPLC is only suitable to analyse species in the size range up to several oligomers, as bigger particles would be stuck in the column resin. In AF4 reversible aggregates might be overseen due to the high shear stress [6]. Light obscuration suitable for low-viscosity samples [7] encounters its limitation measuring partially transparent particles and does not pay any attention towards the shape of the particles. When using static and dynamic light scatting for size measurements, one has to be aware that encountering multimodal distribution the results might be biased towards the larger species.

Protein aggregation might involve structural changes. Beside Fourier transformed infrared spectroscopy (FTIR), 2nd derivation of the UV spectrum and near/far circular dichroism (CD), a standard method for characterization of changes in protein structure is fluorescence spectroscopy [8; 9; 10]. In extrinsic fluorescence, fluorescence dyes, which non-covalently interact with protein molecules, are used to characterize unfolding and denaturation [11] and to detect protein aggregation, e.g., in FM [1; 6; 8; 12]. An overview of commonly used fluorescent dyes is given in table 2. Demeule et al. used Nile Red diluted in ethanol in the FM analysis to determine diameter and number of immunoglobulin aggregates in a high concentration protein formulation [12]. Furthermore, they used Nile Red to study human calcitionin aggregation kinetics [1] and to visualize trastuzumab aggregates formed upon reconstitution with 5% dextrose solution [6]. The observations could be confirmed by other techniques, such as light obscuration particles counting, AF4, circular dichroism, fluorescence spectroscopy and transmission electron microscopy [6]. Reversible aggregates formed by weak interactions easily disrupted during AF4 could be best assessed by FM [12]. Compared to bright-field microscopy the higher

sensitivity of FM by a better contrast enabled the detection of 2-4 µm aggregates present at low quantity [1]. Thioflavin T might be used to stain amyloidal protein aggregates [1]. Another commonly used non-covalent, extrinsic fluorescent dye for protein characterisation is 4,4´-bis-1-anilinonaphthalene-8-sulfonate (BisANS). It enables the observation of changes in protein structure by monitoring the increase of fluorescence intensity due to the interaction of the dye with the hydrophobic surfaces of the protein that become exposed during unfolding [8; 13; 14].

In this study a method was developed combing quantitative and qualitative analysis to analyse protein aggregates with high sensitivity on filter surfaces by using the extrinsic fluorescent dye BisANS and FM on a Keyence BZ-9000 fluorescence microscope (Keyence, Germany). FM is already a very well established tool in life science research for live cell and tissue imaging [15]. For 3D imaging a confocal laser scanning microscope (CLSM) may be used, enhancing the grade of fluorescence images by avoiding the out of focus fluorescence [15]. Moreover, single molecule FM is already successfully used in biochemical and biophysical techniques analysing and tracing enzymes, proteins, telomerases, RNA, genes, viruses and receptors in cell membranes [16]. For reaching deeper tissue layers in living animals infrared microscopy might be used penetrating up to 600 µm [17]. Using FM one should be aware of several potential pitfalls. E.g., crosstalk between fluorophores, photo-bleaching, and detector saturation can lead to difficulties in quantification [15]. Also, a perfect analytical technique should observe protein aggregation without changing the local environment of the protein dramatically, e.g. by dilution or re-buffering [18]. FM addresses those requests, as no preparation is necessary, but as soon as particles are retained on the filter surface the environment is obviously changed.

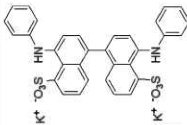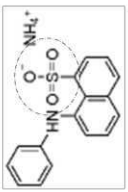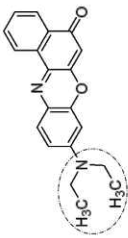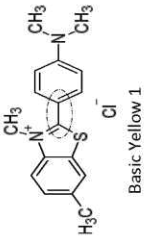Two different filter materials were used in this study. Polyethersulfone (PES) applied as ready-to-use syringe filter and as membrane in Vivaspin500 tubes and cellulose acetate (CA) filters were utilised as membrane disc filters. Hydrophilic PES membranes are supposed to bind less protein, and to show less extractables. Furthermore, they provide a high fluid filtration capacity and a greater strength than

_____

other cellulose based membranes, like acetate or nitrate. CA membranes combine high flow rates and thermal stability with low adsorption characteristics and are therefore used in, e.g., pressure filtration devices. White CA membranes with black grids were used, as the printed grid divides the filtration area into squares (3.1x3.1 mm) enabling the counting of particles. As ready-to-use syringe filter with PES membrane Minisart syringe filters for sterile filtration, particle removal and ultra-cleaning were used for pre-filtration to remove larger particles. In additon, in this study Vivaspin500 concentrators with PES membranes and a molecular weight cut off of 30 kDa were used. Table 1 provides an overview of filters used in this chapter.
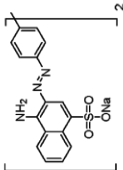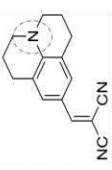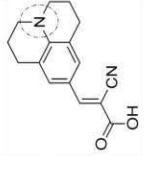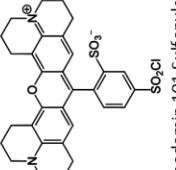
Filter	Supplier	Filter Material	Pore Size / Cut Off	Surface Diameter / Capacity
Minisart	**Satorius Stedim Biotech**	Polyethersulfone (PES)	5 µm	28 mm
CA, white, gridded	**Satorius Stedim Biotech**	Cellulose Acetate (CA)	0.45 µm	50 mm
Vivaspin500	**Satorius Stedim Biotech**	Polyethersulfone (PES)	30 kDa MWCO	0.5 mL
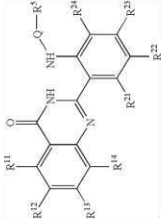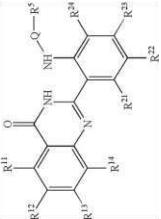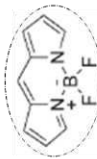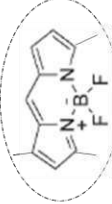
Table 1: Overview of employed filter types, their surface material and the used pore size respectively cut off.

As different stress methods lead to different aggregate species varying quantitatively and qualitatively, (see Chapter 2 and 3), we selected acidic pH, elevated temperature, freeze/thaw, and light exposure as typical stress methods, to create different aggregates qualities [19 – 24]. By staining the induced protein aggregates with BisANS and retaining them on filter surfaces it should be possible to visualize them in the FM, and obtain information about their apparent size, shape and amount. Compared to other analytical methods, such as turbidity and light obscuration particle counting, the benefit of the microscopic method lies clearly in providing further information regarding the shape of the protein particles. In addition, in might provide insights into the status of protein unfolding. The obtained fluorescence microscopic results were compared to the results from turbidity measurements, light obscuration particle counting, fluorescence spectroscopy, SDS-PAGE, bright-field microscopy using the protein detection kit (reversible protein detection kit, Sigma Aldrich, Germany) and further analytical tools.

_____

a in water; blue shift in hydrophobic environment
b in the presence of amyloids
(twisted) intramolicular charge transfer reactions (T)ICT

Noncovalent Extrinsic Fluorecent Dyes	Chemical Structure (IUPAC resp. Synonym)	Application In / Technique	Detection Of / Mechanism of Fluorescence / Sensitive To / Observed Effect	Excitation (nm) / Emission maximum (nm) / Extinction Coefficient (m-1cm-1)/ Stock solution / Typical Conc.(µM)
BisANS	4,4'-Dianilino-1,1'-binaphthyl-5,5'-disulfonic acid dipotassium salt	• protein stability study • spectroscopy, microscopy	• surface hydrophobicity, unfolding/folding, aggregation at early stages, conformation change • hydrophobic interactions • Polarity • intensity increase, maximum shift	385-400 / 515a / 16790 (385 nm, water) / aqueous, methanol, ethanol / 1-20
ANS	8-Anilino-1-naphthalenesulfonic acid ammonium salt	• protein stability studies • spectroscopy, microscopy	• surface hydrophobicity, unfolding/folding, aggregation at early stages, conformation, molten globular intermediates, denaturation, protein structure in ice, protein crystals • ion pairing • Polarity • intensity increase, maximum shift	350-380 / 505a / 5000 (350 nm, water) or 4950 (350 nm, water) / aqueous, ethanol / 1-30
Nile Red	Nile Blue A Oxazone	• protein conformation • microscopy, staining SDS-page	• detection of intracellular lipid droplets, surface hydrophobicity, unfolding/folding, aggregation conformation, amyloid fibrills • electron transfer, TICT • Polarity • intensity increase, maximum shift	540-580 / 660a / 19600 (552 nm, DMSO) / DMSO, ethanol, DMF / 0.5-20
Thioflavin T	Basic Yellow 1	• amyloid fibrils analysis • tissue staining, microscopy	• fibrillation, amyloid fibril characterization • angle change (37°-> 90°), interaction with ß-sheet (tunnels), formation of micelles, excimer formation • Viscosity • intensity increase, maximum shift	450 / 480-490b / 36000 (412 nm, water) or 26620 (416 nm, ethanol) Aqueous / 5-40

_____

a in water; blue shift in hydrophobic environment
b in the presence of amyloids
(twisted) intramolicular charge transfer reactions (T)ICT

Noncovalent Extrinsic Fluorecent Dyes	Chemical Structure / IUPAC resp. Synonym	Application In / Technique	Detection Of / Mechanism of Fluorescence / Sensitive To / Observed Effect	Excitation (nm) / Emission maximum (nm) / Extinction Coefficient (m-1cm-1)/ Stock solution / Typical Conc.(µM)
Congo Red	1-Naphthalene sulfonic acid, 3,3′-[[1,1′-biphenyl]-4,4′diylbis(2,1-diazenediyl)]bis[4-amino-,sodium salt (1:2)	• amyloid fibrils analysis • tissue staining	• fibrillation, amyloid fibril characterization • supramolecular ligands • n.a. • shift of UV absorbance, induction of circular dichroism	550 / n.a. 45000 (498 nm, water) or 59300 (505 nm, ethanol) 10 to 40% ethanol / 10-300
DCVJ	9-(Dicyanovinyl)-julolidine	• protein viscosity • spectroscopy	• tubulin structure, microviscosity of proteins, environment rigidity • electron transfer TICT • Viscosity • intensity increase	480-505 / 450 659000 (453 nm, ethanol) ethanol, DMSO / 5
CCVJ	9-(2-carboxy-2-cyanovinyl)-julolidine	• protein viscosity • spectroscopy	• tubulin structure, microviscosity of proteins, environment rigidity • electron transfer TICT • Viscosity • intensity increase	n.n. / n.n. n.n. n.n. / n.n.
Texas Red	Sulforhodamin 101 Sulfonylchlorid	• Cell histology, molecular biology • Real Time quantitative PCR	• n.n. • n.n. • n.n. • n.n.	595 / 615 n.n. n.n. / n.n.

_____

a in water; blue shift in hydrophobic environment
b in the presence of amyloids
(twisted) intramolicular charge transfer reactions (T)ICT

Noncovalent Extrinsic Fluorecent Dyes	Chemical Structure / IUPAC resp. Synonym	Application In / Technique	Detection Of / Mechanism of Fluorescence / Sensitive To / Observed Effect	Excitation (nm) / Emission maximum (nm) / Extinction Coefficient (m-1cm-1)/ Stock solution / Typical Conc.(µM)
SYPRO Orange		• protein stability studies • Gel and membrane staining, such as SDS-page and Western blots, thermal stability measurements Tm	• detection of melting temperature • hydrophobic interactions, when not bound → quenched by O2 • n.n. • fluorescence appearance	472 / 569 n.n. DMSO / 500µL of 5000*
SYPRO Red		• protein stability studies • Gel and membrane staining, such as SDS-page and Western blots, thermal stability measurements Tm	• hydrophobic areas of proteins, determination of melting point during a thermal scan, affinity of ligands • hydrophobic interactions; when not bound → quenched by O2 • n.n. • fluorescence appearance	547 / 635 n.n. DMSO / 500µL of 5000*
Bodipy Dipyrromethen-bor-difluorid 4,4-Difluoro-4-borata-3a-azonia-4a-aza-s-indacen Monostyryl-boradiazaindacene		• nanotechnology, biomaterials, labeling biological macromolecules, detection of protein expression • HPLC, SDS-page, capillary electrophoresis, microfluid chip, fluoroimmunoassay for separating and detecting biological macromolecules, biomarker, chemical sensors (pH sensor for protons in organic solvents), microscopy	• cations, anions, DNA, fructose, NO derivates • intramolecular energy/charge transfer reactions (T)ICT, proton additions, light induced electron transfer • unsensible to polarity • fluorescence appearance	485 –488 / 530 40000 - 110000M-1cm-1 common solvents (not water) / 100 nM
Bodipy-FL XYZ-Dipyrromethen-bor-difluorid		• proteome research, protein expression screening, receptor function study • Dot-Plot expression screening	• G protein • incorporation, binding to the G protein → relieving quenching • n.n. • fluorescence appearance	485 – 488 / 530 40000 - 110000M-1cm-1 common solvents (not water) / 100 nM

Table 2: Overview of commonly used non-covalent, extrinsic fluorescent dyes in biotechnology giving the chemical structure, IPAC name / synonym, field of application, mechanism of fluorescence and analytical settings [1; 8; 11; 21].

_____

2 MATERIALS AND METHODS

2.1 Materials

An IgG1 at 2 mg/ml in 10 mM phosphate buffer at pH 7.2 containing 140mM NaCl (further called as PBS) was stressed and analysed. The protein content of the solution was determined by UV absorption at 280nm ($e_1 = 1.4$ (mg/mL)$^{-1}$cm^{-1}). BisANS powder (SIGMA, Sigma-Aldrich Chemie GmbH, Germany) for extrinsic fluorescence detection was dissolved in PBS. Final solution concentration was measured by UV absorption at 385 nm ($e_2 = 16750$ mol^{-1}cm^{-1}). The filters used are listed in table 1.

2.2 Stress Methods

2.2.1 pH stress

The IgG1 was stressed changing the pH of the formulation to pH 1 by adding the required amount of HCl 1M to the samples. The actual pH was measured by a MP 220 pH meter (Mettler Toledo).

2.2.2 Thermal stress

The IgG1 was stressed at 60°C in a water bath for 40 minutes and cooled back to room temperature.

2.2.3 Freeze/Thaw stress

The IgG1 was stored in a freezer at -80°C for 30 min and then thawed in a water bath at 25°C for another 30 min. This cycle was repeated for 20 times.

2.2.4 Light stress

The IgG1 was stressed in a SUNTEST CPS (Heraeus, Original Hanau) at 54 W/m² by a xenon lamp for 2 days. The chamber was not cooled, and the samples reached 35°C, which is however far below T_m of the protein (71°C).

2.3 Analytical Methods

2.3.1 Visual Inspection

The existence of visible particles was surveyed after gentle rotation of the sample to bring settled particles in motion.

2.3.2 Turbidity

For nephlometry measurements the NEPHLA turbidimeter (Dr Lange, Germany) was used. Light (= 860 nm) was sent through the samples and the scattered light was measured at a 90° angle. The results were given in formazine nephelometric units (FNU).

2.3.3 Light Obscuration Particle Counting

Sub-visible particle counting was performed on a PAMAS device (Rutesheim, Germany) equipped with a laser diode and a photodiode detector for size distribution analysis. Three measurements of a volume of 0.5 ml for each run were analysed with a forerun volume of 0.3 ml. Results refer to a sample volume of 1.0 ml. Between measurements the device was cleaned with water until particle counts correspond to the acceptance criteria of the European Pharmacopoeia (Pharm.Eur. 2.9.19; number of particles >10μm less then 25 particles in 25 mL).

2.3.4 Fluorescence Spectroscopy

Extrinsic fluorescence spectroscopy studies in batch mode were conducted on a Varian Eclipse Fluorescence Spectrometer (Darmstadt, Germany). The fluorescence of the protein solutions before and after filtration via a 5 μm Minisart syringe filter was compared (Fig.1 Step A). The protein solutions were analysed in white 96 well plates (NUNC). The excitation wavelength was set to 385 nm, the obtained maximum emissions at 485 nm were compared, the excitation and emission slits were adjusted to 5 nm each, the PMT detector voltage was regulated to 700 Volts, and a scanning

_____

speed of 120 nm/min was used. The spectra were corrected by subtracting the buffer spectrum.

2.3.5 Fluorescence Microscopy

Visualization of proteineous particles at a size range > 1 µm up to 200 µm was performed with the fluorescence microscope Keyence BZ 9000 (Keyence, Germany) and staining the protein aggregates with BisANS solution. Protein solutions were stressed and pre-filtrated via a 5 µm Minisart filter to remove very large aggregates. The filtrates were spiked with a BisANS stock solution to a final concentration of 10 µM. Gridded 0.45 µm CA filters (25 mm in diameter) were pre-rinsed with 10 mL of corresponding buffer and subsequently the samples were filtrated.

Alternatively, the protein samples were stained with BisANS stock solution directly (10 µM final concentration) after stress exposure, filtrated via the gridded CA filters and thereby, also larger aggregates were retained and analysed on the filter surface. All filtration steps were performed under laminar air flow conditions. 5 mL of a 2 mg/mL IgG1 were filtrated on 4.9 cm² corresponding to a theoretical protein load of 2 mg/cm². The CA filter surface was analysed using a BZ-9000 Fluorescence Microscope, an excitation of 365 nm, an excitation time of 25 ms, 20x magnification, and the BZ-9000 software (Keyence, Germany) (Fig.1 Step B). The microscope was equipped with a monochromatic detector.

In a second step, Vivaspin500 tubes (MWCO 30kDa) were pre-rinsed with 0.5 mL of NaOH 0.2 M, followed filtration by 2x0.5 mL of buffer for formulation. 0.5 mL of protein solution filtrate (obtained after filtration via the CA filters) were concentrated in the Vivaspin500 at 3,000 rpm/g for 20 min. The membrane was then collected by breaking the Vivaspin500 tube and analysed via the fluorescence microscope (Fig.1 Step C).

2.3.6 Bright-field Microscopy

After FM the protein aggregates on the filter surface were further stained with the protein detection kit as described by the supplier (Sigma Aldrich, Germany) by applying 1 mL protein detection kit stock solution onto the filter surface. The protein detection kit could interact for 5 min with the protein aggregates and was then washed out with 10 mL PBS buffer. The filters were analysed with a Keyence digital VHX-500F bright-field microscope (Keyence, Germany) using the zoom objective VH-V100, 2.11 billion pixel CCD camera, 100 W halogen lamp and its software (Fig1: Step D).

2.3.7 Sodium Dodecyl Sulfate - Polyacryl Amide Gel Electrophoresis (SDS-PAGE)

The formation of covalent aggregates and fragments was analysed by SDS-PAGE under reducing and non-reducing conditions in an electrophoresis chamber with a power supply using Bis-Tris gels and Bis-Tris SDS-Running buffer (Invitrogen GmbH, Germany). Samples were diluted to a final concentration of 0.025 mg/mL with SDS buffer or, when using reducing conditions, with a 10% DDT containing SDS solution. The samples were heated at 95°C for 20 minutes and a sample load of 10 µL was used. A standard silver staining protocol including washing, fixing, staining, de-staining and drying was employed for the protein detection.

_____
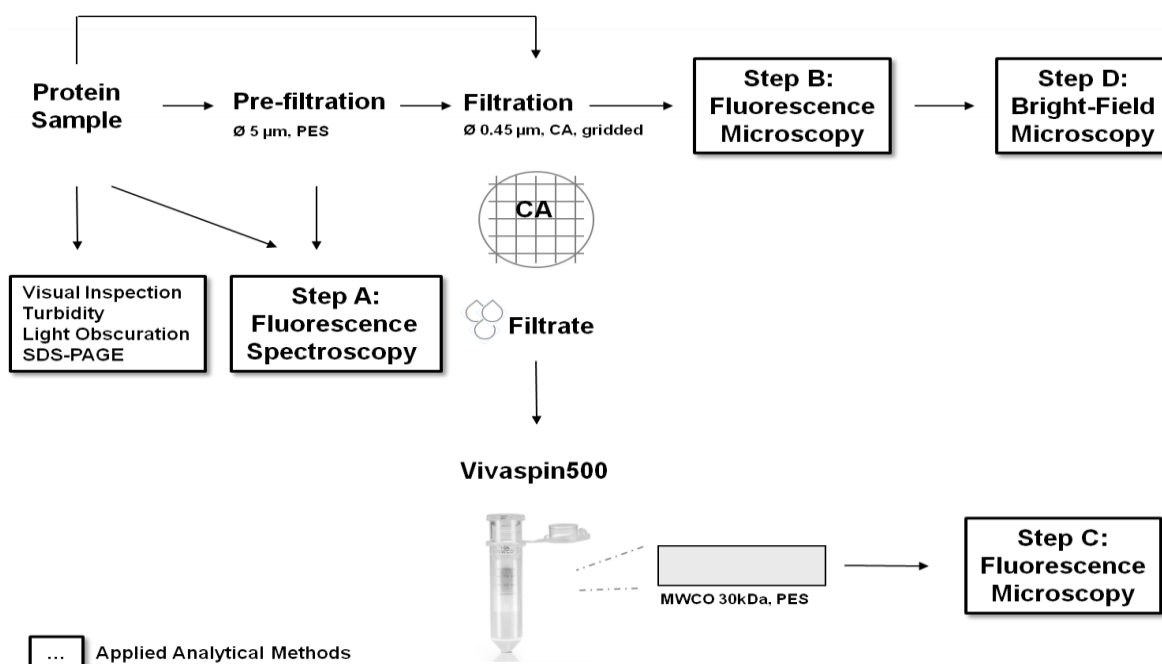
Figure 1: A schematic drawing of the analysis of protein aggregates via FM and spectroscopy and bright-field microscopy.

3 RESULTS AND DISCUSSION

3.1 Visual Inspection and Turbidity

All samples were firstly analysed by naked eye to detect the appearance of visible particles. Whereas the initial IgG1 material and the samples after pH, temperature and light stress remained essentially free of visible particles, the F/T stressed samples showed many small particles. The light stressed samples turned slightly yellowish indicating oxidation and further linkage resulting in chromophores in the protein. Regarding the turbidity, the highest turbidity values resulted for pH 1 stressed material with ~ 9 FNU (Fig.2). Furthermore, a rather high turbidity was observed for F/T stressed samples with 8.7 FNU. The turbidity of temperature and light stressed samples was slightly increased compared to the bulk material with 4.9 FNU. The turbidity for the bulk material showed a value of ~ 1.6 FNU.

_____
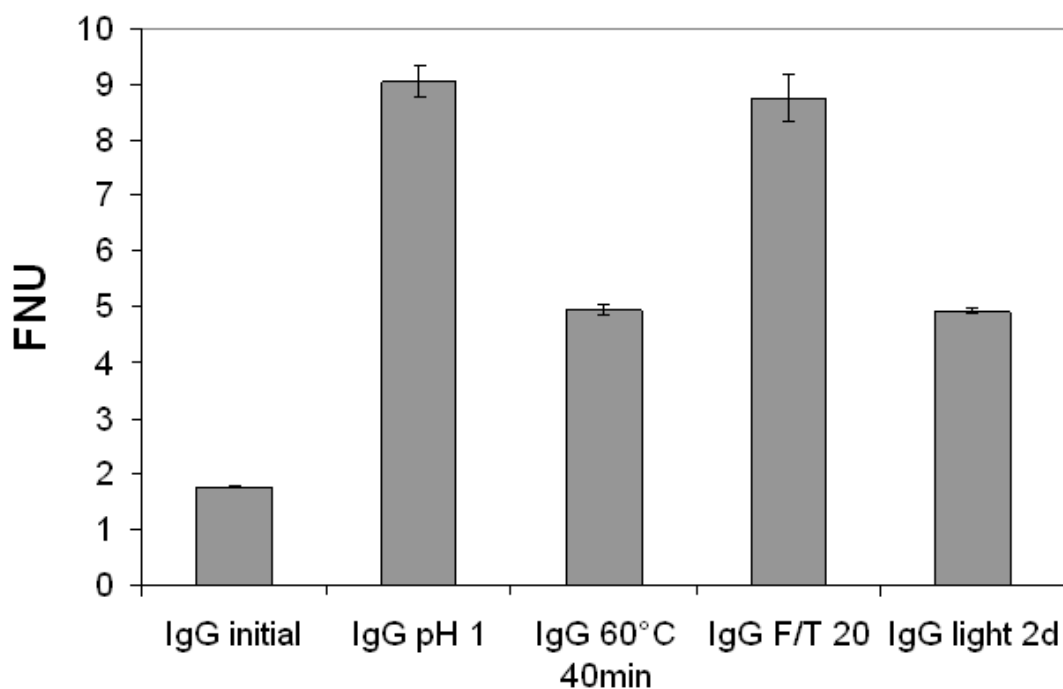
Figure 2: Turbidity as measured via the Nephlometer for stressed protein solutions before filtration.

3.2 Light obscuration particle counting

The number of particles detected by light obscuration particle counting revealed an increase in particles > 1µm for all stressed samples (Fig.3). The IgG1 formulation initially exhibited 1,611 particles larger than 1µm. The pH 1 stressed sample showed an enormous increase in particles > 1 µm with 48,706 particles/mL. Temperature stressed samples showed 21,688 particles > 1 µm. The highest amount of particles > 1 µm was obtained in the F/T stressed sample with ~ 84,000 particles/mL. The light stressed sample showed a number of particles > 1 µm of 52,000 particles/mL. Thus, the number of particles > 10 µm and > 25 µm was increased after stress exposure as well. Whether these particles are unfolded or not, is still unclear.

_____
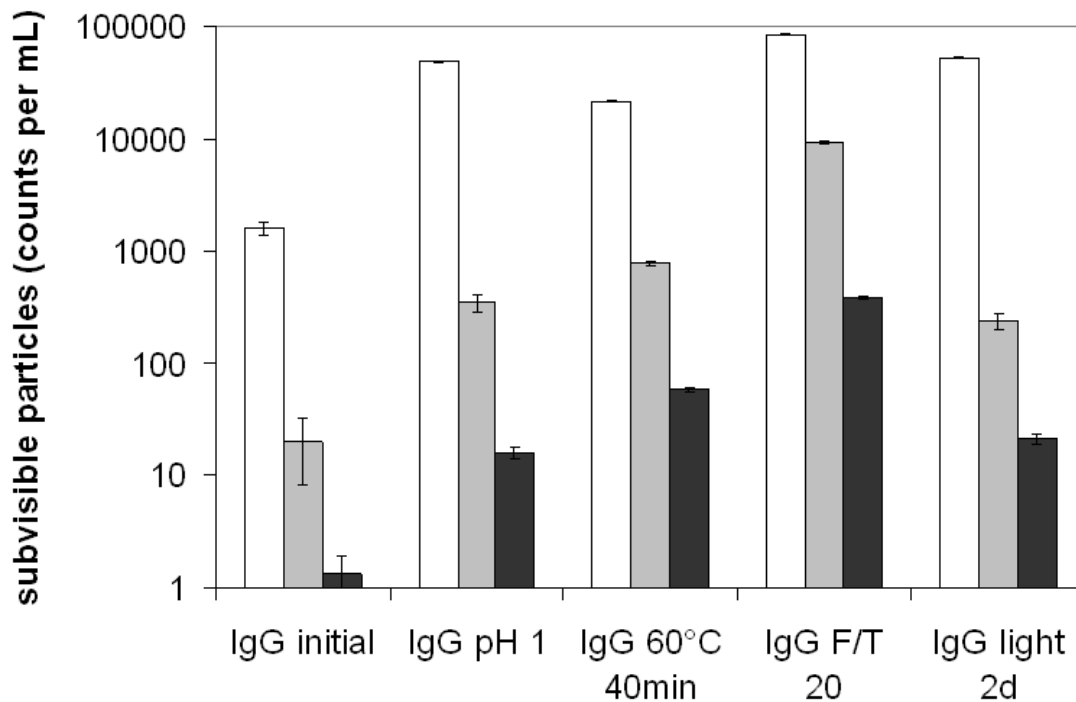
Figure 3: Light obscuration particle counting of stressed protein samples before filtration revealed the presence of particles > 1 µm (white columns), > 10 µm (grey columns), and > 25 µm (black columns).

3.3 Sodium Dodecyl Sulfate - Polyacryl Amide Gel Electrophoresis (SDS-PAGE)

Except for the light stressed samples, both the non-reduced and the reduced SDS-PAGE showed the bands typical for an IgG1 (Fig.4). For light stressed samples aggregates of approx. 300 – 450 kDa could be detected indicating the formation of covalent aggregates by bonds, which can not be reduced.
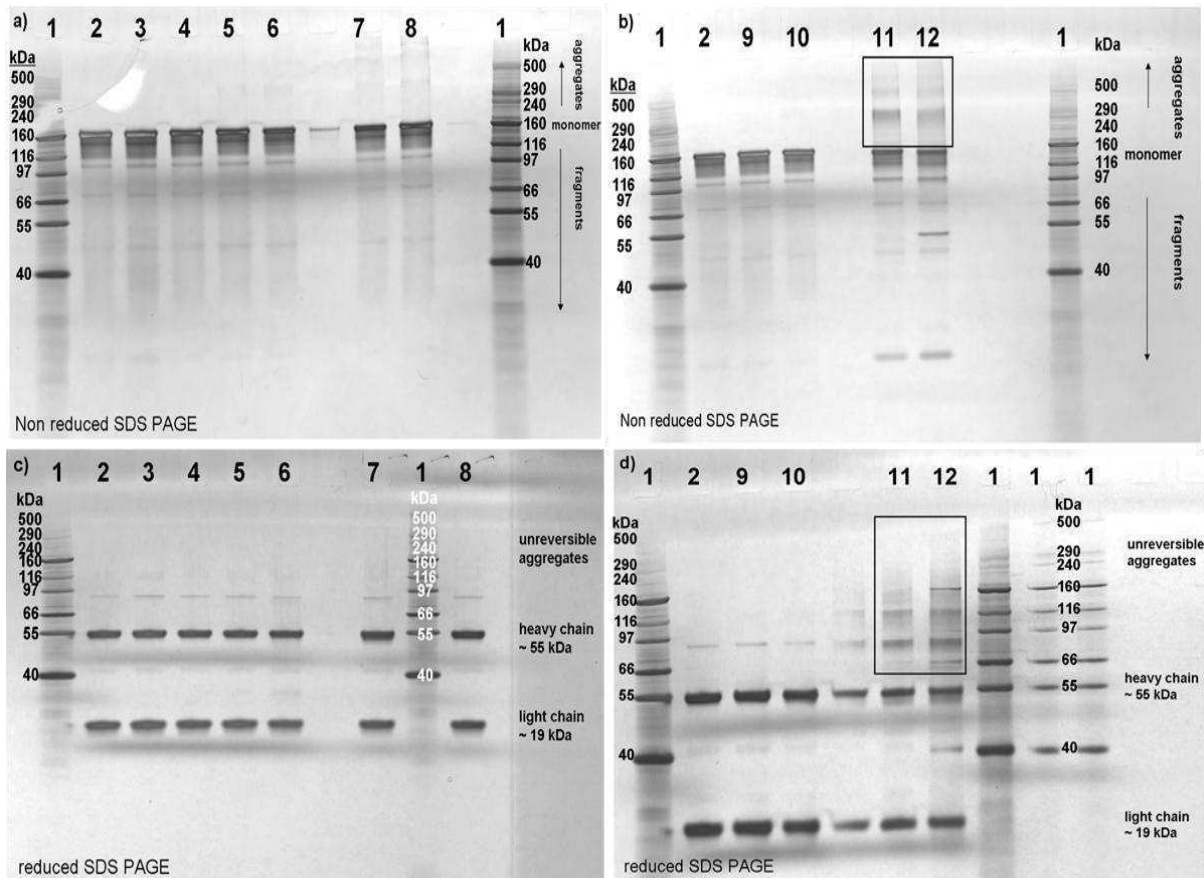
Figure 4: Non-reduced (a-b) and reduced (c-d) SDS-Page of stressed protein solutions before filtration (marker (1), IgG1 initial (2), pH 1 (6), 60 °C 20min (7), 60 °C 40min (8), F/T 10 (9), F/T 20 (10), light 1d (11), light 2d (12)).

3.4 Fluorescence Spectroscopy

The fluorescence intensity was increased for all stressed samples. pH 1 and temperature stressed samples showed the highest increase. In addition, it clearly could be shown that larger particles (> 5 µm) contribute substantially to the fluorescence intensity, as after filtration the intensity for all tested stressed samples dropped by approximately 50 % (Fig.5). The fluorescence intensity observed in the F/T stressed samples was almost only due to larger particles and could be nearly completely removed and down-regulated to the level of the IgG1 initial. In contrast, for the pH 1, temperature and light stressed samples a significantly higher fluorescence intensity remained in fluorescence spectroscopy after filtration. This

indicates the presence of structurally altered small aggregates and potentially monomers.
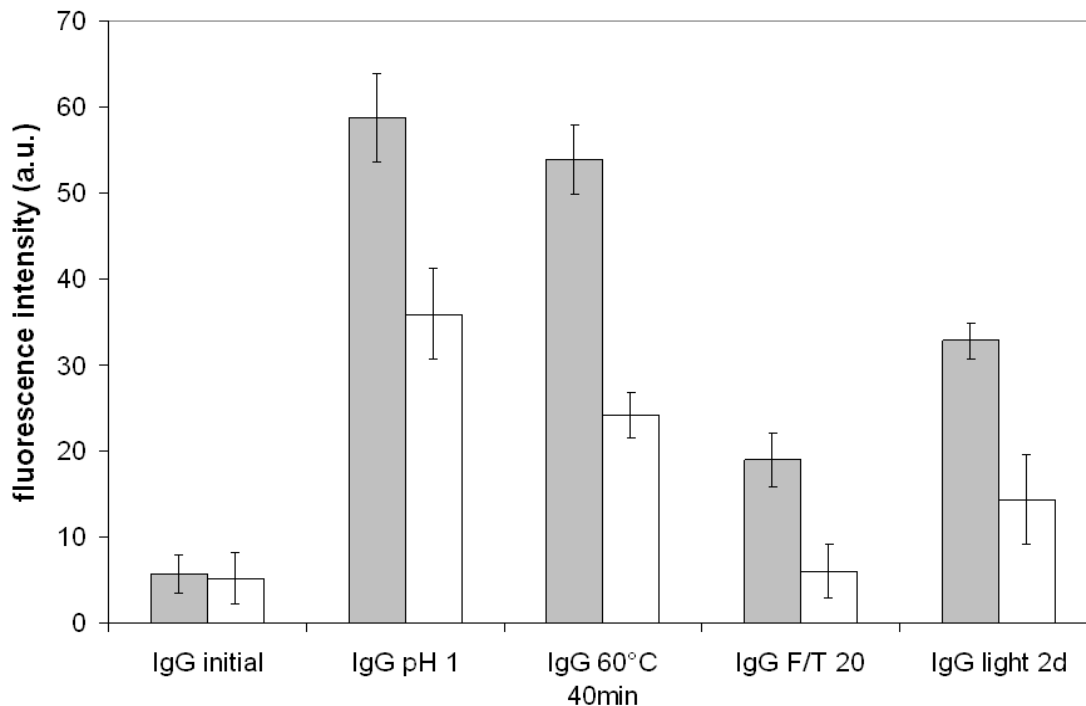
Figure 5: Extrinsic fluorescence spectroscopy (ex. 385 nm, em. 485 nm) of stressed protein solutions before and after pre-filtration via Minisart PES.

3.5 Fluorescence Microscopy

3.5.1 Protein aggregates directly on 0.45 µm CA filter surface

Using FM it was possible to detect protein aggregates stained with BisANS (Fig.6 and 7). It was also possible using bright-field microscopy after staining with the protein detection kit (Fig.8 and 9). The filtration of PBS and IgG1 initial material rendered no, respectively only few fluorescent particles on the filter surface as seen in the FM images (Fig.6a and b). However, the filtration of stressed protein material resulted in a high number of large fluorescent protein aggregates on the filter surfaces (Fig.6c-f). Interestingly, the retained protein aggregates differed in size and quantity depending on the stress expose. IgG1 samples stressed at pH1 showed the

_____

formation of many big protein aggregates species in the size range of 100 µm up to several mm in length (Fig.6c).

The protein aggregates obtained after temperature stress (60°C 40min) appeared also in high quantity in a similar size range from < 100 µm up to several mm. Compared to the big aggregates observed in the pH1 stressed sample, the aggregates of the temperature stress sample seemed to be more fibrous in appearance (Fig.6d). The different shape of the induced aggregates became even more pronounced in the observed protein aggregates of the F/T 20 stressed samples (Fig.6e). Here many smaller particles (< 100 µm) were found showing a spherical shape. Protein aggregates induced by light stress appeared to be less showed a rather fibrous shape in a size range < 100 µm. By comparing the appearance of the induced protein aggregates, the diverse effect of different stress methods on the protein aggregates structure became obvious. Especially the spherical shape of protein aggregates, which appeared after F/T stress exposure, is interesting. This might be a result of a potential phase separation, which the protein is subjected to while freezing. Phase separation is not occurring during pH, temperature, light or shaking stress and here the protein aggregates do show a different shape. Thus, FM may be a good tool to obtain further information on size and shape of the larger aggregates formed in protein formulation.

3.5.2 Protein aggregates after pre-filtration via 5 µm Minisart on 0.45 µm CA filter surface

To reduce the induced protein aggregates in number and to remove the very large particle fraction (> 50 µm), protein samples were pre-filtrated via 5 µm Minisart syringe filters, subsequently stained with BisANS stock solution and filtrated via the 0.45 µm CA filters. The obtained FM images are shown in figure 7. No fluorescent particles were observed in the PBS and the initial IgG material (Fig.7a-b), whereas many small particles (< 50 µm, most particles < 10 µm) were observed in the pH1 (Fig.7c), temperature (Fig.7d), F/T (Fig.7e) and light (Fig.7e) stressed samples. Due to the pre-filtration step however, the differences in information in appearance of the

protein aggregates in shape, size and amount got lost. Most observed particles were found in a size range < 10 µm. Due to the good contrast gained by the fluorescence, protein aggregates of a size down to 1 µm could be detected and size estimated. Thus, FM was rather sensitive to smaller particles.

3.6 Bright-field Microscopy

3.6.1 Protein aggregates directly on 0.45 µm CA filter surface

Using the protein detection kit and a digital microscope VHX 500F (Keyence, Germany) it was possible to observe protein aggregates in the protein samples after stress exposure as well [2]. No, or hardly any protein particles could be observed in PBS and the IgG1 starting material (Fig.8a-b).

Protein aggregates were retained on the filter surface and appeared as purple spots. In pH1 stressed samples (Fig.8c), big particles in a size range > 100 µm as well as smaller protein particle dots of ~ 10 µm could be visualized. After temperature stress a network of big flake-like and fibrous particles was detected in a size range of several 100 µm as well as some smaller particles (Fig.8d). In the F/T stressed samples rather spherical particles in a size range of < 100 µm were found (Fig.8e). In the light stress samples protein aggregates appeared to be less present and showed needle-like, fibrous shapes in a size range < 100 µm (Fig.8f).

Compared to the FM after staining with BisANS, less aggregates appeared to be present. Thus, the bright-field microscopy seems to be less sensitive to smaller particles compared to the FM. Hence, FM was revealed to be a suitable orthogonal tool for the analysis of protein particles > 1 µm, especially after 5 µm pre-filtration.

_____

3.6.2 Protein aggregates after pre-filtration via 5 µm Minisart on 0.45 µm CA filter surface

No protein aggregates were observed in PBS and the initial IgG1 solution after pre-filtration via 5 µM Minisart filters (Fig.9a-b). Also in the stressed protein samples after pre-filtration, particles could hardly be detected in the bright-field microscopy images (Fig.9c-f). Those particles, which could be detected as purple spots, showed a size range of approx. 10 µm and larger (Fig.9c-f). However, due to the filtration step the quantity of the protein aggregates was reduced. But, although using 5 µm Minisart filters, particles exceeding a size of 5 µm were observed suggesting rapid reformation from colloidally instable smaller aggregates.

_____
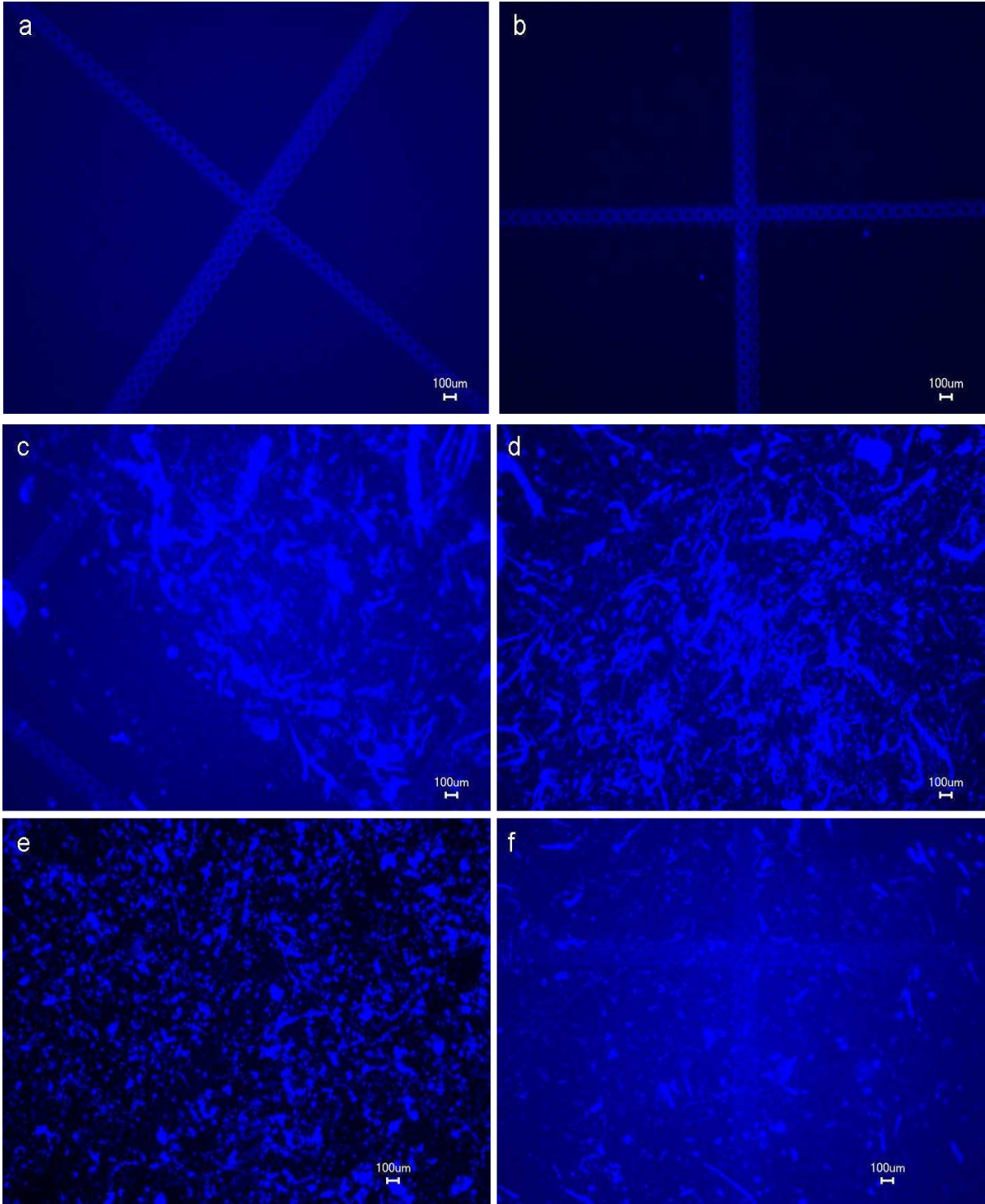
Figure 6: FM images of gridded 0.45 µm CA filter surface after filtration of PBS (a) and IgG1 bulk material (b) and IgG1 after stress exposure for pH 1 (c), 60°C 40min (d), F/T 20 (e) and light 2d (f) stained with BisANS.

_____
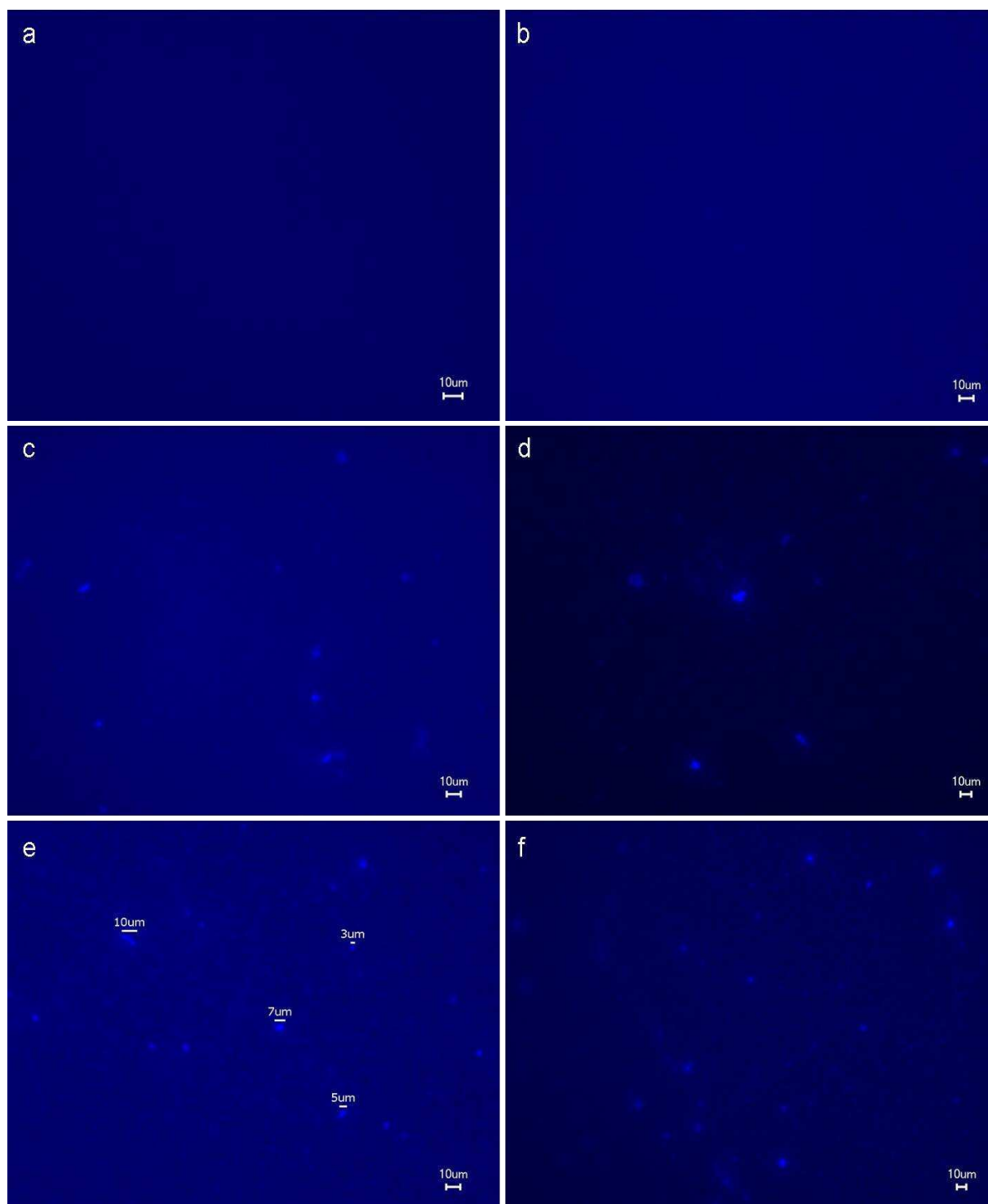
Figure 7: FM images of gridded CA filter surface (Ø 0.45 µm) after filtration of pre-filtrated (Minisart Ø 5 µm) PBS (a) and IgG1 bulk material (b) and IgG1 after stress exposure for pH 1 (c), 60°C 40min (d), F/T 20 (e) and light 2d (f) stained with BisANS.

_____
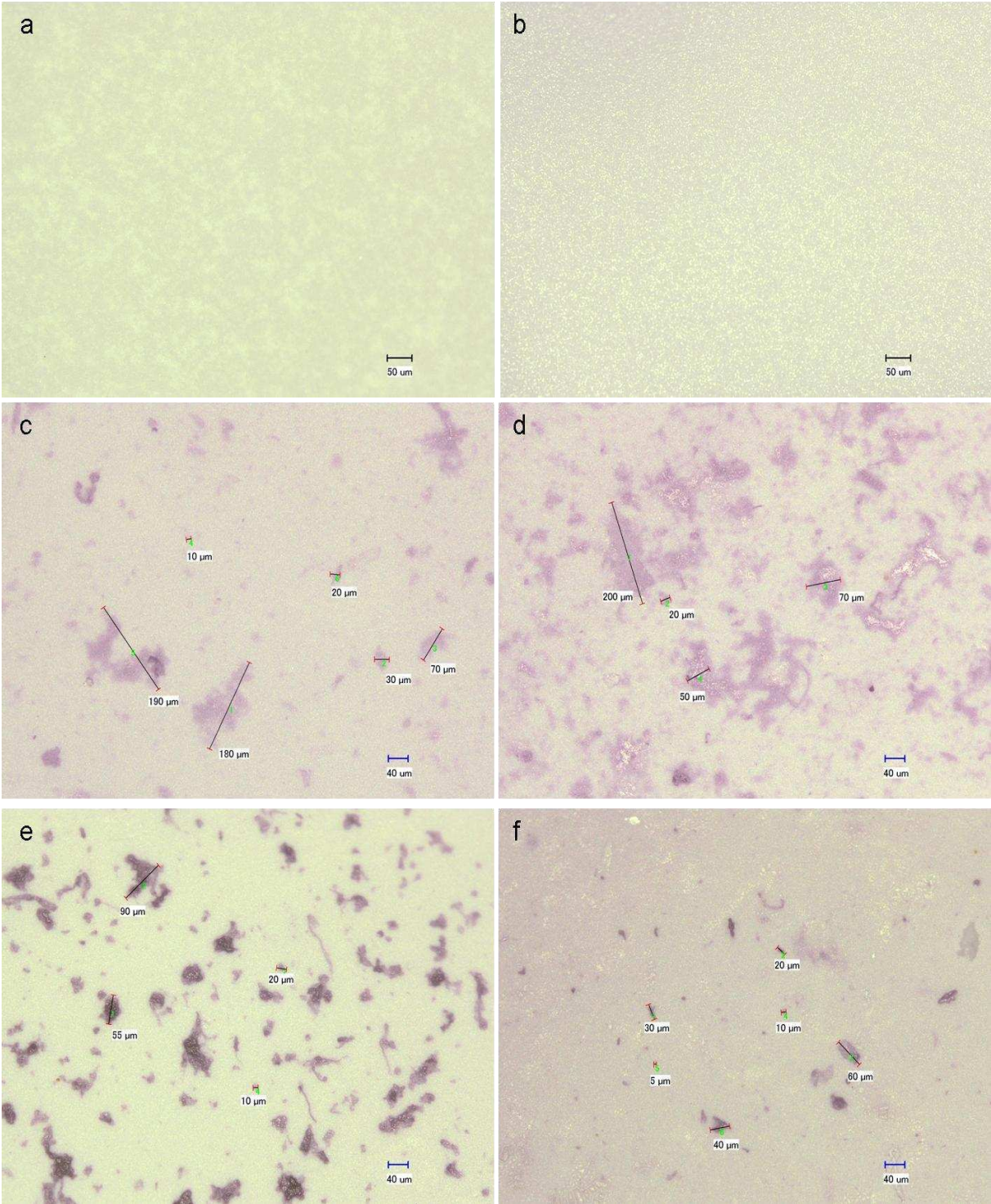
Figure 8: Bright-field microscopy images of gridded CA filter surface (∅ 0.45 µm) as seen after filtration of PBS (a) and IgG1 bulk material (b) and IgG1 after stress exposure for pH 1 (c), 60 °C 40min (d), F/T 20 (e) and light 2d (f) stained with protein detection kit.

_____
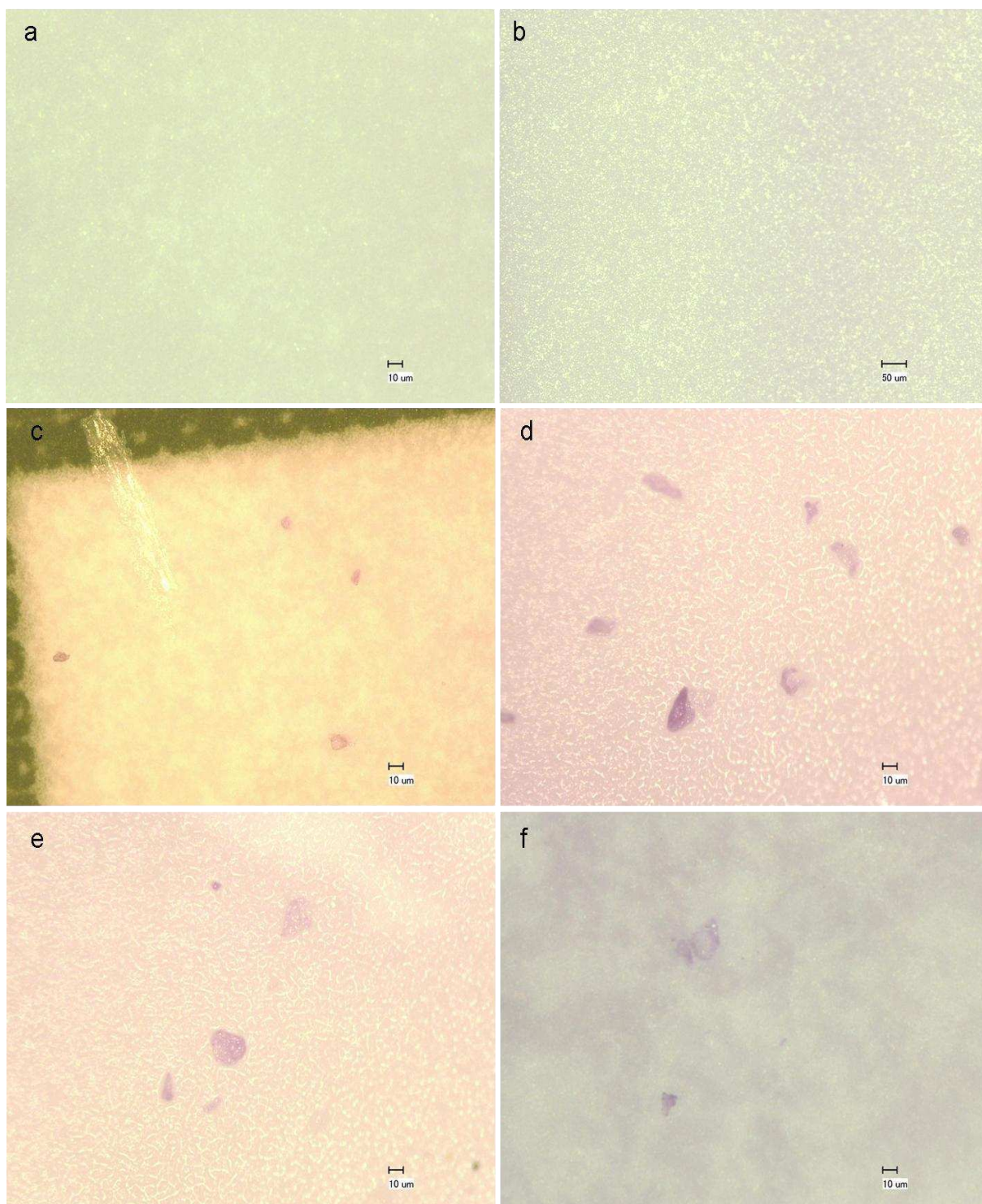
Figure 9: Bright-field microscopy images of gridded CA filter surface (Ø 0.45 µm) after filtration of pre-filtrated (Minisart Ø 5 µm) PBS (a) and IgG1 bulk material (b) and IgG1 after stress exposure of pH 1 (c), 60 °C 40min (d), F/T 20 (e) and light 2d (f) stained with protein detection kit.

3.7 Fluorescence Microscopy on Vivaspin500 (MWCO 30kDA) filter surface

In an effort to further analyse the small formed aggregates < 1 µm by an optical method, the filtrate was concentrated on the Vivaspin500 (MWCO 30kDa) membrane. Here no individual particles are visible any more, but rather an overall fluorescence can be detected. Analysing the obtained histograms provided by the Keyence software, a tendency to a higher average and maximum fluorescence intensity for pH 1 (220 / 255 a.u.), temperature (190 / 250 a.u.) and light (220 / 255 a.u.) stressed samples could be seen (Fig.10). Data from SEC with a post-column-derivatisation module showed structural changes for both oligomers and remaining monomer for exactly those stress samples (data presented in Chapter 3). Therefore, the higher fluorescence intensity might be due to structural changes in the aggregates < 0.45 µm and of the remaining monomer accumulated on the Vivaspin500 membrane. In the bright-field microscopy, however, no particles could be detected on the filter surface after pre-filtration. Therefore, FM is again considered to be more sensitive compared to the bright-field microscopy approach.
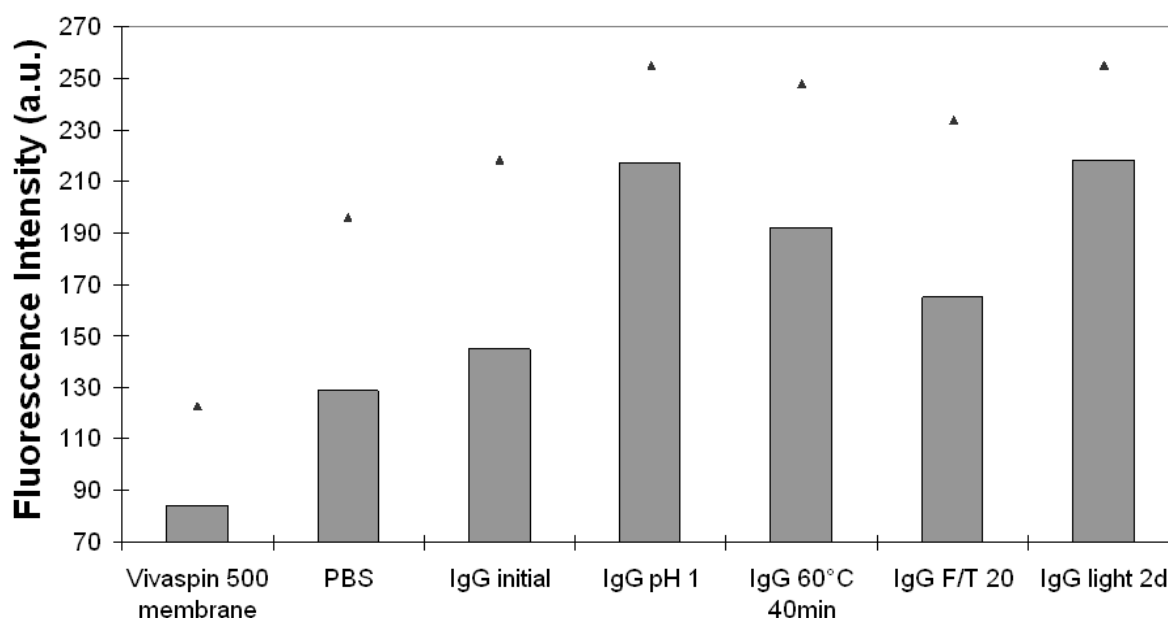
Figure 10: Overall fluorescence of the Vivaspin500 membrane surface (30 kDa) (columns: average fluorescence intensity values (a.u.); triangles: maximum fluorescence intensity).

4 CONCLUSION

FM using BisANS enabled the visualization of particles > 1 µm and was significantly more sensitive for protein particles < 10 µm compared to the bright-field microscopy due to a better contrast. The results obtained by the FM were comparable to light obscuration particles counting and visible particles analysis. By retaining the protein aggregates on the gridded white CA membrane filters, FM enables an easy size estimation using the squares of the grids with a higher sensitivity than the bright-field microscopy. Beyond that, by using FM it was possible to detect different appearances of the protein aggregates formed up on various stress methods. Here, especially the protein aggregates formed upon F/T stress showed a different, rather spherical shape. Therefore, a comparison to the micro-flow imaging would be interesting. Flow microscopy techniques, such as micro-flow imaging (MFI), have the ability to take images of particles > 2 µm. Thus, for the characterization of irregular shaped aggregates, fluorescence flow microscopy techniques might be an interesting combination of FM and particle counting. But both, flow microscopy and light obscuration, as optical particle counting techniques were reported to suffer from the relatively low refractive index (RI) of the protein aggregates in combination with an increased background RI in case of high concentration protein formulation. This can lead to an underestimation of protein aggregates [7]. The possibility of visualizing the shape of protein particles, its suitability for the particle size range 1 – 200 µm and especially its sensitivity to small particles in the size range < 10 µm makes FM an interesting tool in protein aggregate analysis.

5 ACKNOWLEDGEMENTS

6 REFERENCES

[1] Demeule, Barthelemy; Gurny, Robert; Arvinte, Tudor. Detection and characterization of protein aggregates by fluorescence microscopy. International Journal of Pharmaceutics (2007), 329(1-2), 37-45.

[2] Li, Bei; Flores, Jose; Corvari, Vincent. A simple method for the detection of insoluble aggregates in protein formulations. Journal of Pharmaceutical Sciences (2007), 96(7), 1840-1843.

[3] Mahler, Hanns-Christian; Friess, Wolfgang; Grauschopf, Ulla; Kiese, Sylvia. Protein aggregation: Pathways, induction factors and analysis. Journal of Pharmaceutical Sciences (2009), 98(9), 2909-2934.

[4] Schellekens, Huub. Factors influencing the immunogenicity of therapeutic proteins. Nephrology, Dialysis, Transplantation (2005), 20(Suppl. 6), vi3-vi9.

[5] Rosenberg, Amy S. Effects of protein aggregates: an immunologic perspective. AAPS Journal (2006), 8(3), No pp. given.

[6] Demeule Barthelemy; Palais Caroline; Machaidze Gia; Gurny Robert; Arvinte Tudor New methods allowing the detection of protein aggregates: a case study on trastuzumab. mAbs (2009), 1(2), 142-50.

[7] Demeule Barthelemy; Messick Steven; Shire Steven J; Liu Jun Characterization of particles in protein solutions: reaching the limits of current technologies. The AAPS journal (2010), 12(4), 708-15.

[8] Hawe, Andrea; Sutter, Marc; Jiskoot, Wim. Extrinsic Fluorescent Dyes as Tools for Protein Characterization. Pharmaceutical Research (2008), 25(7), 1487-1499.

[9] Kumar, Vineet; Sharma, Vikas K.; Kalonia, Devendra S. Second derivative tryptophan fluorescence spectroscopy as a tool to characterize partially unfolded intermediates of proteins. International Journal of Pharmaceutics (2005), 294(1-2), 193-199.

[10] Lindgren, Mikael; Soergjerd, Karin; Hammarstroem, Per. Detection and characterization of aggregates, prefibrillar amyloidogenic oligomers, and protofibrils using fluorescence spectroscopy. Biophysical Journal (2005), 88(6), 4200-4212.

[11] Gabellieri, Edi; Strambini, Giovanni B. ANS fluorescence detects widespread perturbations of protein tertiary structure in ice. Biophysical Journal (2006), 90(9), 3239-3245.

[12] Demeule Barthelemy; Lawrence M Jayne; Drake Alex F; Gurny Robert; Arvinte Tudor Characterization of protein aggregation: the case of a therapeutic immunoglobulin. Biochimica et biophysica acta (2007), 1774(1), 146-53.

[13] Hawe, Andrea; Friess, Wolfgang; Sutter, Marc; Jiskoot, Wim. Online fluorescent dye detection method for the characterization of immunoglobulin G aggregation by size exclusion chromatography and asymmetrical flow field flow fractionation. Analytical Biochemistry (2008), 378(2), 115-122.

[14] Matulis, Daumantas; Lovrien, Rex. 1-Anilino-8-naphthalene sulfonate anion-protein binding depends primarily on ion pair formation. Biophysical Journal (1998), 74(1), 422-429.

[15] Brown, Claire M.. Fluorescence microscopy - avoiding the pitfalls. Journal of Cell Science (2007), 120(10), 1703-1705.

[16] Dillingham, Mark S.; Wallace, Mark I. Protein modification for single molecule fluorescence microscopy. Organic & Biomolecular Chemistry (2008), 6(17), 3031-3037.

[17] Helmchen, Fritjof; Denk, Winfried. Deep tissue two-photon microscopy. Nature Methods (2005), 2(12), 932-940.

[18] Arvinte, Tudor. Concluding remarks: analytical methods for protein formulations. Biotechnology: Pharmaceutical Aspects (2005), 3(Methods for Structural Analysis of Protein Pharmaceuticals), 661-666.

[19] Kueltzo, Lisa A.; Wang, Wei; Randolph, Theodore W.; Carpenter, John F. Effects of solution conditions, processing parameters, and container materials on aggregation of a monoclonal antibody during freeze-thawing. Journal of Pharmaceutical Sciences (2008), 97(5), 1801-1812.

[20] Strambini G B; Gabellieri E. Proteins in frozen solutions: evidence of ice-induced partial unfolding. Biophysical journal (1996), 70(2), 971-6.

[21] Gabellieri, Edi; Strambini, Giovanni B. Perturbation of protein tertiary structure in frozen solutions revealed by 1-anilino-8-naphthalene sulfonate fluorescence. Biophysical Journal (2003), 85(5), 3214-3220.

[22] Strambini, Giovanni B.; Gonnelli, Margherita. Protein stability in ice. Biophysical Journal (2007), 92(6), 2131-2138.

[23] Chang B S; Kendrick B S; Carpenter J F. Surface-induced denaturation of proteins during freezing and its inhibition by surfactants. Journal of pharmaceutical sciences (1996), 85(12), 1325-30.

[24] Frokjaer Sven; Otzen Daniel E. Protein drug stability: a formulation challenge. Nature reviews. Drug discovery (2005), 4(4), 298-306.

CHAPTER 6

Front Face Fluorescence Spectroscopy of Lyophilized Protein

ABSTRACT

The stabilization of protein against chemical and physical degradation both in liquid and solid formulations is one of the main aspects in protein formulation development. Lyophilized protein formulations are supposed to be more stable during shipment and storage. However, by freezing and drying, the protein is exposed to stress conditions and might unfold and aggregate. Hence, analysing the protein structure in the lyophilised state without reconstitution might bring new insights in the protein aggregation process. In this chapter, front face fluorescence spectroscopy is discussed as a possible method to characterise protein tertiary structure in lyophilised samples. For this purpose the extrinsic fluorescence of BisANS added prior to lyophilisation was analyzed. The extrinsic front face fluorescence spectroscopy was found to be only partially suitable for the analysis of lyophilised proteins. The main challenge was that placebo samples already showed high and variable fluorescence. The measurement of the small incremental changes in the fluorescence of protein containing samples was therefore difficult.

_____

1   INTRODUCTION

The primary objective in protein formulation development is to gain a stable, effective and safe formulation for the market. A major challenge in protein formulation is achieving the stability of the rather sensitive protein molecules [1] within a limited spectrum of variable formulation parameters. Amongst others, the adjustment of the pH value and ionic strength, the choice of buffer species, and the addition of various excipients, such as surfactants, cryoprotectans, lyoprotectans or other stabilizers may be considered in aqueous and lyophilised formulations. In lyophilised systems, the proteins are stabilized in a glassy matrix providing hydrogen bonding to replace the water molecules. Consequently, it is of high interest to gain knowledge about the protein structure directly in the lyophilisate without reconstitution.

Almost 50% of the protein pharmaceuticals on the market are lyophilised. Due to the limited mobility, which restricts conformational flexibility and reduces the number of collisions and by avoiding hydrolytic reactions, aggregation of protein is minimized [2]. However, the freezing and drying process may be disadvantageous for the protein integrity [3]. Freezing of the protein solution may be harmful for the protein structure due to changes in buffer concentration, new interfaces and variations of the pH value [4]. As water is removed during the drying process, the hydration shell of the protein disappears. This may lead to instabilities in protein tertiary structure followed by formation of aggregation [5; 6].

Generally, analytical methods to characterize protein structure or aggregate status may have considerable impact on protein structure due to reconstitution and dilution during analysis. Furthermore, for high-throughput screening and in-process-control, it would be advantageous to have analytical tools on hand to analyse the protein in the dried state. For characterization of protein structure in the dried state, spectroscopic methods have been described [12; 13; 14]. In FT-Raman spectroscopy the substantial interference by excipient signals is a drawback but it is suitable in high concentrated protein formulations. Nevertheless, it might be used to trace alterations in protein tertiary structure in liquids, and regarding disulfide, the microenvironment

_____

data can be gained for solids as well [15]. Infrared spectroscopy works by exciting vibrational motions and thereby changing bond lengths and angles.As the amid 1 band between 1,700 and 1,600 cm^{-1} is influenced by the intramolecular structure of the protein, it is possible to analyse the secondary structure of the protein [16]. By Fourier transform infrared (FTIR) spectroscopy the effect of carbohydrates on dried proteins could be analysed [7].

It was observed that only proteins, which kept their native state in the dried form, were able to regain most of their biological activity after reconstitution. The formation of structurally altered states was also claimed to be a must for irreversible aggregation and sufficient to lead to long-term aggregation [8]. A loss of native structure during drying seems to be in several cases irreversible and leads to denaturation and aggregation after reconstitution [9; 10; 11].

Fluorescence spectroscopy may provide an additional tool for the characterization of protein tertiary structure in the dried state. The results published so far focused on intrinsic front face fluorescence spectroscopy of solid protein formulations in powder or in ice form [5; 8; 17]. Gabellieri et al. [5] focused on freeze-induced structural perturbations in protein tertiary structure in ice analysed by using the fluorescence dye 1-anilino-8-naphthalene sulfonate (ANS). Protein tertiary structure in powders was analysed by Sharma et al. [8] by steady state tryptophan (Trp) fluorescence emission spectroscopy observing a slightly blue-shifted emission maximum compared to the solution spectra, which was assumed to be caused by the absence of water. They investigated the intrinsic fluorescence of vacuum dried protein by fixing the powder via scotch tape. However, due to reported difficulties of reproducible sample loading, no correlation was found between fluorescence intensity and changes in tertiary structure. Ramachander et al. [17] suggested solid state intrinsic protein fluorescence measurements as potentially feasible for long-term stability studies and formulation development. They investigated the fluorescence of lyophilized protein after heat-induced accelerated degeneration. Reproducible fluorescence spectra as well as a correlation between decreasing fluorescence intensity and increasing protein aggregation during long-term stability

_____

were observed. But high background light scattering was a substantial problem. Therefore, our approach was to investigate front face fluorescence spectroscopy for lyophilised protein using the extrinsic fluorescence dye BisANS.

In our approach an IgG1 model protein was lyophilized with different BisANS concentrations (0.2; 1; 5 µM) to analyse which dye concentration would be suitable for the analysis. Trehalose, mannitol, and dextran were used as cryo-/ lyoprotectans. The IgG1 was temperature stressed either prior or after lyophilization. By using a Varian Cary Eclipse solid sample holder equipment and a Steady State Fluorescence Spectrometer FS 920 (Edinburgh Instruments LTD, UK) fluorescence intensities were received for both intrinsic (ex. 280 nm) and extrinsic (ex. 385 nm) fluorescence. The results were flanked by other analytical techniques, such as scanning electron microscopy, X-ray diffraction, and residual moisture analysis. Moreover, FTIR for both liquid and solids was conducted. In addition, fluorescence spectroscopy and SEC were performed after reconstitution.

1.1 Fluorescence Characteristics

Photoluminescence is the ability of photon absorption followed by the emission of photons. It is subdivided into a) fluorescence, where the emitted photons are of lower energy than those absorbed due to the Stokes shift and the loss of energy resp., and b) phosphorescence, where a delayed re-radiation is observed (Fig.1) [18]. Electrons have various energy levels (S0, S1, S2), with various vibration states each (0-2). Absorbed energy can be emitted by molecule collision, vibration or by emitting light, whereby the electron drops down to the lower energy state. Molecules with the ability to fluoresce, show several structural characteristics, e.g., Pi-electrons, which can be activated by photon absorption, a rigid molecule structure to prevent energy loss by rotation or oscillation and a mesomeric system (fluorophore) [18].

Photodecomposition, inner filter effects, cross talking, and the scattering of light (Rayleigh and Raman scattering) may influence the intensity of fluorescence. Fluorescence depends on temperature, pH, viscosity, polarity, and presence of

_____

quenchers [19]. Quenching of fluorescence is induced by all processes that reduce the intensity of the emitted fluorescence, e.g., excited state reactions, molecular rearrangements, energy transfer, and ground state complex formations. The fluorescence lifetime represents the average time that a fluorophore remains in the excited state [18].

The natural and intrinsic fluorescence resp. of proteins and peptides is based on the aromatic amino acids tryptophan, tyrosine and phenylalanine (Fig.2), whereby most of the emission is due to excitation of tryptophan. At 295 nm, the tryptophan emission spectrum is dominant over the weaker tyrosine and phenylalanine fluorescence [19]. The aromatic amino acids contain fluorophores, which are sensitive to the polarity of the local environment. By analysing their fluorescence intensities and maxima, it is possible to monitor structural changes in a protein or peptide. During protein unfolding, the microenvironment of the fluorophores in the molecule might change. The aromatic amino acids may be easier reached or deeper buried and thereby the excitation characteristic is changed leading to an alteration in fluorescence intensity and shifts in maxima [18]. Fluorescence maxima of tryptophan are, e.g., blue-shifted (lower wavelengths, higher energy), if tryptophan encounters polar environment and is highly buried and vice versa [17].

To analyse extrinsic fluorescence characteristics of protein, non-covalently linked fluorescent dyes may be considered [19]. Hereby, fluorescence intensity is increased due to hydrophobic interactions of the dye with unfolded patches on the surface of the protein (see Chapter 3). As a non-covalently linked extrinsic fluorescent dye BisANS was used in our study (Fig.2).

_____
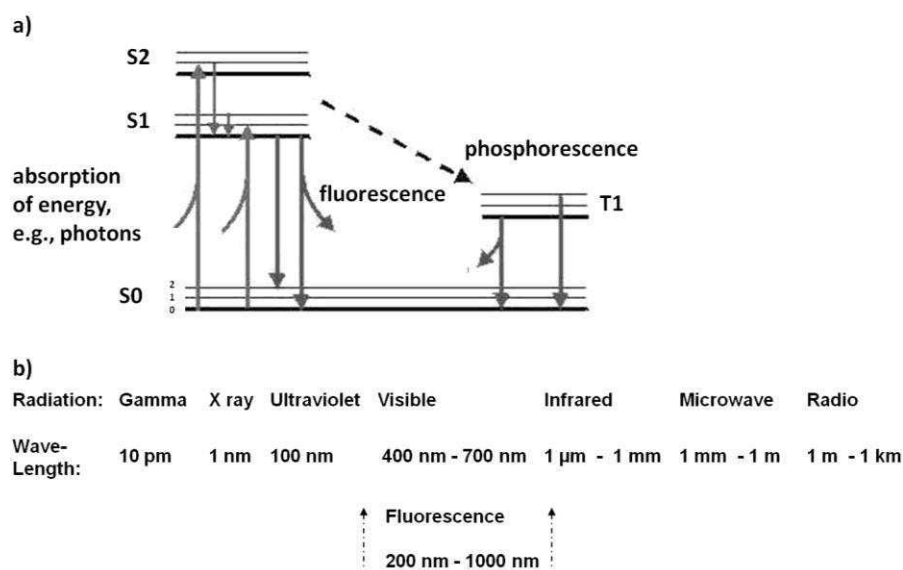
Figure 1: a) The Jablonski diagram shows absorption and emission of energy in electrons with S0 being the ground electronic state of low energy, S1, S2 and T1 representing the excited electronic states of higher energy, and the levels of various vibration states 0, 1, 2. b) The electromagnetic wave spectrum.
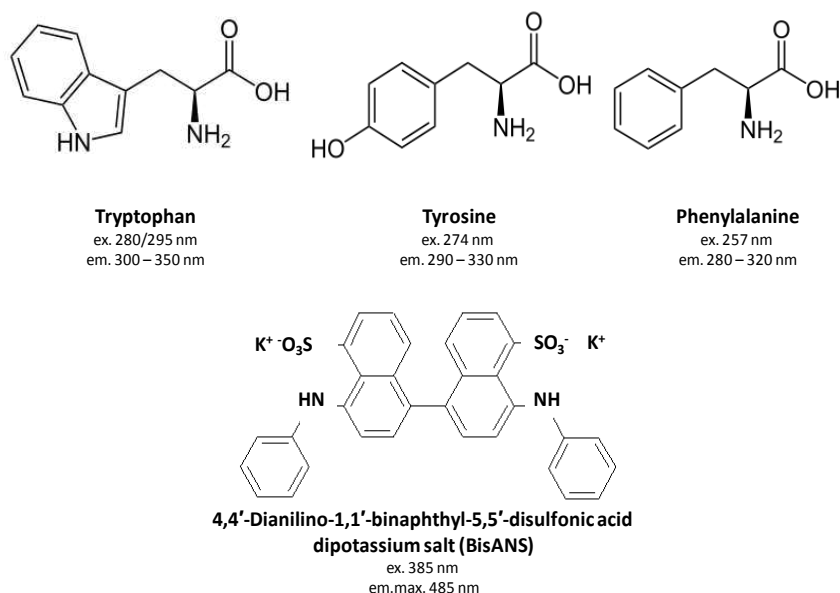
Figure 2: The chemical structures of the aromatic amino acids and BisANS and the corresponding excitation wavelength and emission range.

_____

Fluorescence characteristics of molecules can be analysed by fluorescence spectroscopy, which belongs into the field of electromagnetic spectroscopy (Fig.1). Fluorescence is frequently measured for low concentrated and clear solutions at a 90° angle relative to the excitation light to avoid interference of the transmitted excitation light. For high-throughput, well plates might be used to measure fluorescence from the top at an excitation/emission angle of $> 90°$ but $< 120°$. Furthermore, the fluorescence can also be measured from the front, which is done for turbid or opaque samples.

2 MATERIAL AND METHODS

2.1 Materials

A glycosylated IgG1 (148 kDa) at 2 mg/ mL in 10 mM phosphate buffer containing 140 mM NaCl at pH 7.2 (further called PBS) was donated by Merck, Germany. The protein content of the solution was determined by UV absorption at 280nm (e1 = 1.4 (mg/mL)-1cm-1). 2 mL of protein solution, heat stressed or bulk material, were used. BisANS (SIGMA, Sigma-Aldrich Chemie GmbH, Germany) was added prior to lyophilisation to a final concentration of 5 µM, 1 µM or 0.2 µM as a 121 µM stock solution in PBS. Final solution concentration was measured by UV absorption at 385 nm (e = 16750 (mol)-1cm-1). 300 mg trehalose, mannitol (D-Mannitol puriss. p.a., Riedel-deHaen) or dextran 70 kDa (Leuconostoc ssp, Fluka BioChemika) were added to the protein samples to a final sugar concentration of 10% (m/V) as a 300 mg/mL stock solution in water. Samples were lyophilised in 6R vials and closed with rubber stoppers. All other chemicals used were of analytical grade unless stated otherwise.

2.2 Methods

2.2.1 Lyophilisation

An Epsilon 2-12D Pilot Freeze Dryer (Christ Freeze Dryers, Germany) was used for lyophilisation via freezing to -45°C at a rate of 0.5 K/min, a hold for 5h at -45°C, primary drying at -15°C, 0.08 mbar for 25h and secondary drying at 20°C at the same

_____

pressure for 20h. The chamber was gassed with nitrogen before closing with rubber stoppers. The lyophilisates were stored in a desiccator at room temperature.

2.2.2 Stress Methods

For heat stressing, protein solutions were heated at 70°C for 10 minutes and cooled back to room temperature in 2 mL safe-lock tubes (Eppendorf). Afterwards, BisANS solution and required excipients were added and samples were lyophilised. Other samples were first lyophilised and afterwards heated for periods at 50°C (13h/25h), at 60°C (6h) or at 70°C (4h).

2.2.3 Residual Moisture

As remaining water content and hygroscopicity might possibly influence the fluorescence, residual moisture was measured by Karl-Fischer titration (Karl-Fischer-Titrator AQUA 40.00 with headspace module, analytic Jena AG, Elektrochemie Halle, Deutschland), heating the powders up to 80°C a) directly after the lyophilisation, b) after sample preparation for measurement in the vials and c) after sample preparation for measurement in an air-conditioned room.

2.2.4 X-ray powder diffraction (X-RPD)

Whether lyophilisates showed an amorphous or crystalline structure, was determined by a X-Ray Diffractometer XRD 3000 TT (Seifert, Ahrensberg, Germany) at a scanning rate of 0.05° (2°Theta) within a range of 5 to 40°2Theta (Cu-K α-radiation λ = 0.15418 nm of 40 kV, 30 mA). The diffractograms were measured with the ScanX-Rayflex application. For relative humidity controlled experiments an X´Pert Pro MPD (Panalytical, Kassel, Germany) in combination with the Temperature Humidity Chamber (THC) was used. Analysis of the X-Ray diffractograms was performed with X`Pert High Score®.

2.2.5 Scanning Electron Microscopy (SEM)

The particle morphology of lyophilised protein was analysed using a scanning electron microscope JSM – 6500F (JOEL LTD, Joel Germany GmbH, Eching, Germany) by fixing the samples with self-adhesive tapes on aluminium stubs (PLANO, W. Plannet GmbH, Wetzlar, Germany) and sputtering with a thin carbon layer under vacuum (Bal-Tec Med 20 Coating System; Bal-Tec AG, Balzers, Principality of Liechtenstein). Imaging was done in a vacuum chamber applying an accelerated voltage of 4 kV, a working distance of 10 mm and a spot size of 9.

2.2.6 SEC

IgG aggregation was determined by SEC on a Series 1100 Agilent Instruments (Agilent Technologies, Waldbronn, Germany) using a TSKgel G 3000 SWXL column (7.8 mm ID x 30 cm TOSOH BIOSEP, Tosoh Bioscience, Stuttgart, Germany) with a guard column (TSKgel SWXL Guardcolumn 6mm ID x 4 cm TOSOH BIOSEP). As running buffer PBS was used. The analytics were performed at a flow rate of 0.5 mL/min with UV detection at 280 nm and fluorescence detection (Ex. 384nm / em. 486 nm). The volume of injection was set at 100 µL.

2.2.7 Fourier Transform Infrared Spectroscopy (FTIR)

A Tensor 27 Spectrometer (Bruker Optik GmbH, Ettlingen, Germany) using the Confocheck AquaSpec system for liquids and the PIKE MIRacle system (ATR-system) for powder was employed. Each spectrum was measured with 240 scans at a single beam mode with a 4 cm $^{-1}$ resolution using the software Protein Dynamics for OPUS 6.5 (Bruker Optik GmbH, Ettlingen, Germany) gaining spectra as vector-normalized second derivation. For liquid samples the according buffer was used as background. Solid samples were analysed against air as background and buffer spectra were subtracted manually with a factor of 0.5.

_____

2.2.8 Steady State Fluorescence Spectroscopy

Intrinsic and extrinsic fluorescence spectroscopy in batch mode was conducted on a Varian Eclipse Fluorescence Spectrometer (Darmstadt, Germany) after reconstitution of the protein sample and analysed in white 96 well plates (NUNC®). The spectra were corrected by subtracting the dye containing buffer spectrum. The excitation and the emission range were set to ex. 280 nm / em. 290-500 nm and ex. 385 nm / em. 390-600 nm resp., the excitation and emission slits were adjusted to 5 nm each, the PMT detector voltage was regulated to 700 Volts, and a scanning speed of 120 nm/min was used.

2.2.9 Front Face Fluorescence Spectroscopy

The Steady State Fluorescence Spectrometer FS 920 (Edinburgh Instruments LTD, UK) with the solid sample holder kid from Varian and software F900 was used at and in cooperation with Leiden University. Lyophilised protein cake was milled with a spatula inside the 6R vial minimizing contact with atmospheric moisture. The powder was filled in the solid sample holder ensuring a complete covering of the silica disk in the shell cavity. Measurements were done in triplicates. For measurements the FS 920 used a Xe900 light source and R928P detector cooled at -20°C. The excitation and the emission range were set to ex. 280 nm / em. 300-400 nm and ex. 385 nm / em. 420-520 nm resp. nm with 1 nm steps, dwell time of 0.5 sec and excitation and emission slits of 2 nm each.

3   RESULTS AND DISCUSSION

In the presented preliminary experimental set-up, all samples were analysed before and after lyophilisation and reconstitution resp. In order to focus the discussion on the most relevant findings, the results presented relate mostly to the extrinsic front face fluorescence spectroscopy of trehalose and mannitol containing samples exposed to heat stress prior to lyophilisation and the trehalose samples spiked with different amounts of BisANS (0.2 – 5 µM).

3.1 Residual Moisture

Residual moisture was measured for all samples stabilized with mannitol, trehalose or dextran 70 kDa to be less than 2 % after lyophilisation. However, while transferring the cakes into the hermetically sealed sample cell, the samples pulled moisture resulting in a water content of 3-5 %.

3.2 X-ray powder diffraction (X-RPD)

To analyse the morphology of the powders containing different sugars, X-RPD measurements were performed. The data showed a crystalline characteristic of the mannitol samples (Fig.3), seen as the mannitol hydrate modification by its characteristic peak at 17.9° 2-Theta. Trehalose and dextran 70 kDa lyophilisates were present in the amorphous state. The characteristics were not changed after heat stressing the lyophilisates.
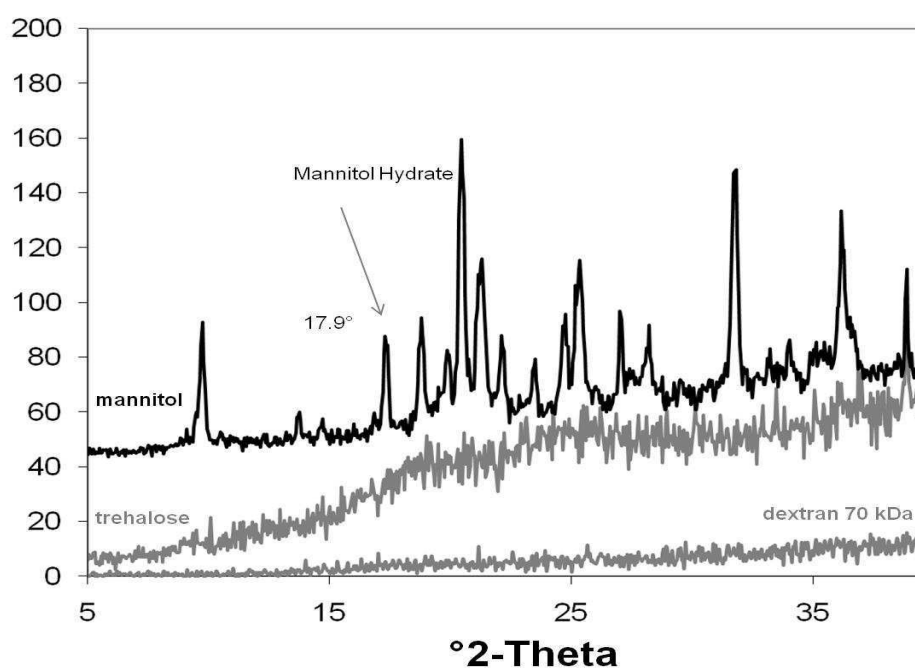
Figure 3: X-RPD of lyophilised protein samples stabilised with mannitol, trehalose or dextran 70 kDa.

3.3 Scanning Electron Microscopy (SEM)

To observe the microscopic surface and the structure of the lyophilisates, SEM images were taken. Mannitol samples revealed a coralline structure and a crystalline nature could be discerned (Fig.4). Trehalose and dextrane 70kD samples displayed a smooth surface. No influence on the structure was observed whether samples contained BisANS or protein aggregates prior to lyophilisation. The effect of heating the lyophilisates was not traceable by SEM, as Tg was not reached.
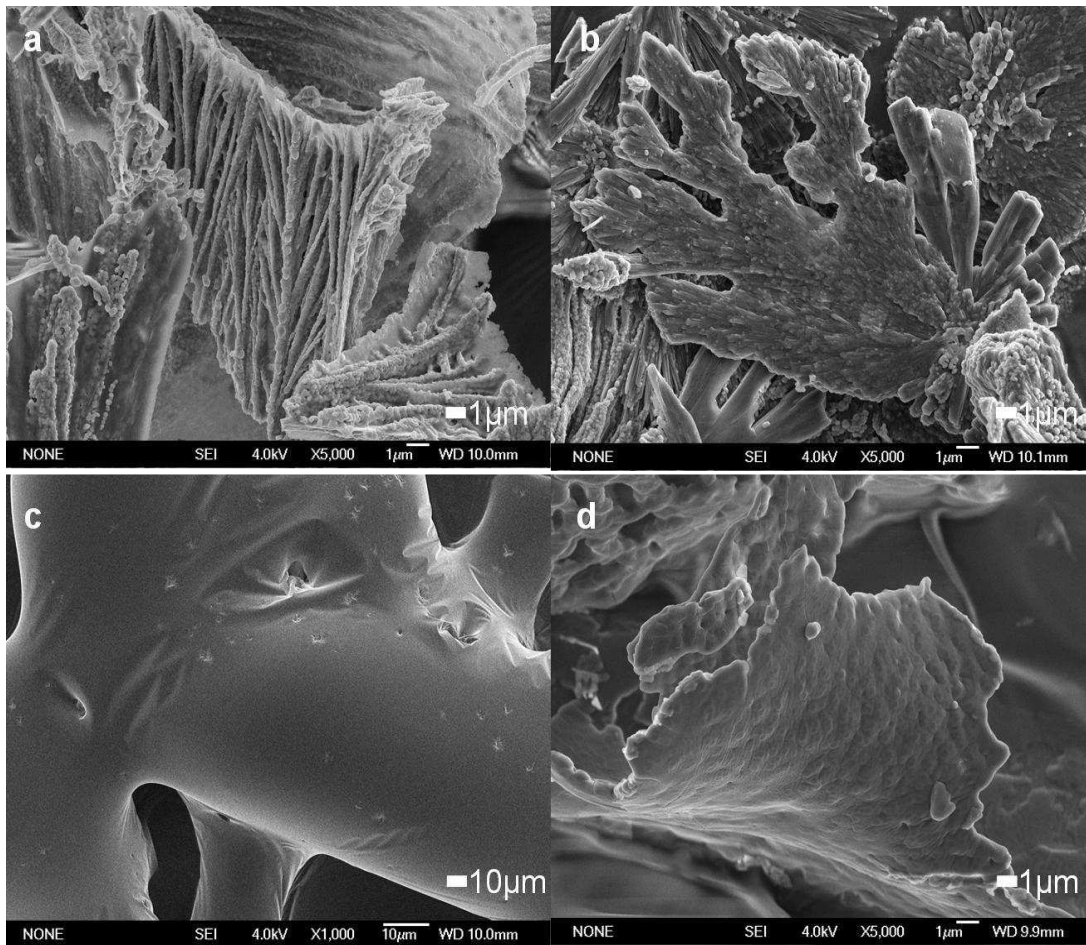
Figure 4: SEM images of lyophilised protein spiked with BisANS 1 µM containing protein aggregates a) without sugar; or stabilized with b) mannitol, c) trehalose, or d) dextran 70 kDa.

_____

3.4 SEC with UV and fluorescence detection

To analyse and prove the presence of induced protein oligomers and remaining monomer after heat stress exposure and lyophilisation, SEC with UV and fluorescence detection was performed after reconstitution. Different amounts of BisANS (0.2-5 µmol) showed no effect on the formation of protein oligomers (Fig.5a), neither in trehalose, nor in mannitol, nor in dextran 70kDa containing formulations. The stabilising effect of mannitol and dextran 70kDa was inferior compared to trehalose as indicated by the lower amount of protein oligomers and higher remaining monomer concentration in the trehalose samples after lyophilisation and reconstitution without any further stress exposure. In the samples stressed before lyophilisation / trehalose samples, > 40 % protein oligomers were observed after reconstitution. Trehalose samples heated after lyophilisation prior to reconstitution did not show any increase in the amount of oligomers. Mannitol and dextran samples showed an increase in the amount of oligomer along with a decrease in remaining monomer after stress exposure and reconstitution. The mannitol sample stressed prior to lyophilisation revealed the highest amount of oligomers (>48 %). Regarding fluorescence intensity, the oligomers contained in the trehalose (74 a.u.) and the mannitol (95 a.u.) samples stressed prior to lyophilisation showed the highest intensity indicating protein unfolding of the aggregates (Fig.5b).

The aggregates formed in unstressed samples during lyophilisation in presence of mannitol or dextran 70 kDa showed substantial fluorescence indicating at least partial unfolding. Also, the aggregates formed in the mannitol samples by heating post lyo must be unfolded to a higher degree. In the dextran 70 kDa samples a slight fluorescence increase was also observed for the remaining monomer (trehalose monomer fluorescence intensity < 2 a.u. / dextran monomer fluorescence intensity > 11 a.u.) indicating a partial unfolding of the monomer under the above mentioned conditions as well. Hence, the fluorescence data revealed an inferior stabilising effect of mannitol and dextran 70 kDa followed by unfolding of the protein, which is in good accordance to the results obtained in the SEC UV detection.
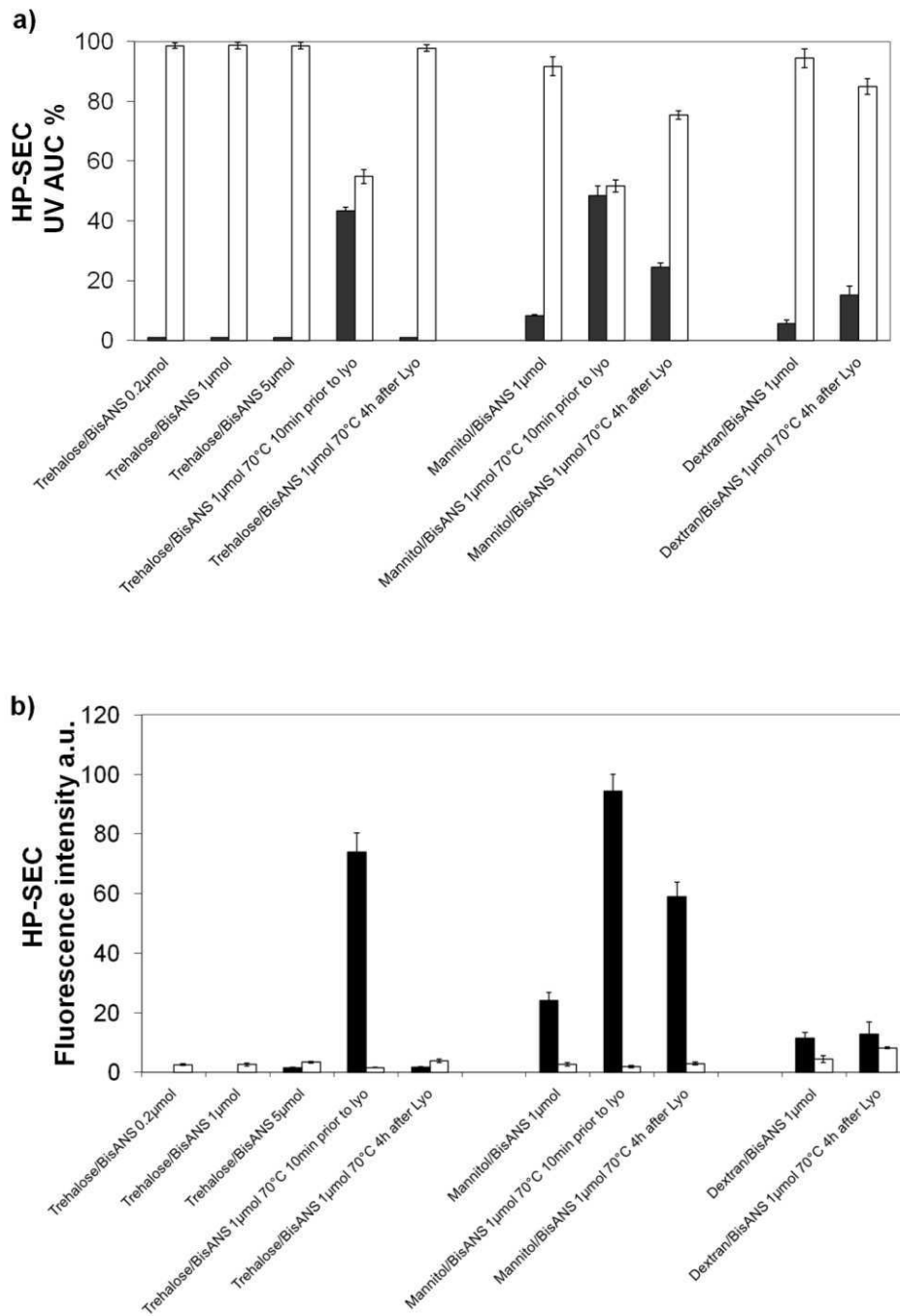
Figure 5: Oligomers (black columns) and monomer (white columns) after reconstitution of lyophilised protein with different sugars stressed prior and after lyophilisation.

3.5 Fourier Transform Infrared Spectroscopy (FTIR)

The investigation of the secondary structure (α-helix and ß-sheet) of the protein by FTIR showed no significant differences between the formulations. No significant changes in wave numbers or intensities could be observed, neither in the solid samples after lyophilisation nor in the liquid samples after reconstition. Moreover, heating did not show any effect on the secondary structure, independent of whether the liquid samples were heated prior to lyophilisation or the solid powders of the lyophilisates were exposed to heat stress. Analysing the solid samples via the PIKE MIRacle system (ATR-system) for powders, however, was challenging as the background scattering was high due to the relative high sugar concentration of 10 % (i.e., 300 mg) compared to 2 mg/mL (i.e., 4 mg) protein.

3.6 Steady State Fluorescence Spectroscopy

Additionally the fluorescence in protein solutions was analysed prior to lyophilisation and after reconstitution. Trehalose samples spiked with 5 µM BisANS prior to lyophilisation gave a significantly higher fluorescence intensity compared to samples containing 1 and 0.2 µM BisANS (Fig.6). This indicates a good protein stabilising effect of trehalose avoiding significant changes in protein structure during lyophilisation and reconstitution.

_____
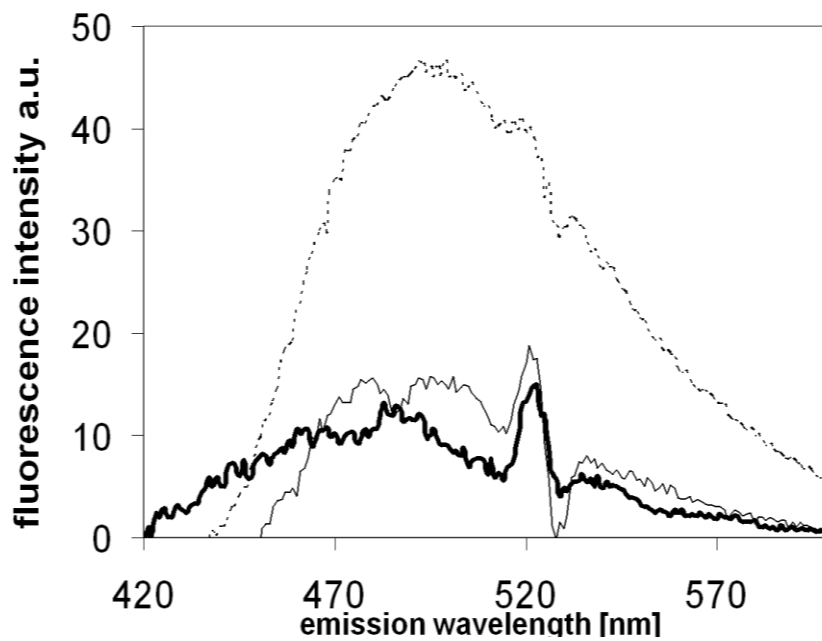
Figure 6: Steady state fluorescence spectroscopy of reconstituted protein samples stabilised with trehalose spiked with 5 µM (dotted thin line), 1 µM (solid thin line) and 0.2 µM (solid thick line) BisANS.

Protein oligomers induced prior to lyophilisation were traceable after lyophilisation (Fig.7). Trehalose and mannitol samples containing protein aggregates showed a significantly higher fluorescence intensity compared to the non stressed samples after reconstitution. However, the fluorescence intensity of the mannitol samples was observed to be increased as well leading again to the assumption of the inferior stabilising effect of mannitol during lyophilisation, as the protein had suffered from structural changes.

_____
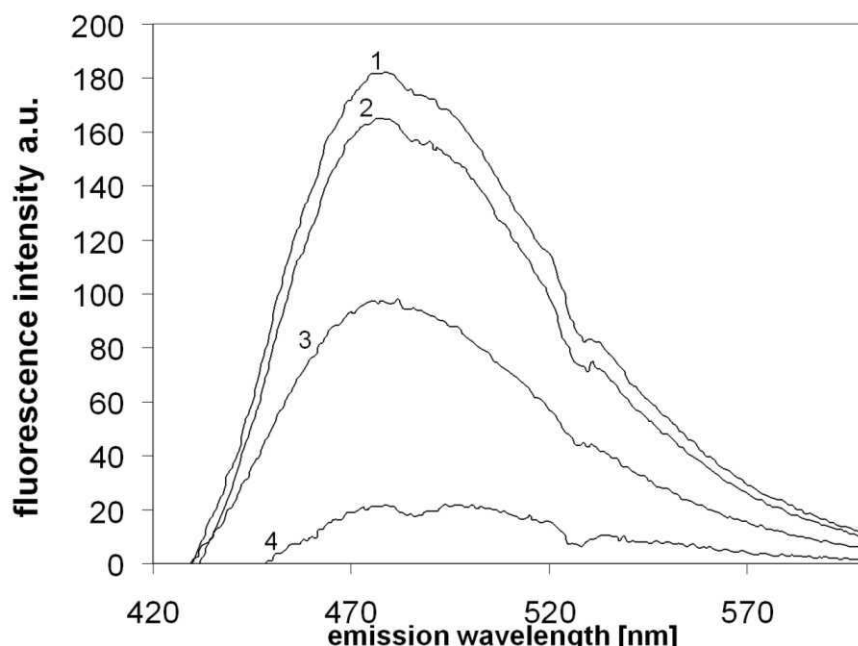
Figure 7: Steady state fluorescence spectroscopy of reconstituted protein samples with 1 µM BisANS of trehalose sample stressed prior to lyophilisation (1), mannitol sample stressed prior to lyophilisation (2), mannitol sample non-stressed (3) and trehalose sample non-stressed (4).

3.7 Front Face Fluorescence Spectroscopy

In order to test front face fluorescence spectroscopy as a method to assess the tertiary structure of proteins in a lyophilised powder state, intrinsic and extrinsic fluorescence were investigated. Firstly, intrinsic fluorescence intensity, observing tryptophan residues in the protein, was analysed. Changes in fluorescence maxima as well as varying intensities were observed, however the observed intrinsic intensities were too weak to be conclusive.

Regarding the extrinsic fluorescence, a possible bleaching effect was investigated. Using the solid sample holder equipment, the sample powder was excited 10 times in the same area without changing any parameter (Fig.8a). Fluorescence intensity differed randomly between 440,000 and 470,000 counts/sec, but no trend could be observed. Therefore, bleaching of the powder was negated, but high standard deviations were observed. In a next step the focus was laid on the sample holder

_____

position. When the sample holder was slightly changed within the limits of the holder fixings, the intensities differed significantly between 650,000 and 50,000 counts/sec. This led to the conclusion that the sample holder position affecting the angles of excitation and emission is of maximum importance. Exact and reproducible positioning was assured by fixing the samples holder cell to the extreme corner of the sample holder.
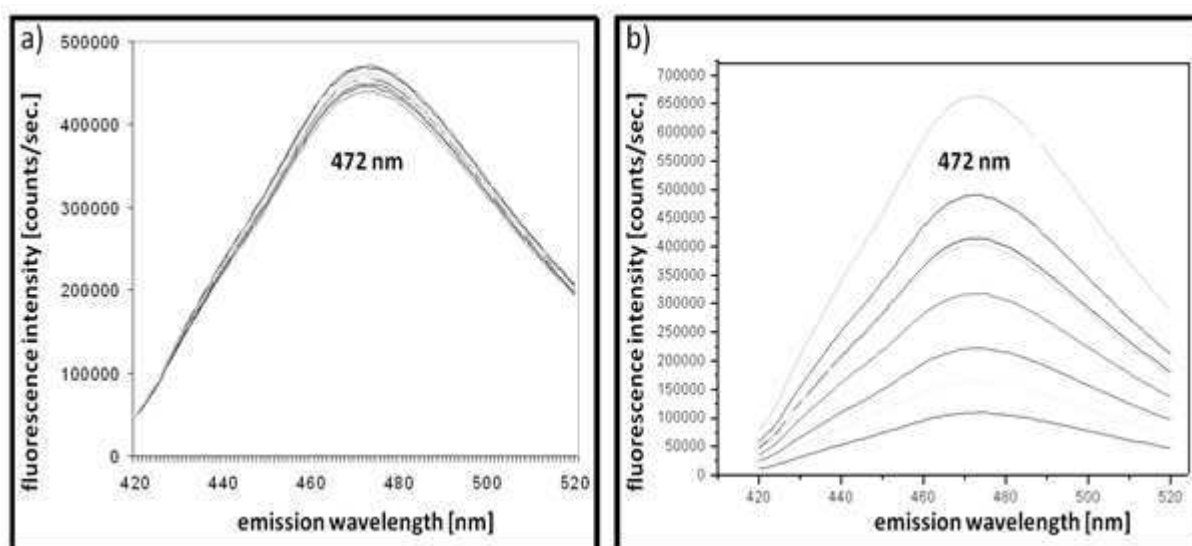
Figure 8: a) Front face fluorescence spectroscopy of lyophilised protein/trehalose samples spiked with 1 µM BisANS measured various times without changing any parameter and b) changing the sample holder position slightly.

Analysing the extrinsic fluorescence characteristics of lyophilised samples, diverging high fluorescence intensities for placebos were observed. Looking at the protein containing samples the fluorescence intensity varied significantly. It was increased in most samples compared to placebo but sometimes reduced. Comparing the fluorescence maxima, a shift of the BisANS fluorescence maximum could be observed (Fig.9). Giving an intensity maximum in liquids at 485 nm, the protein samples containing mannitol and dextran 70kDa as sugar stabiliser showed a blue shifted maximum in the dried state at 481 nm, while in trehalose samples the maximum was blue shifted to 472 nm.

fluorescence maxima	PBS	IgG
mannitol	489 nm	481 nm
dextran 70kD	480 nm	481 nm
trehalose	478 nm	472 nm

fluorescence intensity	PBS	IgG
mannitol	41,800	90,000
dextran 70kD	340,000	210,000
trehalose	510,000	390,000
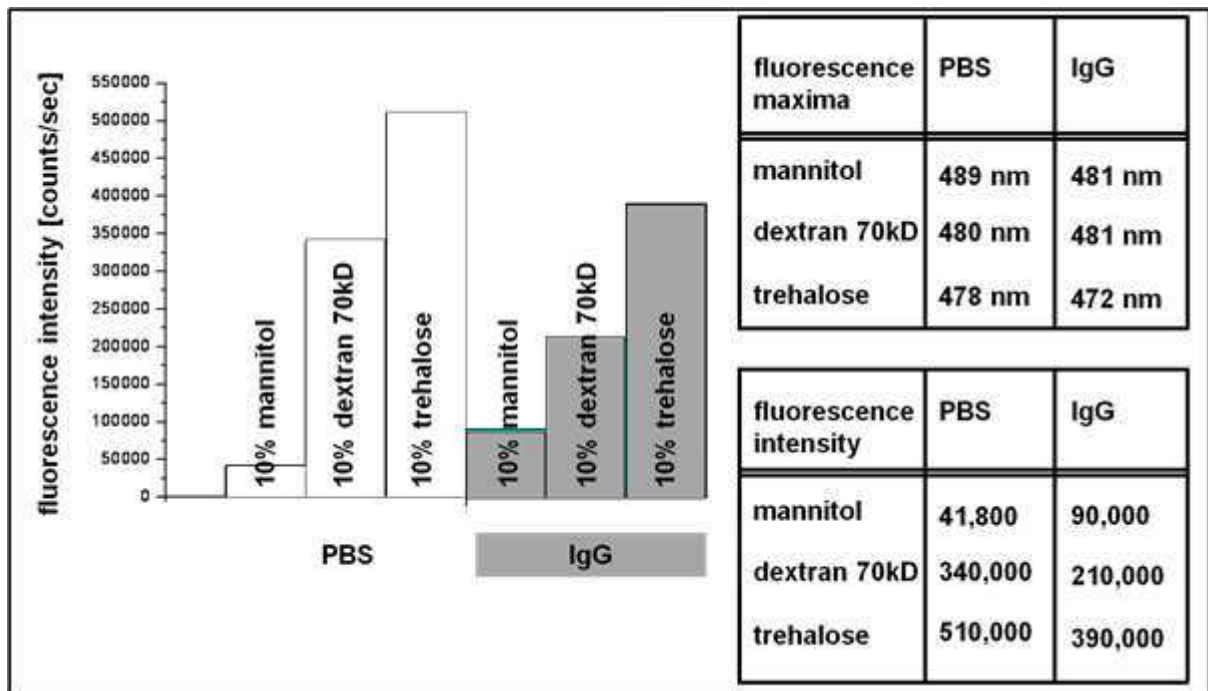
Figure 9: Comparing fluorescence maxima and intensities dependant on sugar and protein content containing 1 µM BisANS.

Fig. 10a shows the effect of different BisANS concentrations on the spectra obtained for unstressed protein / trehalose samples. The sample containing 5 µM BisANS showed the highest fluorescence intensity of > 800,000 counts / sec and the intensity clearly decreased with less BisANS (Fig.10a). Analysing samples spiked with 1 µM BisANS containing protein aggregates formed by stress prior to lyophilisation showed higher fluorescence intensity compared to the protein samples, which were not exposed to heat stress before lyophilisation (Fig.10b). Comparing the results on an absolute scale is not feasible as the individual settings differed slightly.
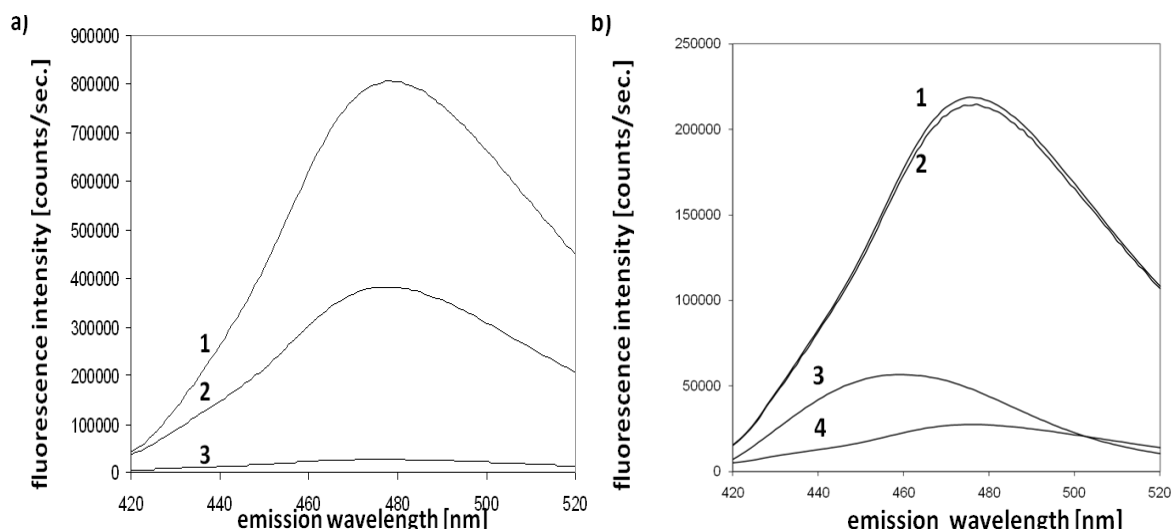
Figure 10: a) Front face fluorescence spectroscopy of lyophilised protein / trehalose samples spiked with 1) 5 µM BisANS, 2) 1 µM BisANS and 3) 0.2 µM BisANS and b) lyophilised protein samples spiked with 1 µM BisANS of mannitol sample stressed prior to lyophilisation (1), trehalose sample stressed prior to lyophlisation (2), unstressed mannitol sample (3) and unstressed trehalose sample (4) in the solid state.

Due to the fact that BisANS becomes fluorescent when interacting with hydrophobic surfaces and the water removal during lyophilisation reduces the polar and hydrophilic environment, random fluorescence intensities and maxima shifts were observed in extrinsic front face fluorescence spectroscopy. As intensities differed extremely among the samples, finding the most suitable settings was challenging. In summary, the extrinsic front face fluorescence spectroscopy may have potential as analytical method to investigate protein aggregation in the dried state. But the method is highly sensitive to minute changes in the experimental setup, particularly the sample holder position. In the present study, the high background fluorescence of the dye in the placebo systems limited the interpretation of the results. BisANS responds to hydrophobic surfaces formed upon water removal in the lyophilisates. Consequently, another dye is needed that does not increase fluorescence intensity when in contact with hydrophobic surfaces, but rather interacts differently with denaturised protein. Thioflavin T could be one possibility. It is used in amyloidal fibrils analysis in tissue staining and fluorescence microscopy to detect protein fibrillation [19]. The mechanism of fluorescence is explained by the interaction with ß-sheets.

However, Thioflavin T is also sensitive to viscosity. Another option would be Congo Red, which is used in amyloidal fibrils analysis as well [19]. It becomes fluorescent due to the formation of a so called supermolecular-ligands-complex. DCVJ (9-(Dicyanovinyl)-julolidine) is capable to detect tubuline structure and its fluorescence is explained by a TICT (twisted intramolecular charge transfer reactions) [19]. But DCVJ is also sensitive to viscosity changes.

4 CONCLUSION

After reconstitution, the conditions for a lyophilised protein change dramatically and do not reflect the situation in the dried state. Considering the well established methods to assess protein stability in liquids, alternative methods that allow to investigate protein integrity in the lyophilised state are desirable. In this context, front face fluorescence spectroscopy is one suitable approach, which could allow analysis of the tertiary structure of lyophilised proteins. We attempted to use the extrinsic fluorescence by adding BisANS to the samples. The presence of protein aggregates in stressed samples was proven by SEC and fluorescence analysis in liquid samples demonstrated protein unfolding. Furthermore, X-RD, SEM and residual moisture analysis ensured the effectiveness of the chosen lyophilisation conditions. Having defined the appropriate test conditions for the front face fluorescence spectroscopy we obtained high background fluorescence of placebo samples as BisANS is sensitive to the newly formed interfaces during lyophilization. Thus, the sometimes higher fluorescence intensities in protein containing samples might be associated with protein aggregates, but this does not provide conclusive evidence. To improve the described approach, different dyes should be tested, whereby particularly Thioflavin T, Congo Red or DCVJ could be alternatives to yield a better understanding of protein conformation in the lyophilised state.

5 ACKNOWLEDGEMENTS

6 REFERENCES

[1] Mahler, H.C.; Friess,W.; Grauschopf,U.; Kiese,S. Protein aggregation: Pathways, induction factors and analysis. J. Pharm Sci. 2008.

[2] Shire,S.J.; Shahrokh,Z.; Liu,J. Challenges in the development of high protein concentration formulations. J. Pharm Sci. 2004, 93 (6), 1390-1402.

[3] Chilson,O.P.; Costello,L.A.; Kaplan,N.O. Effects of freezing on enzymes. Fed Proc. 1965, 24, S55-S65.

[4] Carpenter,J.F.; Crowe,J.H. The mechanism of cryoprotection of proteins by solutes. Cryobiology 1988, 25 (3), 244-255.

[5] Gabellieri,E.; Strambini,G.B. ANS fluorescence detects widespread perturbations of protein tertiary structure in ice. Biophys. J. 2006, 90 (9), 3239-3245.

[6] Gabellieri,E.; Strambini,G.B. Perturbation of protein tertiary structure in frozen solutions revealed by 1-anilino-8-naphthalene sulfonate fluorescence. Biophys. J. 2003, 85 (5), 3214-3220.

[7] Carpenter,J.F.; Crowe,J.H. An infrared spectroscopic study of the interactions of carbohydrates with dried proteins. Biochemistry 1989, 28 (9), 3916-3922.

[8] Sharma, Vikas K.; Kalonia, Devendra S. Steady-state tryptophan fluorescence spectroscopy study to probe tertiary structure of proteins in solid powders. Journal of Pharmaceutical Sciences (2003), 92(4), 890-899.

[9] Prestrelski,S.J.; Tedeschi,N.; Arakawa,T.; Carpenter,J.F. Dehydration-induced conformational transitions in proteins and their inhibition by stabilizers. Biophys. J. 1993, 65 (2), 661-671.

[10] Chang, Liuquan; Pikal, Michael J.. Mechanisms of protein stabilization in the solid state. Journal of Pharmaceutical Sciences (2009), 98(9), 2886-2908.

[11] Heljo, Ville Petteri; Jouppila, Kirsi; Hatanpaa, Timo; Juppo, Anne M. The Use of Disaccharides in Inhibiting Enzymatic Activity Loss and Secondary Structure

_____

Changes in Freeze-Dried Galactosidase during Storage. Pharmaceutical Research

[12] Pelton,J.T.; McLean,L.R. Spectroscopic methods for analysis of protein secondary structure. Anal. Biochem. 2000, 277 (2), 167-176.

[13] Costantino,H.R.; Griebenow,K.; Mishra,P.; Langer,R.; Klibanov,A.M. Fourier-transform infrared spectroscopic investigation of protein stability in the lyophilized form. Biochim. Biophys. Acta 1995, 1253 (1), 69-74.

[14] Schule,S.; Friess,W.; Bechtold-Peters,K.; Garidel,P. Conformational analysis of protein secondary structure during spray-drying of antibody/mannitol formulations. Eur. J. Pharm Biopharm 2007, 65 (1), 1-9.

[15] Spiro T G; Gaber B P Laser Raman scattering as a probe of protein structure. Annual review of biochemistry (1977), 46 553-72.

[16] Van De Weert, Marco; Hering, Joachim A.; Haris, Parvez I. Fourier transform infrared spectroscopy. Biotechnology: Pharmaceutical Aspects (2005), 3, Methods for Structural Analysis of Protein Pharmaceuticals, 131-166.

[17] Ramachander, Ranjini; Jiang, Yijia; Li, Cynthia; Eris, Tamer; Young, Meagan; Dimitrova, Mariana; Narhi, Linda. Solid state fluorescence of lyophilized proteins. Analytical Biochemistry (2008), 376(2), 173-182.

[18] Jiskoot, Wim; Crommelin, J. A. Methods for Structural Analysis of Protein Pharmaceuticals. [In: Biotechnol.: Pharm. Aspects, 2005; 3]. (2005), 678 pp.

[19] Hawe A; Sutter M; Jiskoot W. Extrinsic Fluorescent Dyes as Tools for Protein Characterization. Pharmaceutical Research (2008), 25(7), 1487-1499.

[20] Eisinger, Josef; Flores, Jorge. Front-face fluorometry of liquid samples. Analytical Biochemistry (1979), 94 (1), 15-21.

_____

_____

CHAPTER 7

General Summary and Outlook

Recombinant proteins gain more and more importance on the pharmaceutical market. One major challenge during formulation development is the design of a stable formulation in order to assure the protein integrity during manufacturing, shipping and storage. Various types of chemical and physical protein instabilities, such as oxidation and aggregation, induced by different stress exposures, have been described. Protein instability is undesirable in regards to safety, efficacy and quality requirements. In this context, immunologic side effects of protein aggregates in patients have to be considered. It is best practise to use a combination of orthogonal methods to analyze the protein stability. Complementary analytical approaches are deemed necessary to fully characterize and understand structural changes and the quality of aggregates formed. Hence, the focus of this thesis was the investigation of complementary methods to assess protein-protein interactions and protein unfolding. These two effects can be seen as first steps of protein aggregation. In particular, B22 and extrinsic fluorescence of individual protein species after size separation by SEC are described. Their benefits as additional methods for a better understanding of protein instability to enable adequate formulation development are discussed.

In CHAPTER 1, the techniques most commonly used in protein formulation development to analyze protein aggregates and particles are reviewed. Beyond the assessment of benefits and limitations of today's standard techniques, also newly developed methods, such as lab on a chip gel electrophoresis and the use of robotic systems are introduced. One major aspect discussed is the stability testing of liquid protein pharmaceuticals simulating stress impact on protein caused by formulation

_____

processes, shipment and static storage. In this, the limits of protein aggregation extrapolation to long term stability and up-scaling are discussed. Furthermore, the possibilities of protein aggregation artefacts are reviewed as in the case of HPLC, AF4 and DLS analytics where they might be caused due to the measuring system, or in DLS with its incapability to differentiate exogenous particles. Finally, challenges in high concentration protein formulations and in dried protein pharmaceuticals are discussed. Overall, the review of the currently used analytical methods indicated a fundamental need to find further alternatives to characterize protein aggregation pathways.

In CHAPTER 2, a new technique to characterise protein-protein interactions via B22 analysis was investigated. B22 is a number, either positive or negative, expressing the strength of protein-protein interactions and can be derived using different analytical approaches. The data for our calculation was generated through simultaneous measurements of protein concentration and scattered light intensity after size separation on an SEC column. Going beyond previous investigations, this technique was unique, in that it enables the B22 calculation of both monomer and soluble aggregates individually. We observed that the negative B22 values of the initial protein monomer decreased upon thermal stress for both the monomer and the newly formed aggregate species. This decrease indicates an increase in attractive protein-protein interactions. The decrease of B22 came along with soluble aggregate formation. These results reflect the partial protein unfolding augmenting hydrophobic attractive interactions. Overall, B22 analysis may allow predicting formulation conditions, which provide adequate colloidal stability avoiding aggregate formation, although the correlation of B22 values and long term stability requires further investigation.

_____

In CHAPTERS 3 to 6, extrinsic fluorescence techniques to analyze protein unfolding are investigated. The use of extrinsic fluorescent dyes, e.g., BisANS, allows observing changes in protein tertiary structure. Due to protein unfolding, hydrophobic surfaces of the protein become exposed. The fluorescent dye can interact with the hydrophobic protein patches resulting in an increase of fluorescence intensity. In CHAPTER 3 a Post Column Module (PCM) technique was developed, that adds BisANS after SEC and UV detection, but prior to fluorescence detection. The method enables a monitoring of protein unfolding simultaneously with size analysis. An increase in fluorescence for both oligomers and monomer after stress exposure was observed via PCM. While acidic pH, temperature and light stress resulted mostly in the formation of unfolded oligomers, freeze/thaw (F/T) and shaking stress induced only few native-like soluble aggregates. Thus, unfolding can specifically be assigned to monomer and/or the aggregated species. Furthermore, different degrees of monomer and aggregate unfolding after pH, temperature and light stress are observed. The observation of the unfolding of the monomer still needs to be linked to protein activity and long term stability.

In CHAPTER 4, the changes in protein aggregates during storage of stressed samples were monitored. Using visual inspection, turbidity measurement, light obscuration particle counting, and SEC with UV and PCM fluorescence detection, the protein aggregates induced by acidic pH, heat, F/T and light stress exposure were monitored over 3 months. Both reversibility of protein aggregation along with re-dissolution to monomer species and progression of aggregation to form protein aggregates > 1 µm due to a nucleation effect could be negated in this study. Instead, the induced protein particles were considered to be stable.

In CHAPTER 5, fluorescence microscopy (FM) enabled the visualization of particles > 1 µm retained on filters by using BisANS. FM proved to be more sensitive for protein particles < 10 µm compared to the bright-field microscopy due to a better contrast. FM enabled also size estimation and counting of the protein particles. Moreover, with FM it was also possible to detect different appearances of the protein aggregates formed upon various stress methods. In contrast to the other protein aggregates generated, protein aggregates formed upon F/T stress showed a unique, spherical shape. Thus, FM could be a complementary tool to micro-flow imaging in protein aggregate analysis, as (i) FM has the ability to visualize the shape of protein particles, (ii) FM is suitable for the particle size range 1 – 200 µm and (iii) FM is especially sensitive to small particles in the size range < 10 µm.

In CHAPTER 6, front face fluorescence spectroscopy was discussed as one suitable approach allowing the analysis of lyophilised proteins. After reconstitution, the conditions for a lyophilised protein change dramatically and do not reflect the situation in the dried state. Considering the well established methods to assess protein stability in liquids, alternative methods that allow investigating protein integrity in the lyophilised state are desirable. As novel approach, we attempted to use extrinsic front face fluorescence by adding BisANS prior to lyophilisation. Having defined the appropriate test conditions for the front face fluorescence spectroscopy we obtained high background fluorescence of placebo samples as BisANS was sensitive to the newly formed interfaces during lyophilization. Protein containing samples sometimes exhibited higher fluorescence intensities, indicating protein unfolding, but ultimately no conclusive evidence could be provided. In order to improve the described approach Thioflavin T, Congo Red or DCVJ could be tested as alternative dyes to yield a better understanding of protein conformation in the lyophilised state.

_____

By using the presented methods of B22 analysis and extrinsic fluorescence, complementary knowledge on protein aggregates could be generated. These techniques were able to provide advantageous, supplementary information regarding protein-protein interactions and protein structure of both the protein aggregates as well as of the monomer, due to prior size-separation. Attractive or repulsive protein-protein interactions as well as the state of protein folding could be determined for the different protein species simultaneously and individually. As both B22 and fluorescence analysis can be conducted in combination with SEC, probably the most widely spread and best established technique, the investigated methods represent easily accessible and complementary approaches to shed more light on protein interactions and aggregation in formulation development. Thus, they may help to analyze the induction factors and the sequence of events in protein aggregation in a better way.

_____

LIST OF ABBREVIATIONS

A

AF4	asymmetrical field flow field fractionation
AFM	atomic force microscopy
ANS	8-Anilino-1-naphthalenesulfonic acid ammonium salt
ATR	attenuated total reflectance
AUC	analytical ultracentrifugation
AUC	area under the curve
a.u.	arbitrary units

B

BisANS	4,4′-Dianilino-1,1′-binaphthyl-5,5′-disulfonic acid dipotassium salt
BSA	bovine serum albumin
β-LG	β-lactoglobulin

C

CA	cellulose acetate filter membrane
CD	circular dichroism spectroscopy
CE	capillary electrophoresis
CMC	critical micelle concentration

D

Da	Dalton
DLS	dynamic light scattering

E

EMA	European Medicines Agency

F

Fab	antigen binding fragment
Fc	fragment crystallisable region
FDA	U.S. Food and Drug Administration
FFF	flow field fractionation
FNU	formazine normalized/nephlometric units
FTIR	Fourier transformed infrared spectroscopy

H

HC	heavy chain
HIC	hydrophobic interaction chromatography
HMW	high molecular weight
HPLC	high performance liquid chromatography
HSA	human serum albumin

I

i.m.	intramuscular
i.v.	intravenous
IEC	ion exchange chromatography
IEF	iso-electric focusing
IEP	iso-electric point
IgG	immunoglobulin class G
IgG1	immunoglobulin G subclass 1
IgG2	immunoglobulin G subclass 2

J

JP	Japanese Pharmacopoeia

_____

K

kDa   kilo Dalton

L

LC   light chain

LMW   low molecular weight

M

mAB   monoclonal antibody

MALLS   multi-angle laser light scattering

MWCO   molecular weight cut off

µDSC   micro-differential scanning calorimetry

N

n.a.   not applicable

n.d.   not detected

n.t.   not tested

NMR   nuclear magnetic resonance

nDSC   nano-differential scanning calorimetry

P

PAGE   polyarcylamide gel electrophoresis

PBS   phosphate buffered saline

PEG   polyethylene glycol

PES   polyethersulfone

Ph. Eur.   European Pharmacopoeia

Phe   Phenylalanine

pI   iso-electric point

ppm   parts per million

_____

PS	polysorbate
PVA	polyvinyl alcohol
PVP	polyvinyl pyrrolidone

R

r.h.	relative humidity
RMS	root mean squared error
RPC	reversed phase chromatography
RP-HPLC	reverse phase high performance chromatography
rpm	rounds per minute
RT	room temperature

S

s.c.	subcutaneous
SDS	sodium dodecyl sulphate
SDS-PAGE	sodium dodecyl sulphate polyacrylamide gel electrophoresis
SE	sedimentation equilibrium
SEC	size exclusion chromatography
SE-HPLC	size exclusion high performance chromatography
SEM	scanning electron microscopy
SLS	static light scattering
SV	sedimentation velocity

T

TEM	transmission electron microscopy
TFF	tangential flow filtration
Tm	transition/melting temperature
Trp	Tryptophan
Tyr	Tyrosine

U

USP   United States Pharmacopeia

UV   ultraviolet spectroscopy

V

v/v   volume per volume

W

w/o   without

w/v   weight per volume

WFI   water for injection

X

XRPD   X-ray powder diffraction

_____

PUBLICATIONS

RESEARCH PAPER

2012   Miriam Printz, Wolfgang Friess.
         Simultaneous detection and analysis of protein aggregation and protein
         unfolding by Size Exclusion Chromatography with post column addition
         of the fluorescence dye BisANS.
         Journal of Pharmaceutical Sciences (2012), 101(2), 826-837.

2012   Miriam Printz, Devendra S. Kalonia, Wolfgang Friess.
         Individual Second Virial Coefficient Determination of Monomer and
         Oligomers in Heat Stressed Protein Samples using Size Exclusion
         Chromatography – Light Scattering.
         Journal of Pharmaceutical Sciences (2012), 101(1), 363-372.

2007   Hanns-Christian Mahler, Miriam Printz, Robert Kopf, Rudolf Schuller,
         Robert Müller. Behaviour of Polysorbate 20 During Dialysis,
         Concentration and Filtration Using Membrane Separation Techniques.
         Journal of Pharmaceutical Sciences (2007), 97(2), 764-774

BOOK CHAPTER

2012   M.Printz, W.Friess.
         Formulation Development and Its Relation to Protein Aggregation and
         Particles in *Analysis of Aggregates and Particles in Protein
         Pharmaceuticals*, H.C. Mahler (Editor) and W. Jiskoot (Editor), John
         Wiley & Sons, Inc. ISBN: 978-0-470-49718-0

_____

POSTER PRESENTATIONS

2010   M.Printz, D.S.Kalonia, W.Friess.

Analysing B22 in multiple protein species formed upon thermal stress.

FIP PSWC 2010 / AAPS Annual Meeting and Exposition,

New Orleans, USA, 14-18th November

2010   M.Printz, S.R.Kar, D.S.Kalonia, W.Friess.

A chromatographic determination of second virial coefficient and

unfolding of both protein monomers and higher molecular weight

species. 7th World Meeting on Pharmaceutics, Biopharmaceutics and

Pharmaceutical Technology, Valetta, Malta, 8-11th March

2009   M.Printz, W.Friess.

SEC with UV and fluorescence detection by BisANS and the influence

of PS 20. Protein Stability Conference,

Breckenridge, USA, 16-18th July

2009   M.Printz, W.Friess.

Simultaneous detection of changes in protein tertiary structure and

aggregation by SEC with post column addition of BisANS

AAPS National Biotechnology Conference, Seattle, USA, 21-24th June

2008   M.Printz, W.Friess.

Detection of Small Protein Aggregates with Fluorescence Microscopy

using Extrinsic Fluorescence Dyes

6th World Meeting on Pharmaceutics, Biopharmaceutics and

Pharmaceutical Technology, Barcelona, Spain, 7-10th April

_____

SUPERVISION OF STUDENT-DRIVEN RESEARCH PROJECTS

2009   Characterisation of Protein Aggregates by Post Column Addition of
            BisANS and Assessing the Possible Interaction of Surfactants with
            Fluorescent Dye
            Madeleine Witting
            Master Research Practical Course A

2009   Characterisation of protein aggregates by Fluorescence Detection
            Elena Ivanchenko
            Master Research Practical Course A

2008   Analysis of Liquid and Lyophilised Protein Formulations by FTIR and
            HP-SEC
            Caroline Schweimer
            Master Research Practical Course A

2008   Front Face Fluorescence Spectroscopy of lyophilised proteins
            Madeleine Witting
            Bachelor Thesis

2008   Evaluating different techniques to analyse protein aggregates
            Bérengère Thouroude
            International Erasmus Student Internship

2008   Analysis of temperature stressed IgG1 by HP-SEC with fluorescence
            detection
            Caroline Schweimer
            Bachelor Thesis

2007   Formulation Development of Poorly Water Soluble Drugs for Pediatric
            Use
            Stephanie Buser, Gülsen Özer, Bernd Sterner
            Compulsory Optional Subject (Wahlpflichtfachpraktikum)

_____

CURRICULUM VITAE

MIRIAM PRINTZ

PHD THESIS

2007 – 2010	**"The Value of Fluorescence and B$_{22}$ Techniques as Complementary Approaches in Protein Stability Analyses"** **Ludwig Maximilians University of Munich (LMU)** Department of Pharmacy Pharmaceutical Technology and Biopharmaceuticals Prof. Dr. Wolfgang Friess	Germany

International Research Exchanges

2010 / 2009	**University of Connecticut** School of Pharmacy Prof. Dr. Devendra S. Kalonia	USA
2008 / 2007	**University of Leiden** Leiden Amsterdam Center for Drug Research Prof. Dr. Wim Jiskoot	Netherlands

Professional Development

2007 – 2010	**Certification as** **Specialist in Pharmaceutical Technology** "Fachapotheker in Pharmazeutischer Technologie" Bayerische Landesapothekerkammer / LMU	Germany

STUDY OF PHARMACY

2006	**Certification of Approbation as Pharmacist** Regional Government Düsseldorf	Germany
2006	**Internship - Kristall Apotheke** Public Pharmacy, Hürth	Germany
2005 – 2006	**Internship - F. Hoffmann-La Roche** Department of Research and Development Biologics	Switzerland
2004 – 2005	**University of Valencia** School of Pharmacy, International Exchange Semester	Spain
2003	**Internship - St. Franziskus Hospital** Clinical Pharmacy, Cologne	Germany
2001 – 2005	**University of Bonn** School of Pharmacy	Germany